PROCEEDINGS OF THE 3rd INTERNATIONAL WORKSHOP ON THERMOACOUSTICS

EDITORS
Theo van der Meer
Philippe Blanc-Benon
Kees de Blok
Joris Oosterhuis

26 - 27 October, 2015
University of Twente, The Netherlands

UNIVERSITY OF TWENTE.

Faculty of Engineering Technology
Laboratory of Thermal Engineering

Logos by Jullian Claus & Hieu Nguyen
Cover and lay-out by Joris Oosterhuis
Printed by Gildeprint drukkerijen, Enschede
GILDEPRINT

ISBN: 978-90-365-3974-6
DOI: 10.3990/1.9789036539746

PREFACE

I am proud and happy to present the proceedings of the 3rd International Workshop on Thermoacoustics, which is organised as a Eurotherm Symposium 107.

This meeting brings scientists and researchers from academia and industry together to share their progress on thermoacoustic heat pumps, coolers and engines and to discuss the future of this research field. On purpose we have narrowed down the topic as much as possible in order to stimulate in depth discussions. For the same reason we avoided as much as possible parallel sessions. Now it is up to the participants to make it a real Workshop.

It is a pleasure for the organising committee to welcome around 50 researchers from 11 different countries to the University of Twente and we hope that you will have a fruitful workshop.

On behalf of the co-chairs and the local organizing committee,

Theo van der Meer
(chair, University of Twente)

Sponsors

The following organizations and companies are sponsoring the Third International Workshop on Thermoacoustics through either organizational or financial support.

UNIVERSITY OF TWENTE.

ÉCOLE CENTRALE LYON

ASTER THERMOACOUSTICS

BOSCH

EUROTHERM

Local organizing committee

- Theo van der Meer *(chair)*
- Sally Kloost *(secretary)*
- Coby van Houten *(finance)*
- Joris Oosterhuis *(organization)*

CONTENTS

WORKSHOP SCHEDULE

Sunday 25 October

16:00	**18:00**	**Registration and drinks**	**Hotel Drienerburght**

Monday 26 October

8:30	**9:30**	**Registration and coffee**	**The Gallery**
9:30	9:45	Welcome and introduction	Reactor
9:45	**10:30**	**Keynote 1**	**Erlenmeyer**
		Guillaume Penelet	*Thermoacoustic engines: from what we know to what we do not understand*
10:30	**11:00**	**Coffee**	**The Gallery**
11:00	**12:20**	**Session 1**	**Erlenmeyer**
	TS03	*Bakhtier Farouk*	*Thermoacoustic refrigeration systems: recent developments*
	TS02	*Paweł Owczarek*	*Details and experimental results of a stand-alone container cooled by a solar driven multi-stage traveling wave thermoacoustic system*
	TS04	*Chris Lawn*	*Optimization of the loop in a travelling-wave thermo-acoustic engine*
	TS05	*Maurice-Xavier Francois*	*The VALTA project: full scale conversion of CHP engine flue gas heat into electricity*
12:20	**13:20**	**Lunch**	**Grand café**
13:20	**14:40**	**Session 2a**	**Erlenmeyer**
	AE05	*Douglas Wilcox*	*Development of a compact thermoacoustic-Stirling electric generator*
	AE02	*Jeffrey Lin*	*High-fidelity simulations of a standing-wave thermoacoustic-piezoelectric engine*
	AE04	*Bakhtier Farouk*	*Signal conditioning of carbon nanotube loudspeaker*
	AE01	*Ken Kaneuchi*	*Evaluation of bi-directional turbines using the two-sensor method*
14:40	**14:50**	**Coffee**	**The Gallery**
14:50	**16:10**	**Session 3a**	**Erlenmeyer**
	AE03	*Johan Brussen*	*Modeling and controlling the generator of a thermoacoustic Stirling engine*
	AE06	*Maurice-Xavier Francois*	*Space thermoacoustic radio-isotopic power system: SpaceTRIPS*
	TS15	*Hiroaki Hyodo*	*Dynamics of forced synchronization in thermoacoustic system*
16:10	**16:20**	**Coffee**	**The Gallery**
16:20	**17:20**	**Session 4a**	**Erlenmeyer**
	TC01	*Marialuisa Napolitano*	*The role of stack non acoustic parameters on thermodynamic performance of standing wave devices*
	TC02	*Esmatullah Maiwand Sharify*	*CFD study of oscillatory flow around parallel plates in a traveling-wave thermoacoustic engine*
	TC03	*Ahmed Ibrahim Abd El-Rahman*	*Simulation of flow and heat transfer in thermoacoustic refrigerator using a 3-D periodic cell structure*
17:20	**18:00**	**Discussion**	**Erlenmeyer**
19:30		**Dinner**	**De Grolsch Veste**

Monday 26 October *parallel sessions*

13:20	**14:40**	**Session 2b**	**Reactor**
	SN06	*Kazuto Kuzuu*	*Numerical investigation of heat exchange between fluid and solid wall of oscillatory flow*
	SN05	*Dmitry Uglanov*	*Estimation of different numerical pulse tube thermoacoustic refrigerator models*
	SN10	*Jan-Aiso Lycklama à Nijeholt*	*CFD modelling of the effect of oscillating jets on streaming heat losses in a torus-shaped thermoacoustic engine*
	SN07	*Carlo Scalo*	*High-fidelity and low-order modeling of a traveling-wave thermoacoustic engine*
14:40	**14:50**	**Coffee**	**The Gallery**
14:50	**16:10**	**Session 3b**	**Reactor**
	SN01	*Gaëlle Poignand*	*Simplified modeling of a thermo-acousto-electric engine forced by an external sound source*
	SN03	*Nobumasa Sugimoto*	*On general expressions of temporal means of mass flux, shear stress and heat flux due to thermoacoustic waves*
	SN04	*Svetlana Nekrasova*	*A mathematical model of acoustic thermal excitation for pulse tube engine*
	SN12	*Anne de Jong*	*A fast one-dimensional nonlinear thermoacoustic code*
16:10	**16:20**	**Coffee**	**The Gallery**
16:20	**17:20**	**Session 4b**	**Reactor**
	ET01	*Mahening Citra Vidya*	*A traveling wave termination for a thermoacoustic setup*
	ET02	*Mariko Senga*	*Comparison of acoustic power amplification by wet/dry-walled thermoacoustic engine*
	ET04	*Philippe Blanc-Benon*	*Analysis of the acoustic field in a thermoacoustic system using time-resolved particle image velocimetry and constant-voltage anemometry*

WORKSHOP SCHEDULE

Tuesday 27 October

8:30	**9:00**	**Coffee**	**The Gallery**
9:00	**9:45**	**Keynote 2**	**Erlenmeyer**
		Kees de Blok	*A way out of the acoustic to electric conversion limitations*
9:50	**10:30**	**Session 5**	**Erlenmeyer**
	TS06	*Adam Ruziewicz*	*The analysis of hybrid solar powered cooling/heating system with the travelling-wave thermoacoustic refrigerator*
	TS07	*Remi Bessis*	*Dual thermoacoustic core compact heat-pump for automotive application*
10:30	**11:00**	**Coffee**	**The Gallery**
11:00	**12:20**	**Session 6**	**Erlenmeyer**
	TS08	*Hassan Tijani*	*Bench scale electrically driven thermoacoustic heat pump*
	TS01	*Tao Jin*	*Study on a looped 2-stage thermoacoustic engine*
	TS11	*Alexander Kruse*	*Simulation and experimental validation of a looped thermoacoustic generator with stub*
	TS17	*Catherine Weisman*	*Load effect on the starting performance of a standing wave thermoacoustic engine*
12:20	**13:20**	**Lunch**	**Grand café**
13:20	**14:20**	**Session 7**	**Erlenmeyer**
	SN02	*Sudipto Mukhopadhyay*	*Numerical simulation of minor losses in oscillating flow*
	SN08	*Joris Oosterhuis*	*Performance measurements of jet pumps with multiple holes*
	SN09	*Michael Timmer*	*Reducing flow separation in jet pumps*
14:20	**14:30**	**Coffee**	**The Gallery**
14:30	**15:50**	**Session 8**	**Erlenmeyer**
	TS18	*Steven Garrett*	*Self-powered thermoacoustic sensors for nuclear reactors*
	TS12	*Kenichiro Tsuda*	*The amount of water required to decrease the critical temperature difference of a standing wave thermoacoustic engine*
	TS16	*Robert Keolian*	*Trillium: an inline thermoacoustic-Stirling refrigerator*
	TS14	*Hiroaki Hyodo*	*Thermoacoustic Stirling engine with liquid piston*
15:50	**16:00**	**Closing ceremony**	**Erlenmeyer**
16:00	**17:30**	**Drinks**	**Grand café**

GUIDELINES FOR PRESENTATION

To streamline the technical sessions at the workshop, please pay attention to the following guidelines when preparing your oral presentation:

- The presenting time is limited to 15 minutes. An additional 5 minutes is available for questions and switching speakers.
- The allowed presentation formats are MS Powerpoint 2010 or PDF. Any other formats are not supported. If you would like to use fonts that are not included in the base installation of Windows 7, please make sure to embed them in the presentation file.
- The presentation room is equipped with computer facilities, it is not possible to use your own laptop or tablet.
- Please bring your presentation on a USB flash drive 10 minutes before the start of the session you are scheduled in. Assistants will help you to transfer your file to the presentation computer.

KEYNOTE LECTURES

Thermoacoustic engines: from what we know to what we do not understand

Guillaume Penelet

Associate professor, Laboratoire d'Acoustique de l'Université du Maine, LAUM UMR-CNRS 6613 Avenue Olivier Messiaen, 72085 Le mans cedex 9, France

The design and the development of thermoacoustic engines already has a three-decade history and there exists several examples of devices able to reach high performances. However, despite their simplicity in terms of geometry, thermoacoustic engines are not very well understood due to the complexity and the variety of the phenomena saturating heat transport and sound amplification.

This talk will be organized into two parts. The first part will be devoted to a general, academic presentation of thermoacoustic engines from the standpoint of acoustics. The second part will give an emphasis on some processes which are still poorly understood (notably entrance effects or acoustic streaming). As an illustrative example of the challenges that need to be taken up to get further insight into the operation of thermoacoustic engines, a focus will be given on recent research at LAUM, in which digital interferometric holography is used to characterize the highly nonlinear density fluctuations generated in the vicinity of the stack during the transient regime of wave amplitude growth in a standing wave thermoacoustic self-sustained oscillator.

A way out of the acoustic to electric conversion limitations

Kees de Blok

Aster Thermoacoustics, Smeestraat 11, NL8194LG Veesen, The Netherlands

Thermoacoustics is a key enabling technology for the conversion of heat into acoustic power. Nowadays thermoacoustics in itself is well understood and has proven to be a generic applicable and efficient conversion technology. For practical and economic viable applications however, still two issues have to be solved in a practical and cost effective way. (1) heat to be converted need to be supplied at high or medium temperature and rejected at a lower temperature with minimal temperature loss and, (2) high acoustic (wave) power generated by the thermoacoustic process has to be converted into electricity. Focus of this keynote presentation is on the conversion of high acoustic power levels into electricity.

A common approach for converting acoustic power from thermoacoustic engines into electricity and vice versa is the use of so called resonant linear alternators or electro motors. These devices however shows severe limitations in terms of cost and scalability. The increase of moving mass when increasing power sets a practical limit to the output power mainly caused by the increase of periodic forces in the construction and by the difficulty to maintain clearance seals (<70 μm) stable over large stroke amplitudes.

Linear alternators make use of the pressure variation of the acoustic wave. There is however no physical reason why not using the periodic velocity component of the acoustic wave. A way to convert such a bidirectional flow into rotation is known from shore and off-shore electricity production plants based on an oscillating water column (OWC). In this type of power stations, waves force a water column in a chamber to go up and down. This chamber is connected to the open atmosphere and the periodic in- and outflow of air drives a bi-directional turbine of which the rotation direction is independent of the flow direction.

In a thermoacoustic system similar periodic flow conditions exist, so in principle, bi-directional turbines can be deployed for conversion of acoustic wave motion as well. While theory of these bi-directional turbine is well understood and documented for air at atmospheric pressure operating at very low frequencies (water waves), information is lacking about the behaviour of such turbines in high frequent acoustic flow fields and at elevated mean pressures.

The idea of converting high acoustic power flow by using bi-directional turbines was introduced early 2012 by Aster, actually as a result of failing to convert the high acoustic power from the 100kW TAP project into 10kW of electricity by deploying linear alternators.

Since then, a lot of progress is made, by experimental and theoretical work, in understanding the principe of operation, modelling and design of such turbines. Results so far are encouraging. The conclusion from the this work is that this type of turbine provide a cost effective device for converting acoustic wave energy into rotation and from there into electricity on any power level. The presentation will address the background and specific issues about the interacton of the turbine with the acoustic flow as well as experimental results obtained in various prototypes.

THERMOACOUSTIC SYSTEMS
&
APPLICATIONS

STUDY ON A LOOPED 2-STAGE THERMOACOUSTIC ENGINE

T. Jin [1,2*], R. Yang[1], Y.L. Liu[1], K. Tang[1] and B.M. Chen[3]

[1]*Institute of Refrigeration and Cryogenics, Zhejiang University, Hangzhou 310027, P.R.China.*
[2] *State Key Laboratory of Clean Energy Utilization, Zhejiang University, Hangzhou 310027, China.*
**Corresponding author's e-mail: jintao@zju.edu.cn*
[3]*Department of Energy and Chemical Engineering, Dongguan University of Technology, Dongguan 523808, P.R.China.*

Keywords: *thermoacoustic prime mover, looped 2-stage configuration, onset temperature, low-grade heat source*

Multi-stage looped thermoacoustic engines have attracted much attention in recent years[1]. This paper presents the looped 2-stage thermoacoustic prime movers schematically shown in Figure 1, which are composed of 2 thermoacoustic cores (including hot heat exchangers, regenerators and main cold heat exchangers) connected by resonators, thermal buffer tubes and secondary cold heat exchangers in series. The two thermoacoustic cores can be arranged in asymmetric or symmetric configuration. The total loop length is about 8 m. Main dimensions of the thermoacoustic core are listed in Table 1. A funnel-shaped fluid director is inserted between the thermoacoustic core and resonator to reduce the flowing loss.

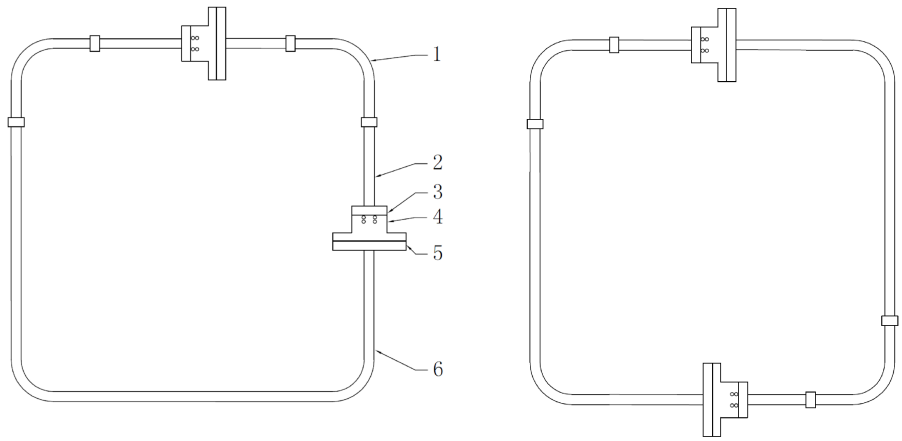

Figure 1: *Schematic of the looped 2-stage thermoacoustic prime movers: 1. Secondary cold heat exchanger; 2. Thermal buffer tube; 3. Hot heat exchanger; 4. Regenerator; 5. Main cold heat exchanger; 6. Resonator.*

Table 1: *Dimensions of the thermoacoustic core*

Components	Hot heat exchanger	Regenerator	Main cold heat exchanger
Length (mm)	30	30	30
Diameter (mm)	99	99	99

Numerical simulations with the DeltaEC program[2] and systematic experiments on the looped 2-stage thermoacoustic engine with an asymmetric configuration (see Figure 1 on the left) have been conducted with helium as the working fluid. Figure 2 presents the relation between pressure amplitude and heating temperature with the filling pressure of 2 MPa, containing the results from both experiments and simulations. Figure 3 shows the onset temperatures under different filling pressures in our experiments. A lowest onset temperature of 64°C (under a cooling temperature of 13°C) was achieved with the filling pressure of 2.3 MPa.

A symmetric configuration of the thermoacoustic prime mover (see Figure 1 on the right), in which the two thermoacoustic cores are placed with a distance of half-wavelength, has also been tested, but failed to oscillate even at 600 °C with helium as working fluid.

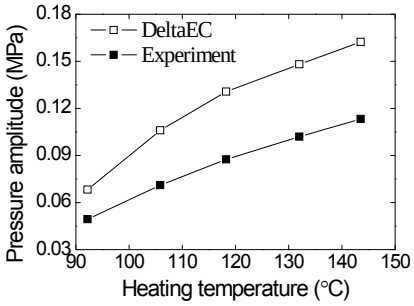

Figure 2: *Pressure amplitude versus heating temperature*

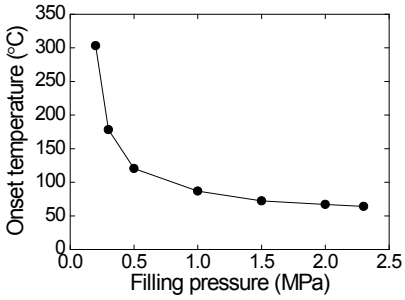

Figure 3: *Onset temperature versus filling pressure*

In summary, the results show that the looped 2-stage thermoacoustic prime mover with an asymmetric configuration can oscillate under a quite low heating temperature, showing the promising usability of low-grade heat source.

Acknowledgements

This work is supported by the National Natural Sciences Foundation of China (No. 51276154).

References

[1] de Blok K. Novel 4-stage Traveling Wave Thermoacoustic Power Generator, Proceedings of ASME 2010 3rd Joint US-European Fluids Engineering Summer Meeting and 8th International Conference on Nanochannels, Microchannels, and Minichannels , 2010, Montreal, Canada , 2-4 August,(2010).

[2] Ward B., Clark J., Swift G. Design Environment for Low-amplitude Thermoacoustic Energy Conversion (DeltaEC software), Version 6.2, Los Alamos National Laboratory (2008).

DETAILS AND EXPERIMENTAL RESULTS OF A STAND-ALONE CONTAINER COOLED BY A SOLAR DRIVEN MULTI-STAGE TRAVELING WAVE THERMOACOUSTIC SYSTEM

P. Owczarek[1*], C.M de Blok[2]

[1] *Future Energy Management, Weegschaalstraat 45, 7521CC Enschede, The Netherlands.*Corresponding author's e-mail: pawel.owczarek@futureenergymanagement.nl*
[2]*Aster Thermoacoustics,Smeestraat 11, 8194LG Veessen, The Netherlands..*

Keywords: *thermoacoustics, solar cooling,*

Abstract
Nowadays in many solar rich countries, up to 40% of the electric power is consumed for cooling and air conditioning only. From sustainable and energy point of view this is not a efficient situation, due to many energy conversion steps and energy loses.

A way out from this dead end road is to convert solar heat directly into cold. One technology to perform such action is thermoacoustic energy conversion. In particular a multi-stage travelling wave thermoacoustic system is capable for direct converting medium temperature solar heat into cold. The process includes only two conversion steps, 1) from heat into acoustic power and 2) acoustic power into cold. In addition such a system lacks any mechanical moving parts in the process, except for the optional circulation pumps.

Since the start of thermoacoustics in the eighties of last century onset and operating temperatures of thermoacoustic engines is drastically lowered enabling for the use of vacuum tube solar collectors (VTSC) as input heat source for SOlar ThermoAcoustic Cooling (SOTAC) systems .

In order to test the SOTAC concept we have build a stand-alone sea container size cooler driven by a multi-stage travelling wave thermoacoustic system. On the roof of the container 9 m^2 VTSC are installed which should be sufficient to generate about 1.5kW of cooling power at a temperature of 8°C with an outdoor temperature of 30°C. The container is divided inside in two spaces; one accommodating the thermoacoustic system and one for cold storage. The "technical room" is depicted in Figure 1.

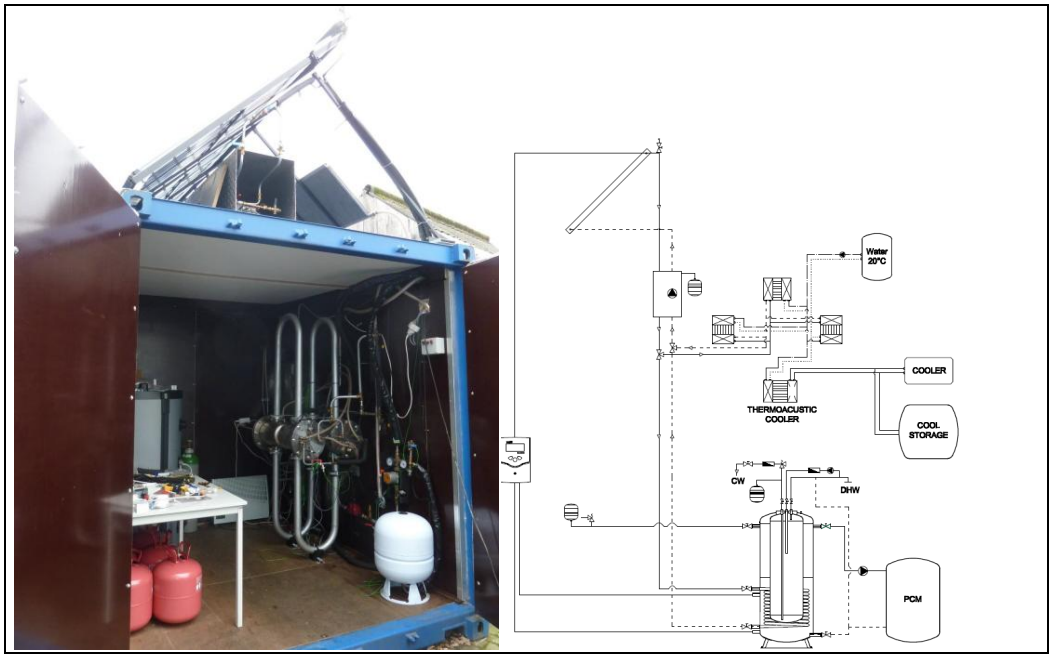

Figure 1: *Picture of the thermoacoustic cooling installation and scheme of the installation.*

While the thermoacoustic process is well understood and described, emphasis in this project is on the periphery. In particular the high temperature circuit connecting the VTSC's with the heat exchangers inside the thermoacoustic system turned out to be critical in design, because heat losses and heat transfer directly affect the overall system performance while safety aspects has to be considered as well.
Beside this also dimensioning and implementation of the heat rejection circuit to ambient and cold circuit to the cooling space affect the overall system performance.

The paper and presentation will address the theoretical and practical aspect of the design and build of a solar powered cooling system including periphery and support equipment together with the results from the test runs performed late summer.

THERMOACOUSTIC REFRIGERATION SYSTEMS: RECENT DEVELOPMENTS

B. Farouk[1] and D. S. Antao[2]

[1] *Department of Mechanical Engineering, Drexel University, Philadelphia., PA 19104 U.S.A.*
*. *Corresponding author's e-mail: bfarouk@coe.drexel.edu*
[2] *Department of Mechanical Engineering, Massachusetts Institute of Technology, Cambridge, MA*

Keywords: *Pulse tube, thermoacoustic refrigeration, inertance tube, regenerator phase angle,*

Introduction

In this paper, we first review our recent experimental and computational studies on the orifice-type [1] and inertance-type [2] pulse tube refrigerators along with related optimization studies. The experimental studies are done at various values of mean pressure of helium (~ 0.35 MPa to 2.2 MPa), different amplitudes of pressure oscillations, and frequency of operation and size of inertance length and orifice opening. Time-dependent axisymmetric CFD simulations of the inertance-type and orifice-type pulse tube refrigerators are reported where the transient as well as the cycle-averaged operation of the in-line pulse tube refrigerator is studied for the processes occurring in the system. Phase relation between mass flow and pressure waves are also reported for both systems. These relations play important roles in the performance of thermoacoustic devices. While passive forms of phase shifting is considered in [1, 2], we also present numerical results for a thermoacoustic refrigerator - where active mechanical phase shifting is achieved via a spring-mass system that replaces the inertance tube and the orifice opening - traditionally used in passive phase shifting systems. In an active phase shifting system (see figure below), greater control of phase shifting is achieved - which would produce lower temperatures at the cold spot.

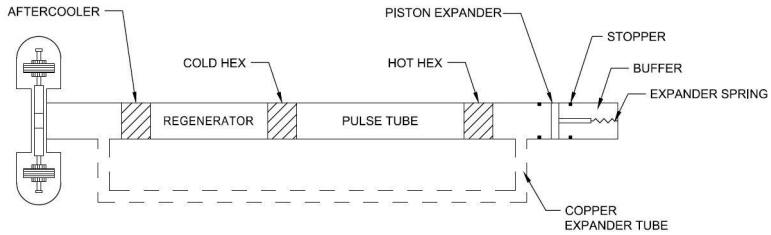

Figure 1: *Schematic of an active phase shifting pulse tube refrigerator* ***[3]***

Computational model

The compressible form of the Navier-Stokes equations is considered for the flow simulations of the pulse tube refrigerators. For the porous media regions (i.e. the regenerator and the heat exchangers), we employ the thermal non-equilibrium porous media model. In the non-equilibrium model, the gas and the solid temperatures are different in the porous media. The effect of heat transfer between the gas and the solid phases are considered in the energy equations of the gas and solid phase regions. The cycle-averaged (quasi-steady) and temporal experimental and computational results are also compared. The comparison between the experimental measurements and model predictions are found to improve when the effects of wall thicknesses of the various components of the pulse tube refrigerators are included in the

CFD model. The computational fluid dynamic model developed has been used to analyze the inertance-type, the orifice-type and the mechanical phase-shifting pulse tube refrigerators with high pressure helium as the working fluid.

Experimental system

An orifice-type pulse tube refrigerator was designed and built. The pressure wave generator used in the experiments was a Q-Drive twin-STAR linear motor. The linear motor has a swept volume of 15.55 cubic centimeters and a maximum operating pressure of 2.5 MPa. The heat exchangers were made from copper tubing (due to its high thermal conductivity) and the other components of the refrigerator were made of 316-type stainless steel tubing (stainless steel exhibits relatively low thermal conductivity and high strength in the temperature range of 350 - .100 K). The various components were connected by flange couplings. The flanges were welded on to the component tubing. Indium wire O-rings were found to provide the best seal for the system operating with high pressure helium and large temperature gradients. The orifice used in the system was a NOSHOK brass needle valve (101-MMB) capable of a maximum flow coefficient of 0.42. The aftercooler, cold and hot heat-exchanger tubing were filled with stacked copper woven square-mesh screen. The mesh screen in the heat exchangers acts as the primary heat-exchanger between the gas refrigerant and the tube walls. The regenerator tubing houses the regenerator material which is a high thermal capacity and low thermal conductivity permeable material. The regenerator is composed of stacked stainless steel woven square-mesh screen.

Results and discussion

Figure 2a shows a typical computed temporal evolution of the gas and solid temperature at the exit of the cold heat exchanger and inlet to the orifice-type pulse tube section. The banded profiles are cyclic variation of the gas temperature in the system. This cyclic nature of both the gas and solid temperature is highlighted in Figure 2b. The gas temperature decreases rapidly at the start; however the decrease in temperature is exponential over time. The solid temperature oscillates too, however the oscillations have much lower amplitude as compared to the gas temperature.

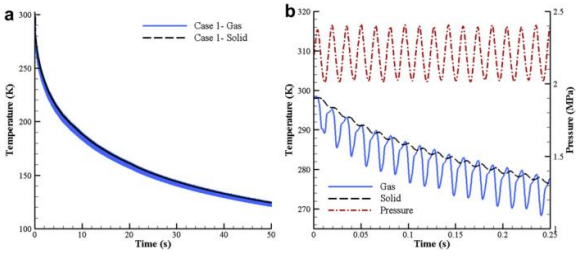

Figure 2. (a) Temporal variation of the gas and solid temperature at the exit of the cold heat-exchanger for the entire simulation, (b) Gas and solid temperature and pressure profiles at the exit of the cold heat-exchanger at the start of the simulations

Computational results for all three systems considered are presented in the paper while only experimental results are presented for the orifice-type pulse tube refrigerator

Acknowledgements

The authors would like to thank Dr. Ray Radebaugh for his continued interest in our work

References

[1] D.S. Antao, B. Farouk, Experimental and numerical investigations of an orifice type cryogenic pulse tube refrigerator, Applied Thermal Engineering 50 (2013) 112e123, 50 (2013) 112-123.

[2] D.S. Antao, B. Farouk, Numerical and experimental characterization of the inertance effect on pulse tube refrigerator performance, International Journal of Heat and Mass Transfer, 76 (2014) 33-44.

[3] R. Radebaugh, Cryocoolers: the state of the art and recent developments, Journal of Physics: Condensed Matter, 21(16) (2009) 164219 (164219 pp.).

OPTIMIZATION OF THE LOOP IN A TRAVELLING-WAVE THERMO-ACOUSTIC ENGINE

C.J.Lawn*

[1] *School of Engineering and Materials Science, Queen Mary University of London, Mile End Rd., E1 4NS, UK*
**Corresponding author's e-mail: c.j.lawn@qmul.ac.uk*

Keywords: *looped thermo-acoustic engines, regenerator boundary conditions, scattering matrix*

Introduction

A number of experimental realizations of thermo-acoustic engines that use an acoustic loop to feed energy back to a regenerator have been reported, mostly of the Thermo-Acoustic Stirling Heat Engine (TASHE) type. An alternative configuration is the simple wavelength loop with the linear alternator in a short side-branch, but with close to travelling-wave phasing on both sides of it. The advantage over the TASHE is that a great deal more power can be extracted for the same stroke-length of the alternator. However, a difficulty with this configuration lies in maintaining the optimum conditions in the regenerator, particularly when the temperature at the hot-end is changing. Attempts by the author to achieve consistent power generation with atmospheric air and a radiative heating system that would be cheaply realizable with a wood-burning stove have been frustrated, with very variable performance, and a thermal to electrical conversion efficiency of less than 1% [1].

This contribution focusses upon finding the optimum acoustic path in the loop feeding the regenerator, so as to give the most favourable conditions within it. Computations with a model of the regenerator have proved capable of reproducing the pressure distribution around the loop with reasonable accuracy [2]. However, attempts to use the model to determine the best loop configuration have been negated by the complex interaction of the parameters. An alternative, semi-empirical approach is described here.

Method for Loop Optimization

Bannwart et al. [3] characterised the regenerator separately from the rest of the loop through calculation of its transfer function from two experiments with different boundary conditions. They then computed the response when this regenerator was placed in a loop with variable length legs on either side of a variable length of branch pipe, and thus identified an optimum configuration, albeit without power extraction.

The approach here is similar, but the optimisation of the boundary conditions for the regenerator is carried out through a procedure recently outlined by Holzinger et al. [4]. They derived the gain in acoustic power from the scattering matrix (Σ) of a two-port element, which here includes the regenerator. The coefficients of Σ can be derived from the coefficients of the transfer matrix, as determined by the two-source method. Computing the eigenvalues of the product of Σ and its adjoint yields the maximum possible amplification factor and power gain relative to the total incident power, and the acoustic impedance required at the two boundaries to achieve this.

Because of the need for at least two-microphones on each side to assess the energy flows, the boundary planes were as shown in Figure 1. To implement the 'two-source' method, the loop was closed with a plate in two different places. Thus energy flowed in different directions through the regenerator and around the loop to an open termination, which was given extra real impedance by inserting a Rockwool plug. Measurements were made for the unheated case, and for three levels of heating, with three frequencies of excitation.

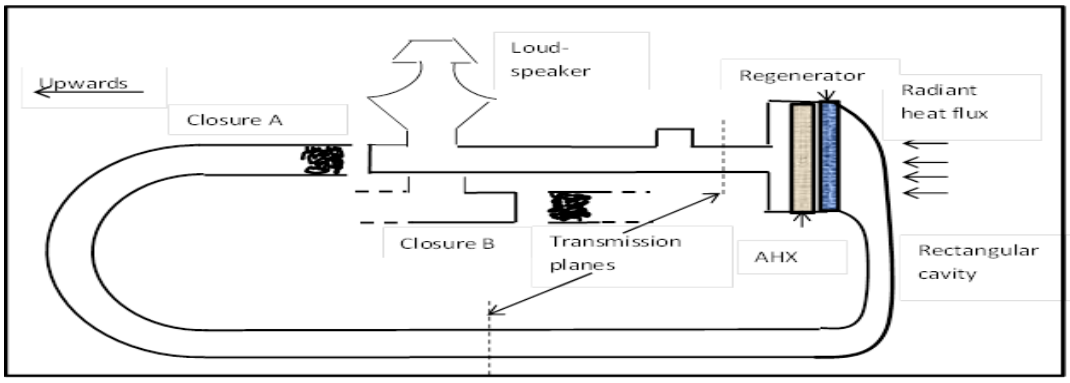

Figure 1: *The loop configuration, showing chosen transmission planes and the two pipe closures*

Results

The maximum and minimum acoustic power gains were thus computed:

Table 1: *Computed Results for the Potential Acoustic Gains of the Regenerator based on Transfer Function Measurements*

T_h	f=68Hz		f=74Hz		f=80Hz	
	Max	Min	Max	Min	Max	Min
295-297K	0.07	-0.25	0.10	-0.25	0.14	-0.33
690-780K	0.47	-0.35	0.37	-0.29	0.35	-0.28
860-920K	0.45	-0.32	0.23	-0.40	0.22	-0.38
1010-1060K	0.40	-0.36	0.38	-0.49	0.26	-0.40

It is seen that for the unheated cases, the deduced gains centre on negative values, because of dissipation, although errors in measurement suggest erroneously that some positive generation could take place. When the temperature of the hot end of the regenerator (T_h) was increased by radiation, maximum potential gains of about 0.4 were deduced, and these values are consistent with those computed in [4] from first principles for the present Womersley number of 0.4. However, the general trend to a reduced maximum gain with temperature is not in accord with theory, and the fall in gain with frequency is too rapid.

References

[1] Lawn, C.J., "Development of a thermoacoustic travelling wave engine", J. Power and Energy, 227(7) (2013) 783-802

[2] Lawn, C.J., "Computational modelling of a thermo-acoustic travelling wave engine", J. Power and Energy, 227(4) (2013) 498-514

[3] Bannwart, F.C., Penelet, G., Lotton, P. and Dalmont, J-P, "Measurement of the impedance matrix of a thermoacoustic core: Applications to the design of thermoacoustic engines", J.Acoust. Soc. Am., 133(5)(2013)

[4] Holzinger, T., Emmert, T., and Polifke, W, "Optimizing thermoacoustic regenerators for maximum amplification of acoustic power", J.Acoust. Soc. Am. 136(5)(2014) 2432-2440.

The VALTA project: Full scale conversion of CHP engine flue gas heat into electricity

Maurice-Xavier Francois[1], Kees de Blok[2], Paul Bouakhao[1], Manuel Niphon[1],Jean Pierre thermeau[1], Bruno Guestin[3], Luc Courtès[3], Denis Clodic[4]

[1]HEKYOM, 2 rue jean Rostand, 91400- ORSAY, France mxfrancois@hekyom.com
[2] ASTER, Smeestraat 11 NL8194LG VEESEEN, The Netherlands
[3] SDMO, 12bis rue de la Villeneuve, 29228 BREST, France,
[4] EReIE, 3 rue de la Croix Martre, 91120 PALAISEAU, France, 12bis rue de la Villeneuve

Exhaust gas from combustion engines in commercial CHP systems or generator sets contains a significant amount of high grade thermal energy. Prior to exhausting this flue gas to open air, part of its thermal energy can be harvested by a thermoacoustic energy converter (TAEC) converting this heat, normally wasted or used for low grade heating, into electricity or cold (tri-generation).

The VALTA project originated in France and lead by HEKYOM aimed to design and build such a downstream energy converter to be applied to a commercial genset, converting 70kW heat flue gas heat into 15 kW electricity. The equipment is supposed to convert exhaust gas enthalpy in the temperature range of 350°C to 200°C into acoustic energy and from there into electricity. The VALTA project was partially funded by ADEME, www.ademe.fr, in a specific program for ”efficiency improving in industrial processes.

The VALTA project associates four Companies, HEKYOM and ASTER for thermoacoustics design and manufacture, SDMO for genset equipment implementation and EReIE for some contribution in heat transfer mechanisms by means of heat pipes
The concept of the VALTA heat recovery system comprises a few innovative embodiments.

One of them is the thermoacoustic geometry proposed by HEKYOM with 3 amplifiers positioned at small mutual distance and acoustically connected in series while thermally connected in parallel. Heat from the flue gas heat exchanger is transferred to the engine heat exchangers by dedicated looped heat pipe circuits. As compared with normal flow through heat exchangers this two-phase heat transfer mechanism significantly reduces temperature drop between the heat source and thermoacoustic process. It is known from Ceperley that thermoacoustic amplification process can be very efficient if the characteristics of regenerator and its local acoustic field are correctly chosen. According to the fact that, on one hand, amplifier acoustic gain, defined as the ration of acoustic power output (Wout) over input value (Win) which can be closed to the ratio of output over input temperature Tout/ Tin, as it may be written as:

Wout/ Win = α Tout/ Tin, where $0,8 < \alpha < 0,95$ and, Wout = Win [α Tout/ Tin]

Moreover, Wout – Win represents the amount of heat converted into acoustic power by the heat engine (amplification) process. It thus may be written:

Wout – Win = η [1- Tin/Tout] *Qwaste with η ≅ 70% as obtained by HEKYOM in a previous one stage engine. Here Qwaste correspond to the part of exhaust gas enthalpy that can be brought to the hot heat exchanger amplifier.
It is seen that the behaviour of each amplifier is has a strong mutual dependency. Moreover, energetic and exegetic efficiencies of each amplifier impact its required amount of heat.
Another innovative embodiment concerns the conversion of acoustic energy into electricity
Initially linear alternators were aimed to convert electricity in acoustic power and vice versa. Then an electric feedback associated with a specific starter device would be necessary in order to make the system autonomous (fig.1).

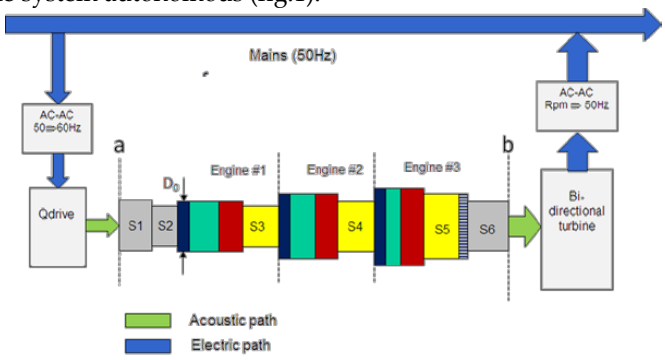

However the increasing moving mass and cost of these alternators at multi kW power level will hamper widespread application.

For VALTA system, it was thus decided, first to replace the electroacoustic wave generator by an acoustic feedback issue from the output acoustic wave, and second to replace the linear alternator providing conversion of acoustic energy to electric energy by a novel linear to rotation conversion of acoustic energy associated to a conventional rotating generator. (fig.2)

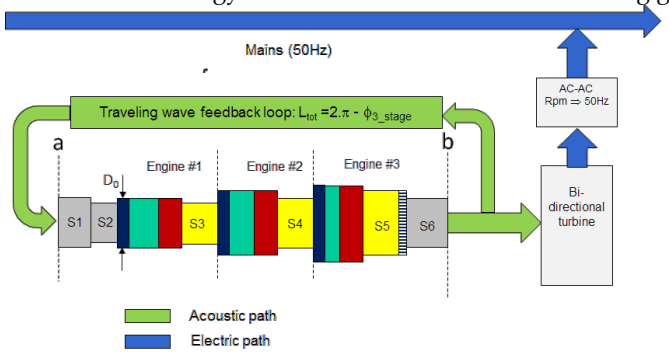

Such linear to rotation conversion of acoustic to mechanical energy system initially proposed by Aster was chosen and developed by Aster in cooperation with HEHYOM. The expected global efficiency will be of the order of 25%.

The presentation will give an overview of the design choices and modifications analysed during the project and of the final design. As an example, electric or acoustic feedback has been considered and the reasons for choosing or discarding them will be mentioned.

The total VALTA budget is about 750k€. The project should be completed by the end of this year. First tests are expected in 2015 December at SDMO factory.

THE ANALYSIS OF HYBRID SOLAR POWERED COOLING/HEATING SYSTEM WITH THE TRAVELLING-WAVE THERMOACOUSTIC REFRIGERATOR

A. Ruziewicz[1*], C.M. de Blok[2] and P. Owczarek[3]

[1] *Faculty of Mechanical and Power Engineering, Wroclaw University of Technology, Poland. *Corresponding author's e-mail: adam.ruziewicz@pwr.edu.pl*
[2] *Aster Thermoacoustics,Smeestraat 11, 8194LG Veessen, The Netherlands.*
[3] *Future Energy Management, Weegschaalstraat 45, 7521CC Enschede.*

Keywords: *thermoacoustic cooling, heating and cooling systems, solar radiation, solar collectors.*

Introduction

One of common applications of thermoacoustic (TA) technology is cold production in a TA device powered by any heat source. This concept, based on combination of TA-engine and TA-heat pump operating on different temperature ranges, allows conversion of heat directly into cold, using an acoustic wave as an energy carrier in between. Unlike electricity generation, heat powered thermoacoustic cooler needs no moving parts by the acoustic side. The solar and waste heat recovery in range of 70-200°C, so far, seems to be the most competitive to conventional systems (possible) TA application [1]. Reaching the satisfying efficiency by such low temperature is possible due to the idea of multistage devices. Connecting more regenerators in series enables decrease of the onset temperature, while the exergetic efficiency of 40% is still possible to achieve [2].

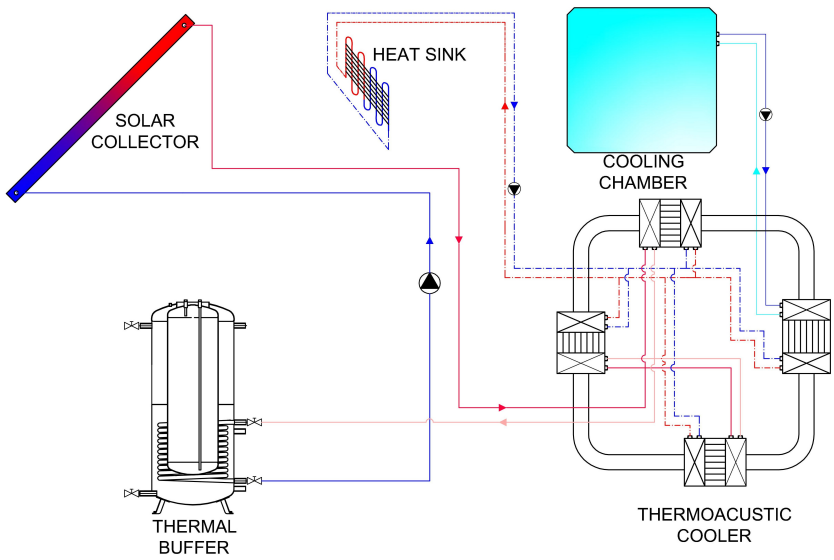

Figure 1: *The scheme of the hybrid system.*

The aim of this work is to analyse the performance of the hybrid cooling and heating system driven by solar energy. The concept is to use vacuum tube solar collectors to drive the multi-stage thermoacoustic cooler, which takes up heat from the cooling room. Since the temperature drop on the heat exchangers of TA cooler is relatively small, the rest of the heat can be used for heating up domestic hot water (DHW). A typical sea container with tube collectors on the roof constitutes the experimental prototype. One part of the container is the cooling room, while the TA device and the DHW tank are located in the second. The simple scheme of the system is shown in the Figure 1.

Combining heating and cooling system driven by the solar power allows better matching between the demand for heat/cold and the provided energy. In the most sunny months, solar excess energy covers higher demand for cooling. In colder months the energy achieved should be enough for DHW purpose. The analysis will consider power of solar radiation and the demand for cooling power throughout the whole year. The calculated energy balance will be compared then for different months and seasons. The results for few different places (longitudes) will be provided as well, thus the viability of such hybrid system in dependence on geographical location can be evaluated.

References

[1] de Blok C.M. "Low operating temperature integral thermoacoustic devices for solar cooling and waste heat recovery". Paris, Acoustics, (2008).

[2] de Blok C.M. "Multi-stage travelling wave thermoaocustics in practise". International Congress on Sound and Vibration, Acoustics, (2012).

DUAL THERMOACOUSTIC CORE COMPACT HEAT-PUMP FOR AUTOMOTIVE APPLICATION

R. Bessis[1*], G. Poignand[2], H. Bailliet[1], H. Lazure[3], J-C. Valière[1], and E. Boudard[3]

[1] *Institut PPRIME, UPR CNRS 3346, Université de Poitiers, ISAE-ENSMA, 6 rue Marcel Doré, 86073 Poitiers, France.*
**Corresponding author's e-mail: remi.bessis@univ-poitiers.fr*
[2] *Laboratoire d'Acoustique de l'Université du Maine (LAUM), UMR CNRS 6613, Université du Maine, Avenue Olivier Messiaen, 72085 Le Mans, France.*
[3] *PSA Peugeot Citroën, Openlab Fluidics@Poitiers, 6 rue Marcel Doré, 86073 Poitiers, France.*

Keywords: *thermoacoustics – heat-pump – automobile – DeltaEC*

In order to reduce environmental impact, the automotive industry investigates alternative "green" technologies. In this context, the use of chemical refrigerants (such as CFCs and HFCs) for vapor-compression refrigeration in air conditioning systems, which are known as potent global-warming gases, has been identified as one of the sources of pollution in a vehicle. Moreover, cooling systems draw significant power from the engine and reduces the overall efficiency of the vehicle. Thermoacoustic cooling devices, which use an inert gas as working fluid, could be a good alternative, especially with the rapid development of hybrid and electric vehicles, although very few thermoacoustic solutions have been adapted to automotive applications because of weight and space restrictions. This paper outlines the design and performance predictions for a compact coaxial thermoacoustic heat-pump with two coupled acoustic sources.

The concept of such device has been developed by Poignand & al. [1]. In this system (Figure 1-a), one end of the thermoacoustic core, comprising the stack - or regenerator - and the heat exchangers, is set on an acoustic source, which creates the displacement field needed in the thermoacoustic process. The second acoustic source is set on the opening of the cavity and creates a quasi-uniform pressure field inside the cavity. The sources are working at the same frequency and their amplitudes and phases can be independently tuned for optimizing the performances of the device, i.e. acoustic pressure and the particle velocity are no longer linked by standing wave or travelling wave conditions. As a direct consequence, the working frequency can be such that the wavelength is much greater than the dimensions of the resonator, so that the compactness of the device is significantly improved.

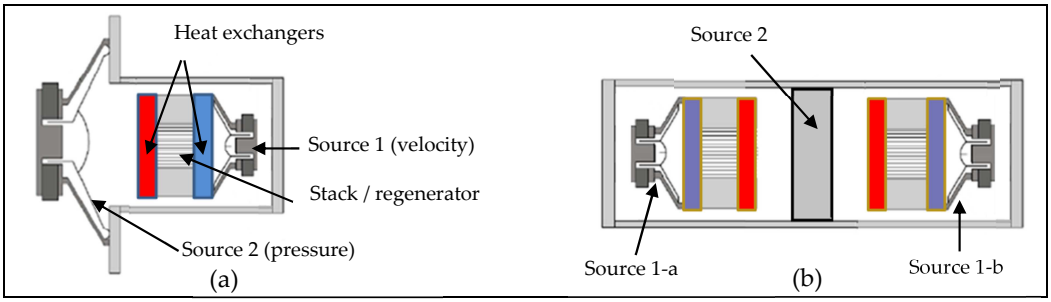

Figure 1: (a) *the compact thermoacoustic device developed by Poignand & al. [1];* **(b)** *the compact thermoacoustic device with two thermoacoustic cores.*

The device described in [1,2] was designed for low power applications, moving about 1 W of heat, the acoustic field being generated by two "commercial" electrodynamic loudspeakers and the device using air at atmospheric pressure. In order to match automotive performances in air refrigeration, it was necessary to increase the amount of heat extracted by the device and its efficiency to reduce the indirect energy-related contributions. For this purpose, we have designed the dual thermoacoustic core compact heat-pump whose sketch is presented in Figure 1-b. In this device, filled with gas Argon under P=40 bars, two thermoacoustic cavities are placed on both sides of the Source "2", which allows doubling the heat pumping of the refrigerator. This configuration permits to use the acoustic energy dissipated at the back of the pressure source to power the additional thermoacoustic cavity.

The device has been designed using DeltaEC [3] in order to fit performances of an air refrigeration system for standard automobile. For this application, it should move 5 kW of heat from the cold heat exchanger at 5°C and rejects heat to the ambient heat exchanger at 55°C. Low-power electrodynamic loudspeakers create the velocity fields in the thermoacoustic cores. The design of heat exchangers is based on elements used in the automotive industry, adapted so that the thickness is about the order of the particle displacement into the regenerator, which consists of metallic meshes stacked together. Numerical simulations permitted to set the characteristics of the thermoacoustic cores as well as the working frequency that satisfies the performances goal. The dimensions of the cavities were optimized, and we ended up with a machine of about the size of a cylinder measuring 33 cm in diameter and 32 cm in height (not including the pressure source), working at f=40 Hz. In the present model, the main acoustic source is not included but simulations allow getting the characteristics for this key element. We plan to design an adapted source based on technologies used in automotive industry. Good candidates for such a high power pressure source are indeed linear motors, as they can create high acoustic pressure fields with an efficiency that usually exceeds 80%, which should permit to achieve the maximum power consumption of about 2.3 kW necessary for this device. With such a source the theoretical overall coefficient-of-performance for the designed device should be equal to 2.2, which is competitive with most efficient thermoacoustic cooling machines to date, as well as with today's automotive air conditioning systems.

Acknowledgements
This project has been made in the context of the OpenLab Fluidics@Poitiers between PSA Peugeot Citroën and the PPRIME institute (Poitiers, France), in collaboration with the LAUM (Le Mans, France).

References

[1] Poignand, G., Lotton, P., Penelet, G., and Bruneau, M. "Thermoacoustic, Small Cavity Excitation to Achive Optimal Performance", Acta Acustica united with Acustica, **97**, (2011), 926-932.
[2] Poignand, G., Podkovskiy, A., Penelet, G., Lotton, P., and Bruneau, M. "Analysis of a coaxial, compact thermoacoustic heat-pump", Acta Acustica united with Acustica, **99**, (2013), 898-904.
[3] Ward, W., and Swift, G.W. "Design environment for low amplitude thermoacoustic engine", J. Acoust. Soc. Am., **95**, (1994), 3671-3672.

Bench scale electrically driven thermoacoustic heat pump

M.E.H. Tijani, J.A. Lycklama à Nijeholt

Energy research Centre of the Netherlands (ECN), P.O. Box 1, 1755 ZG, Petten, The Netherland
**Corresponding author's e-mail: tijani@ecn.nl*

Keywords: *Thermoacoustics, Heat pump, Stirling, Energy.*

Introduction

The application of heat pumps in the industry can lead to large energy savings and reduce global warming emissions. Heat pumps can be used to upgrade waste heat. This enables to reuse the huge quantities of energy that would otherwise be rejected to the environment. One of the industrial applications where the application of a heat pump can be beneficial is the distillation process [1-2]. Distillation is one of the largest energy consumers processes in refining and bulk chemical industries. It is estimated that distillation columns consume about 40% of the total energy used to operate plants in these sectors [3-4]. The distillation process is a very inefficient process as heat at high temperature is supplied to boil a mixture of liquids and most of this heat is released at a lower temperature level during condensation. In a conventional distillation column energy is supplied to the system via the reboiler to evaporate the feed for the separation process. The vapors from the top of the column are liquefied in the (water) cooled condenser. About 95 % of the energy needed for the reboiler leaves the system as waste heat. In a heat pump assisted distillation column, the condenser is linked to the reboiler via the heat pump where the temperature of the vapor from the top of the column is increased and fed to the reboiler where it is condensed. For the Netherlands, the total energy saving potential is estimated to 10-20 PJ/year. The extrapolation to Europe and the world, based on production capacities, leads to more than 100-200 PJ/year for Europe and 300-600 PJ/year for the world.

However, widespread use of large scale heat pumps is not yet common due to the low operation temperatures and limited temperature lifts of conventional heat pumps. Innovative heat pump technologies are needed which can help to overcome these difficulties. One promising innovative heat pump technology is the thermoacoustic heat pump which uses acoustic power to increase the temperature of a waste-heat stream to a higher, useful temperature. Thermoacoustic heat pumps can be electrically or thermally driven and can operate over a large scale of (high) temperatures and can achieve large temperature lifts. This paper presents the design, construction, and test of a bench-scale electrically driven thermoacoustic heat pump (EDTAH) which operates between 60 and 100 °C. The heat pump is designed to deliver 10 kW of thermal power at 100 °C.

Design and construction of the heat pump

A schematic illustration of EDTAH is given in Figure 1. The heat pump is designed to operate with helium gas at an average pressure of 50 bar and an operation frequency of 80 Hz. The linear motor delivers the acoustic power needed by the heat pump. A thermal bench using thermal oil simulates the low temperature heat source (50-80°C) and the high temperature heat sink (100-200°C). A high temperature heat exchanger (HHX) and a low

temperature heat exchanger (LHX) are used to connect the heat pump to the heat sink and heat source respectively. The Heat pump is designed and optimized using DeltaEC code.

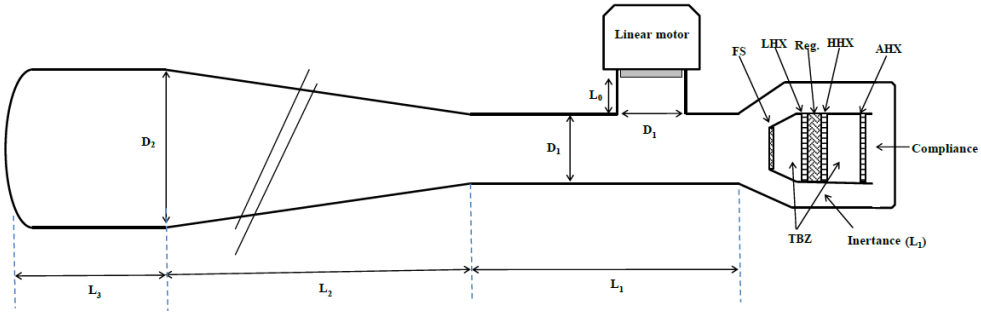

Figure 1: ***Schematic illustration of the heat pump.***

Experimental results

The first test of the bench scale EDTAH shows that the heat pump delivers about 3 kW of thermal power at 109 °C with a COP of 3.02 corresponding to 42 % of the Carnot performance.

References

[1] Spoelstra, S. and Tijani, M.E.H. 2005, "Thermoacoustic heat pumps for energy savings"" Presented at the seminar "Boundary crossing acoustics" of the Acoustical Society of the Netherlands http://intranet.energy.intra/publicaties/

[2] Kiss, A, Landaeta, S., Ferreira, C (2012), "Mastering Heat pump Selection for Energy Efficient Distillation", Chem. Eng. Trans. **29**, (2012), 397-402.

[3] Humprey, J., " Separation processes: playing a critical role", Chemical Engineering Progress **91** (1995). 31-41.

[4] Mix, T.J. , Dueck, J.S., Weinberg, M. 1978, "Energy conservation in distillation", Chemical Engineering Progress **74** (1978), 49-55.

Simulation and Experimental Validation of a Looped Thermoacoustic Generator with Stub

A. Kruse*, T. Schmiel, M. Tajmar

Chair of Space Systems, Institute for Aerospace Engineering, TU Dresden, 01062 Dresden
**Corresponding author's e-mail: alexander.kruse@tu-dresden.de*

Keywords: Looped tube, Matching stub, Acoustic RC load, DeltaEC

Introduction and Concept

Thermoacoustic travelling-wave engines combine a simple design with high efficiency and relatively low operating temperatures which makes them a promising alternative to conventional heat engines. Starting from the one-wavelength loop design proposed by Ceperley in 1979 [1] and set up from Yazaki in 1998 [2], a breakthrough in power and efficiency has been made with the TASHE from Backhaus and Swift in 1999 [3]. They introduced a more complex acoustic network, including a quarter-wavelength resonator, inertance tube, and compliance. This layout sets optimal travelling-wave phasing and impedance in the regenerator, resulting in great thermal to acoustic conversion efficiency. However, a rather large amount of acoustic power is lost in the resonator.
Another option to influence phasing and impedance in the regenerator is by means of an acoustic matching stub and an increase of the cross-sectional area of the regenerator section [4], [5]. At TU Dresden, numerical simulations have shown that position and length of the stub are essential parameters for achieving high performance. They are also greatly influenced by the position of the acoustic load. Therefore, an experimental apparatus is designed to validate the simulation data.

Modelling and Simulation

The researched engine is a one-wavelength loop type with matching stub (see Figure 1). It has a loop length of 4 m and is operated with argon at a pressure of 20 bar, resulting in a resonance frequency of 77 Hz. The regenerator section has a nominal diameter of DN150 that is connected to the DN80 feedback tube via reducing cones.

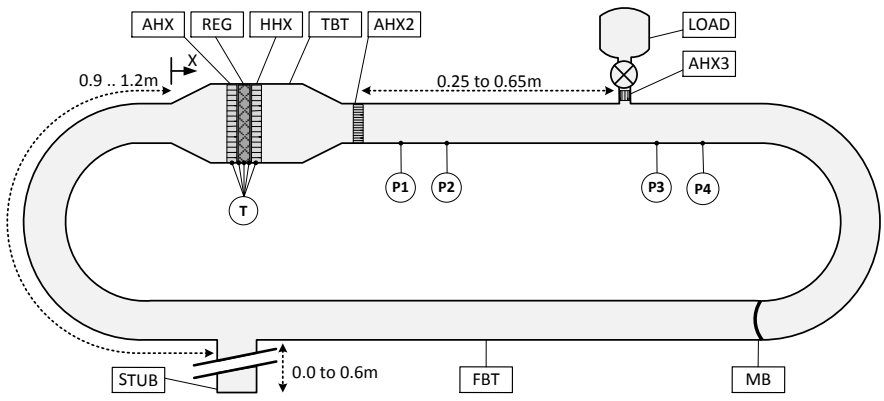

Figure 1: *Schematic view of the test rig (AHX..ambient heat exchanger, REG..regenerator, HHX..hot heat exchanger, TBT..thermal buffer tube, AHX2..secondary ambient heat exchanger, LOAD..acoustic RC load, AHX3..tertiary ambient heat exchanger, STUB..acoustic matching stub, FBT..feedback tube, MB..membrane)*

Acoustic power is removed from the system by use of an adjustable acoustic RC load. The geometrical parameters "load position", "stub position", and "stub length" are variable in the range shown in Figure 1.
Numerical simulation and design is done with DeltaEC [6]. The computer code integrates the one dimensional wave equation in dependence of chosen gas and geometry. Figure 2 presents preliminary simulation results. The left side shows the distribution of pressure amplitude and volumetric velocity along the generator when heat input in the hot heat exchanger is 2000W. The positions of regenerator, acoustic load and stub are indicated by sharp amplitude changes. The right side of Figure 2 illustrates the impact of load position on the temperature difference across the regenerator and load power consumption. Cold side temperature was kept steady at 350K.

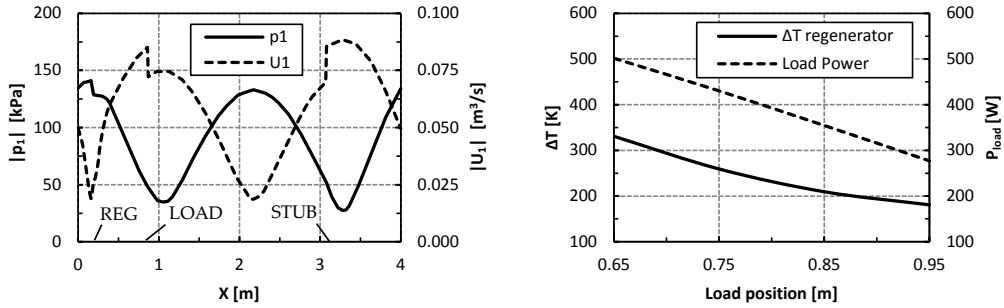

Figure 2: *Pressure amplitude and volumetric velocity along the generator (left), temperature difference between hot and cold side of the regenerator and consumed load power dependent on load position (right)*

Experimental apparatus

The test rig is planned to be made of stainless steel tubing. Stainless steel screens will be used for the regenerator. Heat exchangers will be made of copper blocks drilled with holes. Ambient heat exchangers are water cooled and the hot heat exchanger will be electrically heated. The acoustic load consists of a control valve and a cavity. A flexible membrane will prevent Gedeon streaming. Thermocouples will measure the temperature distribution inside heat exchangers and regenerator. Moreover, four pressure sensors will be used to determine acoustic power gain, consumed power, and feedback power. The gained data will enable a detailed analysis on the acoustical impact of the geometrical parameters.

Acknowledgements

This project is financially supported by the Friedrich-und Elisabeth-Boysen Stiftung.

References

[1] P. H. Ceperley, "A pistonless Stirling engine -The traveling wave heat engine," *J. Acoust. Soc. Am.*, vol. 66, no. 5, pp. 1508–1513, 1979.

[2] T. Yazaki, A. Iwata, T. Maekawa, and A. Tominaga, "Traveling Wave Thermoacoustic Engine in a Looped Tube," *Phys. Rev. Lett.*, vol. 81, no. 15, pp. 3128–3131, 1998.

[3] S. Backhaus and G. W. Swift, "A thermoacoustic Stirling heat engine," *Nature*, vol. 399, pp. 335–338, 1999.

[4] Z. Yu, A. J. Jaworski, and S. Backhaus, "Travelling-wave thermoacoustic electricity generator using an ultra-compliant alternator for utilization of low-grade thermal energy," *Appl. Energy*, vol. 99, pp. 135–145, 2012.

[5] H. Kang, P. Cheng, Z. Yu, and H. Zheng, "A two-stage traveling-wave thermoacoustic electric generator with loudspeakers as alternators," *Appl. Energy*, vol. 137, pp. 9–17, 2015.

[6] B. Ward, J. Clark, and G. Swift, *Design Environment for Low-amplitude Thermoacoustic Energy Conversion. DeltaEC. Users Guide*. Los Almos National Laboratory, 2012.

THE AMOUNT OF WATER REQUIRED TO DECREASE THE CRITICAL TENPERATURE DIFFERENCE OF A STANDING WAVE THERMOACOUSTIC ENGINE

K. Tsuda[1*] and Y.Ueda[1]

[1] *Graduate School of Bio-Application and System Enginnering, Tokyo University of Agriculture and Technology, 2-24-16 Nakacho, Koganei-shi, Tokyo, Japan.*
**Corresponding author's e-mail: 50014701202@st.tuat.ac.jp*

Keywords: *Thermoacoustic engine, standing wave, the low critical temperature, water, vapor, two-phase fluid.*

Abstract

It is well known that the critical temperature difference needed for causing a thermoacoustic oscillation is decreased by the presence of water. R. Reilgh described in his book "Theory of sound"[1] that "the production of sound is facilitated by the vapor in the notice of glass-blowers" and the Kibitsunokama, which is used in Japanese ritual, can generate sound wave by using a rice-grain regenerator and water vapor[2,3]. Furthermore, D.Noda and Y.Ueda demonstrated that water vapor reduces the critical temperature difference from 290 to 56 degree C[4]. However, it has not been found how much water is necessary for the decrease of the critical temperature difference. In this study, we measured the critical temperature difference of a standing wave thermoacoustic engine as a function of the water mass added into the working gas. We increased the water mass from 0 g in increment of 0.05 g. As a result, the critical temperature difference was not changed in the range from 0 g to 0.15 g. On the other hand, when the water mass was 0.20 g, the critical temperature difference was decreased from 144 to 54 degree C. Therefore, it is found that the marginal value of the amount of water required to decrease the critical temperature difference exists. Moreover, we measured the marginal mass of water with changing material of a regenerator.

References

[1] Rayleigh, J.W.S. "Theory of Sound", Dover Publications, Second, (1945), 230-231.
[2] Ueda, A. "*Ugetsu monogatari*", (1776), Kyoto, Japan.
[3] Ueda, Y. "Kibitsunokama -instrument used in historical Japanese shrine ritual-", The 2nd International Workshop on Thermoacoustics, **SD-1**, (2014), Sendai, Japan.
[4] Noda, D and Ueda, A. "A thermoacoustic oscillator powered by vaporized water and ethanol", Am. J. Phys., **81**(2), (2013), 124-126.

THERMOACOUSTIC STIRLING ENGINE WITH LIQUID PISTON

H. Hyodo[1*], R.Uchiya[1], and T. Biwa[1]

[1] *Mechanical Systems and Design, Tohoku University, 6-6-04 Aramaki, Aoba-ku, 980-8579 Sendai, Japan.*
**Corresponding author's e-mail: hyodo@amsd.mech.tohoku.ac.jp*

Keywords: *modeling of thermoacoustic engine, liquid column piston.*

Introduction

The thermoacoustic engine with liquid piston was proposed by West [1] and confirmed its operation by Martini [2] and Li [3]. However, the effects of parameters such as number of liquid column and length of it on the operation of the devices are not discussed. In this study, by modelling the looped thermoacoustic engines with gas-liquid column, we clarify the basic mechanism of the engine.

Analytical model

The thermoacoustic engine with gas-liquid column is modeled by the spring-mass system to examine the characteristic oscillation mode. The liquid column, gas column and effect of gravity force in thermoacoustic engines are replaced with mass point (mass: m), spring (spring constant: k_a) and elastic rod (spring constant: k_g), respectively as shown in figure 1.

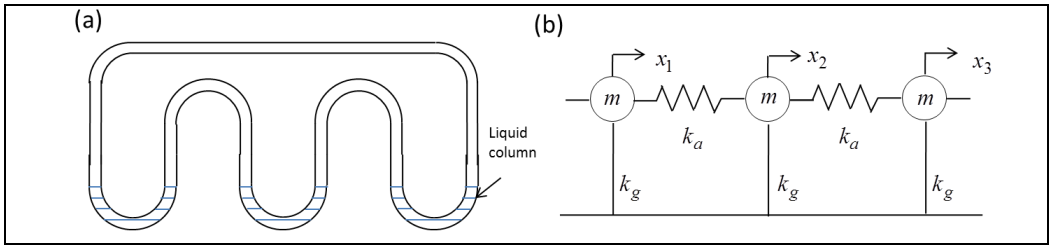

Figure 1: *(a) Liquid piston engine (b) Spring-mass system model.*

The constant k_a and k_g are assumed to be $k_a=AP_m\gamma/l_{gas}$, $k_g=2A\rho_w g$, where A is the cross sectional area of the tube, P_m is the mean pressure of the gas, γ is the ratio of specific heat, l_{gas} is the length of the gas column, ρ_w is the density of the gas and g is the gravity acceleration. When the number of liquid column is n, the equations of motion of this system is expressed by

$$m\ddot{x}_j = -k_g x_j - k_a(x_j - x_{j+1}) - k_a(x_j - x_{j-1}) \tag{1}$$

where x_j (j=1,…n) is the displacement of mass. We focus on the solution that the phase of the complex amplitude of x_j is given by $2\pi j$/n, whereas the magnitude satisfies x_j=const. In this case, frequency equation is written as

$$\omega^2 = \frac{k_g + 2k_a\left(1-\cos\frac{2\pi}{n}\right)}{m}. \tag{2}$$

The pressure p_j and velocity u_j of the gas in the middle of tube between the water column are given by $p_j=k_a(v_{j-1}-v_j)/i\omega A$ and $u_j=(v_{j-1}+v_j)/2$, where v_j is the velocity of mass given by $v_j=\mathrm{d}x_j/\mathrm{d}t$.

Calculating the acoustic impedance from pressure and velocity of gas, we obtain the impedance z_j

$$Z_j = \frac{2k_a}{\omega A}\tan\frac{\pi}{n}. \tag{3}$$

In equation (3), the acoustic impedance is real, which means the pressure and velocity oscillate in phase. Then if regenerator is put at this point, Stirling cycle should be realized regardless to the number of liquid columns.

Calculation by thermoacoustic theory

We calculate further details in more realistic model including regenerator and temperature gradient by using transmittance matrices based on Rott's theory. We consider a looped tube engine in which the regenerators are inserted into the center of the gas column tubes. The apparatus consists of the same shaped three sections as shown in fig2 (a). Setting the parameters as fig 2(a) and imposing periodic boundary condition, marginal conditions of this engine was derived shown in fig 2(b). Fig 2(b) shows the relation of pore radius of regenerator and angular frequency and temperature ratio of hot and cold heat exchangers. The data of dots were results calculated by thermoacoustic theory and dotted line in the graph of frequency was calculated by the equation of spring-mass model. The oscillation frequencies calculated by thermoacoustic theory were around 43, these results agree well with that of spring-mass model. We experimentally confirmed the operation of the apparatus at predicted frequency. This means that the system operates in the characteristic oscillation mode we focused on in the mass-spring model.

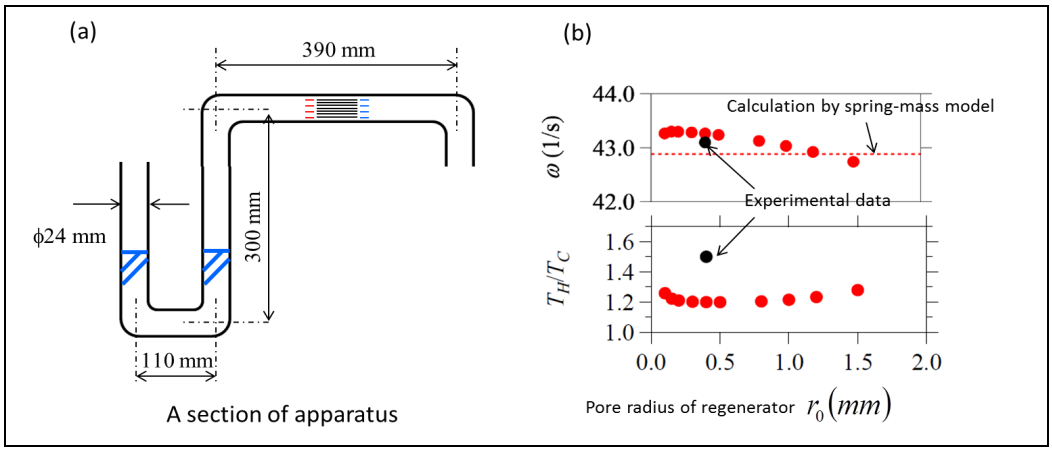

Figure 2: *(a) Parameters of the apparatus (b) Oscillation marginal conditions.*

Summary

We modeled the thermoacoustic engines with liquid piston by the spring-mass system. The characteristic oscillation mode of the system became obvious and Stirling cycle should be realized.

References

[1] West, C.D. "Liquid piston stirling engines", Van Nostrand Reinhold, (1983)

[2] Martini, W. R. "Test on a 4u tube heat operated heat pump" Proc., Intersoc. Energy Convers. Eng. Conf., **2**, (1983), 872–874.

[3] Li, D., Luo, E., Chen, Y., Zhang, L., and Huang, Y. "A looped three-stage traveling-wave thermoacoustic engine with liquid piston", 19th International Congress on Sound and Vibration, (2012)

DYNAMICS OF FORCED SYNCHRONIZATION IN THERMOACOUSTIC SYSTEM

H. Hyodo[1*], Y.Tanizaki[2], and T. Biwa[3]

[1] *Mechanical Systems and Design, Tohoku University, 6-6-04 Aramaki, Aoba-ku, 980-8579 Sendai, Japan.*
**Corresponding author's e-mail: hyodo@amsd.mech.tohoku.ac.jp*

Keywords: *thermoacoustic self-excited oscillation system, forced synchronization.*

Introduction

When an oscillator with a natural frequency f_0 is put under the influence of a periodic force with frequency $f \sim f_0$, a variety of phenomena can be observed. When the influence is unidirectional, 1:1 forced synchronization takes place in a triangular region called Arnold tongue on a plane of detuning $\Delta f = f - f_0$ vs. forcing strength. In the lower part of the synchronization region with relatively weak forcing, the oscillator goes from phase drift to phase locking regions through a saddle-node bifurcation. In the upper part with a strong forcing, it enters suppression region through torus-death bifurcation, where the amplitude of natural oscillations are damped by external force. The boundary between phase drift and suppression or phase locking region has been observed [1], [2]. However, boundary of saddle-node and torus-death bifurcation in synchronous state has not been observed experimentally. In this study, we experimentally observe the dynamics of oscillator in synchronous state in forced synchronization in thermoacoustic system.

Experimental setup

Experiments are performed on thermoacoustic oscillator shown in figure 1. The oscillator with a straight resonant tube is filled with atmospheric air at room temperature. The regenerator is sandwiched by hot and cold heat exchangers. External force is supplied by the acoustic driver composed of the speaker and the bellows. The oscillations of the external forced oscillator system are examined by measuring the acoustic pressure with a pressure transducer mounted on the closed end of resonant tube.

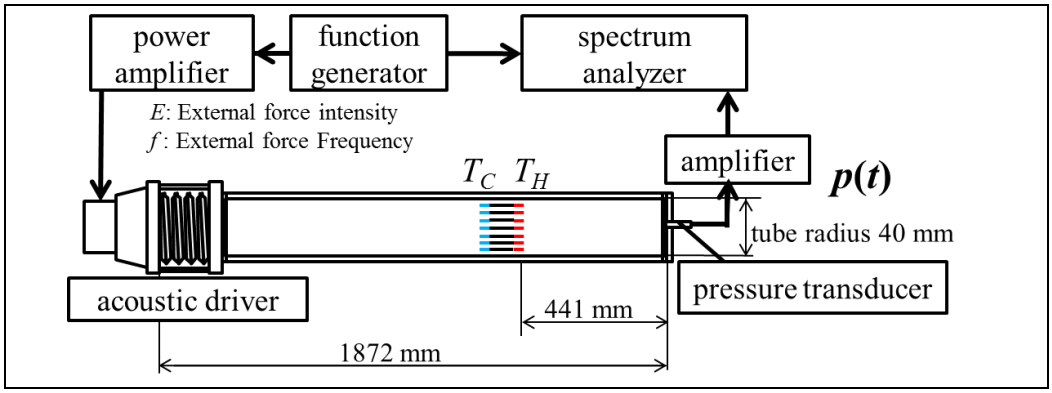

Figure 1: *The experimental setup*

The time-series data of the pressure is projected onto the real part on a complex plane and imaginary part of the signal was obtained by Hilbert transformation. And the complex plane itself is rotated with frequency of external force. When the system is in an asynchronous state, the trajectory of pressure on the complex plane rotates with angular velocity resulting from the frequency difference between external force and oscillator. When the system is synchronized, the trajectory comes to rest. To observe the dynamics of oscillator in synchronous state, we added perturbation to break the synchronous state once and observed trajectory to be synchronous again.

Results

The Arnold tongue and dynamics in synchronous state are shown in figure 2. In the synchronous process with a weak forcing (D−>A), rotation of trajectory became slow and stopped (saddle-node bifurcation). In the synchronous process with a strong forcing (D−>B), trajectory radius became small and stopped (torus-death bifurcation).The trajectory rotated without including the origin in region C (phase modulation). The dynamics of oscillation in synchronous region was different between week forcing and strong forcing region. In the case of weak forcing, trajectory moves along a circular orbit which is traces of natural oscillation (phase locking). However, trajectory does not move along in the case of strong forcing (suppression).

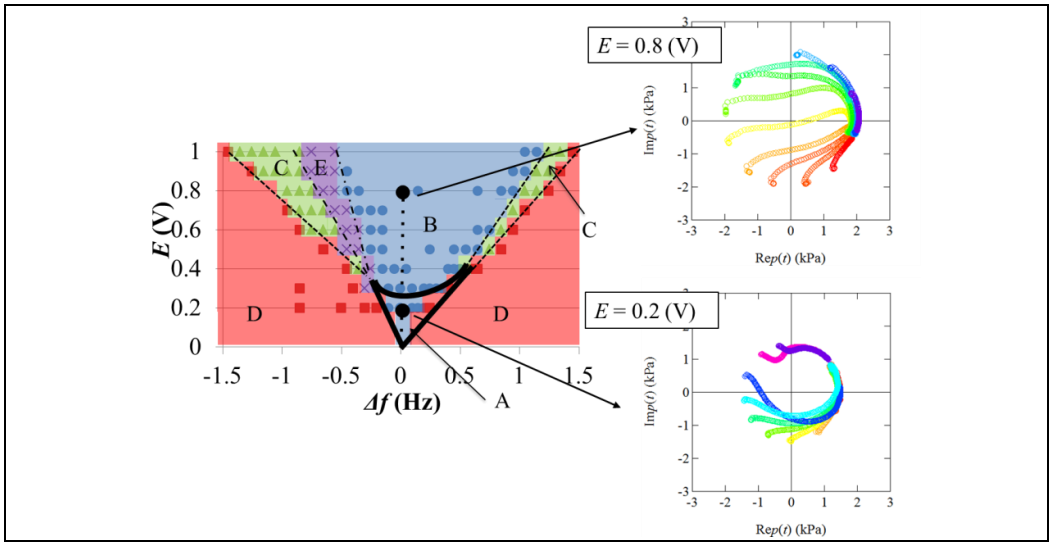

Figure 2: *The synchronous region and synchronous state.*

Summary

The dynamics of oscillator in synchronous state are experimentally observed in forced synchronization in thermoacoustic system by observing the trajectory of oscillation in complex plane. The dynamics of oscillation in synchronous region was different according to the strength of external force.

References

[1] Penelet, G., and Biwa, T. "Synchronization of a thermoacoustic oscillator by an external sound source ", Am. J. Phys., **81**, (2013), 290–297.

[2] Yoshida, T. et al. "Forced Synchronization of Periodic Oscillations in a Gas Column: Where is the Power Source? ", J. Phys. Soc. Jpn., **82**, (2013), 103001.

TRILLIUM: AN INLINE THERMOACOUSTIC-STRILING REFRIGERATOR

R.M. Keolian[1,2*], M.E. Poese[1,2], R.W.M. Smith[1], E.C. Mitchell[1,3], C.M. Roberts[1,3], S.L. Garrett[1]

[1] *Applied Research Laboratory, The Pennsylvania State University, PO Box 30, State College, PA 16804-0030, USA.*
**Corresponding author's e-mail: keolian@psu.edu*
[2] *Sonic Joule LLC, 732 Holmes St, State College, PA 16803-3621, USA.*
[3] *Bose Corporation, The Mountain, Framingham, MA 01701, USA.*

Keywords: *Thermoacoustic, Stirling, alpha-Stirling, refrigeration, multi-stage, vibration balance.*

Introduction

Construction has been completed on an inline refrigerator we call Trillium. It is a prototype for a split-system commercial refrigerator that does not use HCFC or other fluorine based F-gas refrigerants.

Description

The refrigerator is shown in Figure 1. It consists of three thermal stages driven by three linear motors arranged in a row. Vibration balance and quiet operation is achieved by keeping the moving masses of the three stages the same and driving each of the motors 120° out of phase from the others. The 11 bar helium working gas within each thermal stage is compressed and translated by pistons and flexure seals above and below each stage. Each linear motor is rigidly attached to the piston above and below it, except that the bottom motor drives the uppermost piston of the top thermal stage through a lightweight rigid aluminum yoke. The pistons attached to the top and middle motors are heavier than those attached to the bottom motor to compensate for the mass of the yoke. A pressure vessel surrounds the components shown in the figure. Operation is at 82 Hz.

The regenerator at the center of each thermal core is a rolled, 51 micron thick Kapton ribbon that has been dimpled to produce gaps of 60 microns between successive layers. Vacuum brazed aluminum microchannel tube-fin heat exchangers are above and below each regenerator. The fins are folded from 100 micron 3003 aluminum foil with 790 micron outer peak-to-peak amplitude and fin pitch (fin-fin center spacing) of 320 microns. This gives a hydraulic radius of only 84 microns for nearly regenerator-like performance in the heat exchangers. Brazing did not go well and the heat exchangers have suffered multiple helium leaks, which have since been plugged.

In a bid towards commercialization, the flexure seals between the moving pistons and the heat exchangers are made from injection molded fatigue-resistant AvaSpire PAEK or KetaSpire PEEK thermoplastic. Both types have survived for 113 hours or 27 million cycles of a 110% of full amplitude fatigue test. The linear motors are from Qdrive of Chart Industries. They are driven by an off-the-shelf three-phase motor controller.

Unfortunately, the refrigerator and its instrumentation had to be moved before testing could be done, and testing has barely started as of this writing. We expect a COP of 1.4 (37% of Carnot) for 3.5 kW of refrigeration at a refrigerated load temperature of –29°C and heat rejection at 35°C ambient temperature.

The machine as a whole can be considered as a lumped-element version of a looped thermoacoustic-Stirling device, or as three alpha-Stirling devices in-line.

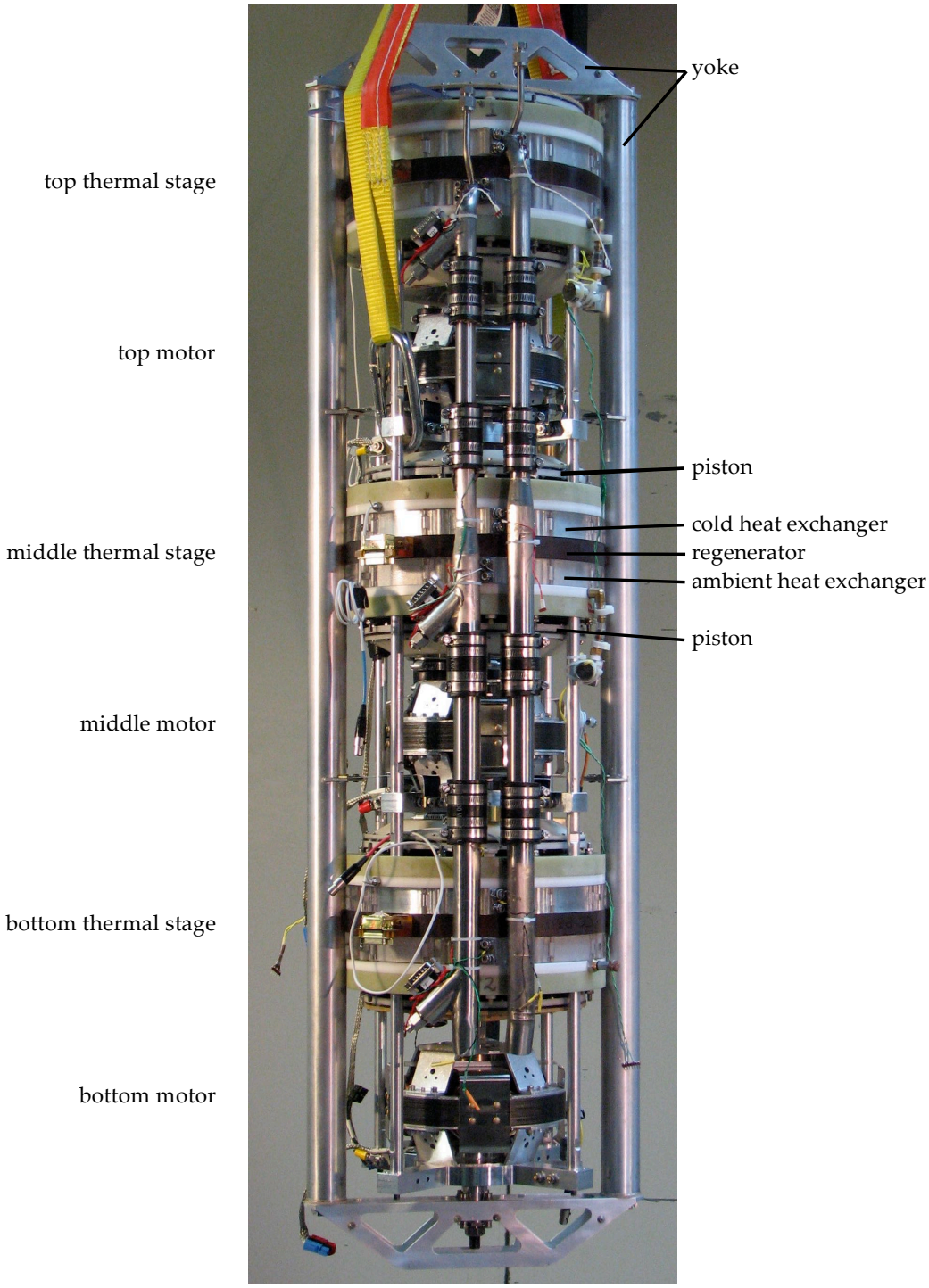

Figure 1: *Internal components of the Trillium refrigerator. Heat exchanger and regenerator OD is 254 mm.*

Acknowledgements
We thank the US Department of Energy's ARPA-E for its support.

LOAD EFFECT ON THE STARTING PERFORMANCE OF A STANDING WAVE THERMOACOUSTIC ENGINE

C. Weisman[1], D. Baltean-Carlès[1*], I. Delbende[1], L. Ma[1], and L. Bauwens[2]

[1] *Université Pierre et Marie Curie UPMC Sorbonne Universités, Laboratoire d'Informatique pour la Mécanique et les Sciences de l'Ingénieur Orsay, France. *Corresponding author's e-mail: baltean@limsi.fr*
[2] *Department of Mechanical and Manufacturing Engineering, University of Calgary, Canada.*

Keywords: *standing wave engine, resistive load, numerical simulation, low Mach number approximation, thermoacoustic instability*

Introduction

A thermoacoustic engine is a device absorbing heat at the hot heat exchanger and releasing heat at the cold heat exchanger while producing acoustic work as an output. Engines are built to carry a load, which in the case of an acoustic device, might include a thermoacoustic refrigerator [4], a (possibly linear) electric generator [2] etc. Coupling between the engine and the load influences both starting performance and steady operation.

The aim of the current work is to study the influence of a variable load on the onset conditions of a standing-wave thermoacoustic engine, through direct numerical simulation of the starting phase. Unstable acoustic modes develop spontaneously in the system. The computed acoustic pressure signal in the active cell is analyzed in order to extract the growth rate and frequency of the dominant modes. Therefore the critical hot exchanger temperature and frequency of the associated mode allowing the engine to start can be determined.

Physical model and numerical simulation

The geometry consists of a long tube, within which an active cell is placed. Flow in the resonator is then described by linear acoustics. The solutions are expressed as a pair of planar traveling waves that move respectively left and right at the speed of sound, using Riemann invariants. The active cell consists of a stack of horizontal solid plates, placed between two heat exchangers also made of solid horizontal plates that have the same periodicity as the stack. There is no empty space between stack and heat exchanger plates, resulting in an optimal configuration for the engine. The geometry can be reduced to a domain consisting of two half-plates plus the gap between them, plus a region that extends away from the solid plates.

Flow in the active cell is described by the two-dimensional Navier-Stokes equations in the low Mach number approximation [1]. The solid stack plate problem is described by the heat conduction equation. In the stack and heat exchanger plates, thermophysical properties of the gas are taken to be constant. In the heat exchangers, uniform, constant temperatures are imposed with dimensionless values $T_c = 1$ in the cooler plates, $T_h > 1$ in the heater plates. Given the periodicity, open active cell boundaries are effectively adiabatic. The flow in the active cell is coupled to linear acoustics model in the resonator, using matched asymptotic expansions in the low Mach number limit [1]. The flow boundary conditions at resonator ends (closed end and loaded end) are then transported along the characteristics to the open end locations of the active cell.

The load is taken to be a resistive load. Instantaneous acoustic pressure and velocity are assumed to be in phase at the loaded end and the load is thus reduced to a real scalar value f measuring the ratio of velocity over acoustic pressure. That condition, carried along the char-

acteristics, results in a relation between the Riemann invariants at the right end of the active cell through a real coefficient $Z = (\gamma - f)/(\gamma + f)$, where γ is the ratio of the gas specific heats. While f goes from zero to infinity, Z has the finite span from -1 for a closed end to $+1$ for an open end, and zero for $f = \gamma$. In the framework of the harmonic approximation, it is possible to relate f or Z to the reflection coefficient at the loaded end hence to the standing wave ratio [3]. The limit values $Z = \pm 1$ correspond to a pure standing wave in the resonator, while the limit case $Z = 0$ corresponds to a pure traveling wave moving from the active cell towards the load. Between those limit cases, the wave is a combination between standing and traveling waves.

Results

The problem in the active cell is solved numerically using a finite volume code [1]. Numerical simulations are carried out for an existing prototype of thermoacoustic engine [1]. The acoustic pressure signal from each simulation is then analyzed. The growth rate and frequency of the dominant modes are extracted from the signal, yielding the critical temperature T_h for which the first unstable mode appears and the frequency of that mode.

Varying the load and reproducing the same procedure for each load value results in a stability diagram, Figure 1 (left), in the (Z, T_h) plane, showing stable and unstable zones. The region above the stability curve corresponds to instability. Results show that for a wide range of intermediate load values (for Z close to zero), the critical temperature ratio is so high that in practice the engine will not start on its own. Figure 1 (right) shows the dimensionless angular

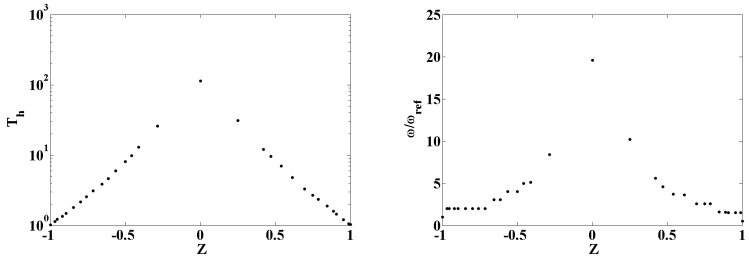

Figure 1: *Left: Stability diagram in the (Z, T_h) plane. The region above the curve corresponds to instability. Right: Angular frequency of the most unstable mode scaled by ω_{ref}, as a function of Z.*

frequency ω/ω_{ref} of the first mode to become unstable as a function of Z. Critical modes near $Z = -1$ are of the closed-end type (multiples of $\lambda/2$) whereas critical modes near $Z = 1$ are of the open-end type (odd multiples of $\lambda/4$). As $|Z|$ decreases, the frequency of the most unstable mode is observed to increase, and higher harmonics are first destabilized. This results in distinct sets of onset frequencies, each set corresponding to a specific harmonic. The load influences the wavelength and changes the optimal relative stack position, so that the most unstable mode shifts from fundamental to first harmonic, second harmonic and so on. These results were found to be in good agreement with an analysis based on Rott's linear theory.

References

[1] Hireche, O., Weisman, C., Baltean-Carlès, D., Le Quéré, P., and Bauwens, L. "Low Mach number analysis of idealized thermoacoustic engines with numerical solution". J. Acoust. Soc. Am., **128**, (2010), 3438–3448.

[2] Miglori, A. and Swift, G. "Liquid sodium thermoacoustic engine". Appl. Phys. Lett., **53**, (1988), 355–357.

[3] Raspet, R., Bruster, J., and Bass, H. "New Approximation Method for Thermoacoustic Calculations". J. Acoust. Soc. Am., **103**, (1998), 2395–2402.

[4] Swift, G. "Thermoacoustic engines". J. Acoust. Soc. Am., **84**, (1988), 1145–1180.

SELF-POWERED THERMOACOUSTIC SENSORS FOR NUCLEAR REACTORS

S. L. Garrett

Graduate Program in Acoustics, Penn State, 201 G Applied Science Bldg. University Park, PA 16802.
**Corresponding author's e-mail: sxg185@psu.edu*

Keywords: *Standing-Wave Engines, Thermoacoustics, Temperature Measurement, Nuclear Reactor Flux Measurement, Fission Heating, Streaming*

Introduction

The core of a nuclear reactor is a particularly harsh environment when functioning properly. When there is a stress event that may include the loss of electrical service, similar to the earthquake and tsunami that struck the Fukushimi Daiichi reactors on 11 March 2011, the need for robust and reliable self-powered sensors becomes acute. The development and testing of very simple standing-wave thermoacoustic engines that can be configured within nuclear fuel rods to exploit the flux of energetic particles (either neutrons or gamma radiation) will be described [U.S. Pat. Appl. No. 2014/0050293 (Feb. 20, 2014)]. The vibrations of such thermoacoustic engines can produce sound that couples to the surrounding heat-transfer fluid to telemeter the information (as frequency and amplitude) to the exterior of the reactor vessel, without requiring electrical power. The resonance frequency is related to the temperature of the heat transfer fluid that surrounds the thermoacoustic resonator [*IEEE Instrumentation and Measurement* **16**(3), 18-25 (2013)] and the amplitude is proportional to the heating, therefore to the neutron or gamma flux [U.S. Patent Application No. 284117-00634 (J1731857-2), 18 April 2013]. Thermoacoustic resonances are maintained without use of a cold heat exchanger, making the engine quite simple. Removal of waste heat from the ambient-temperature end of the stack is enhanced by nonlinear acoustically-induced streaming. The nonlinear hydrodynamic heat transport limits the temperature of the fissionable material or gamma-absorber that provides the heat that drives the engine. This thermoacoustic technique for self-powered "wireless" sensing may be applicable to other processes that generate substantial temperature gradients, such as industrial crucibles for melting glasses and metals.

Acknowledgements
This research is supported by Westinghouse and by Idaho National Laboratory. The author appreciates the services provided by Iain Wilson, Larry Bodendorf, and Brandon Rieck, all of IST Mirion in Cambridge, Ontario, for fabrication of major thermoacoustic resonator parts suitable for service in the core a nuclear reactors.

THERMOACOUSTIC COMPONENTS

THE ROLE OF STACK NON ACOUSTIC PARAMETERS ON THERMODYNAMIC PERFOMANCE OF STANDING WAVE DEVICES

S. Di Filippo*, M. Napolitano, R. Dragonetti, and R. Romano

Department of Industrial Engineering, University of Naples Federico II, P.le Tecchio 80, 80125, Naples, Italy.
**Corresponding author's e-mail: sabato.difilippo@unina.it*

Keywords: *stack geometry, pore cross-section, non-acoustic parameters*

Introduction

The stack is the core of an thermoacoustic standing wave device. In thermoacoustic engines, heat pumps and refrigerators the geometric characteristics of the stack influence the thermodynamic performance. Until now the stack is studied by using viscous and thermal functions that vary with the shape of the pore. However more advantageous general functions can be taken into account to study a complex cross-section of pores and also the tortuosity. These functions involve classic non-acoustic parameters such as the air-flow resistivity, the tortuosity, the thermal and viscous characteristic length. Aim of this work is to introduce these functions in the classical thermoacoustic theory and to study theoretically the effect on the performance of a thermoacoustic engines.

Thermal and viscous averaged functions

The use of thermal and viscous averaged functions are introduced in the thermoacoustic theory by Swift [1] to describe the viscous and thermal interaction inside the stack. Similar functions are also used to describe the acoustic properties of a porous material such as the absorption and the reflection coefficient. However a porous material used in practical applications of sound control is quite different from the stack introduced in the Swift theory because do not exist straight but tortuous pores with various interconnections among them. For these reasons, numerous researchers engaged themself to derive more general models to describe the complex geometry inside a porous material. For example, Biot [2] and Stinson [3] later, found that the sound propagation inside a porous material, having straight pores but different cross-section, can be studied with general thermal and viscous averaged functions, by using an equivalent hydraulic radius or a pore-shape factor. In particular Stinson shows that the viscous interaction can be described by the complex density $\tilde{\rho}$ while the thermal interaction can be described by the complex bulk modulus $\tilde{K}$.
Nowadays, in order to take also into account the tortuosity inside a porous material the most used model is that given by Johnson [4] to describe the viscous interaction and that given by Champoux [5] to describe the thermal interaction. In the Johnson model:

$$\tilde{\rho} = \frac{\rho_0 \alpha_\infty}{\phi}\left(1 + \frac{\sigma\phi}{j\omega\rho_0\alpha_\infty}\sqrt{1 + \frac{4\alpha_\infty^2 \mu\rho_0\omega}{\phi^2\sigma^2\Lambda_v^2}}\right) \tag{1}$$

where ρ_0 is the air static density, μ is the dynamic viscosity, α_∞ is the high frequency limit of the tortuosity, σ is the static air-flow resistivity, ϕ is the open porosity and Λ_v is the viscous characteristic length. In the Champoux model:

$$\widetilde{K} = \gamma P_0 \left(\gamma - \frac{(\gamma - 1)}{1 + \frac{8\mu}{j\Lambda_t^{\prime 2} P_r \omega \rho_0} \sqrt{1 + j \frac{\Lambda_t^{\prime 2} \rho_0 \omega}{16\mu}}} \right)^{-1} \quad (2)$$

where γ is the ratio of isobaric to isochoric specific heats, P_0 is the static air pressure, P_r is the Prandtl number and Λ_t is the thermal characteristic length. These functions are in turn improved by the Pride [6] and Lafarge [7] but other parameters are introduced. In this preliminary study these further models are not considered.

Use of general thermal and viscous averaged functions in the thermoacoustic theory

The complex density and the bulk modulus can be related to the function f_v and f_k used in the Swift theory. A matlab code, tested with DeltaEC, is developed to take into account these new general functions. The non-acoustic parameters can be obtained by numerically solving the thermoacoustic interaction inside a pore without considering the variations in temperature as shown in figure 1.

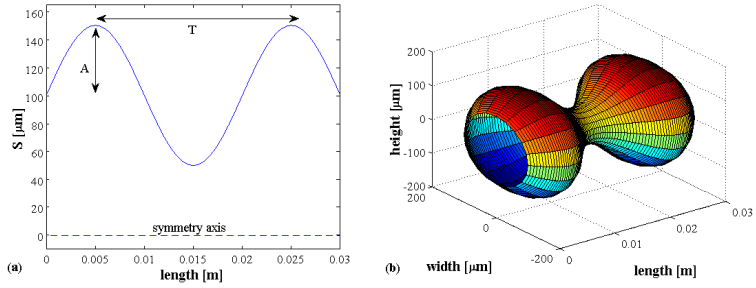

Figure 1: *a) Axial symmetric section and b) 3D view of a typical considered pore shape.*

It is found that this general approach to study the influence of the stack geometry in terms of porosity, air-flow resistivity, tortuosity and thermal and viscous characteristic length is more advantageous than to use different averaged functions for any pore cross-section.

References

[1] Backhaus, S., and Swift, G. "A thermoacoustic-Stirling heat engine: detailed study", J. Acoust. Soc. Am., **107**, (2000), 3148–3166.

[2] M. A. Biot, "Theory of Propagation of Elastic Waves in a Fluid-Saturated Porous Solid. II. Higher Frequency Range", J. Acoust. Soc. Am., **28** , (1956), 179-191.

[3] Stinson, M. R., The propagation of plane sound waves in narrow and wide circular tubes, and generalization to uniform tubes of arbitrary cross-sectional shape . J. Acoust. Soc. Amer., **89**, (1991) 550–8.

[4] Johnson D. L., Koplik J. and Dashen R., Theory of dynamic permeability and tortuosity in fluid-saturated porous media, J. Fluid Mech. **176**, (1987), 379-402.

[5] Champoux Y. and Allard J.-F., Dynamic tortuosity and bulk modulus in air-saturated porous media, J. Appl. Phys., **70**, (1991), 1975-1979.

[6] Pride S. R., Morgan F. D. and Gangi A. F., Drag forces of porous-medium acoustics, Phys. Rev. **B 47**, (1993), 4964-4978.

[7] Lafarge D., Lemarinier P., Allard J.-F. and Tarnow V., Dynamic compressibility of air in porous structures at audible frequencies, J. Acoust. Soc. Am. **102**, (1997), 1995-2006.

CFD STUDY OF OSCILLATORY FLOW AROUND PARALLEL PLATES IN A TRAVELING-WAVE THERMOACOUSTIC ENGINE

Esmatullah Maiwand Sharify[1*], Shun Takahashi[1], Shinya Hasegawa[1]

[1]*Department of Prime Mover Engineering, Tokai University, Kanagawa 259-1292, Japan*
**Corresponding author's e-mail: esmat.maiwand@gmail.com*

Keywords: *CFD simulation, parallel plates, particle displacement amplitudes, frequency, nonlinearity effects.*

Introduction

The stack/regenerator and heat exchangers are the core components whereby the thermoacoustic effect and energy conversion take place [1]. The flow field near the edges of the plates is crucial due to nonlinear behavior which affects the performance of the device significantly [2]. Therefore, there is a need to understand the oscillatory flow processes in the vicinity of such internal structures [3]. In this work, CFD simulation was performed and the oscillatory flow in the vicinity of a parallel plates placed in a traveling-wave thermoacoustic resonator was studied.

Methodology

The finite volume method was used to discretize the Navier–Stokes equations on equally spaced Cartesian grids with a cell-centered arrangement. The wall boundaries of objects were represented by the immersed boundary method using ghost cells of the level-set method [4]. The no-slip boundary condition was used for the velocity and the Neumann boundary condition was imposed on the walls for the pressure. On the other hand, the impedance matching boundary (IMB) condition was used on the both sides of the computational domain, which was developed by Hasegawa and Takahashi [5-6]. Parallel plates were assumed to be periodic in the y direction. The air at atmospheric pressure was used as a working fluid. The temperature gradient as a linear function was added to the plates as isothermal walls of 300 K at left side and 600K at right side of regenerator. Meanwhile, isothermal boundary condition was applied for the temperature.

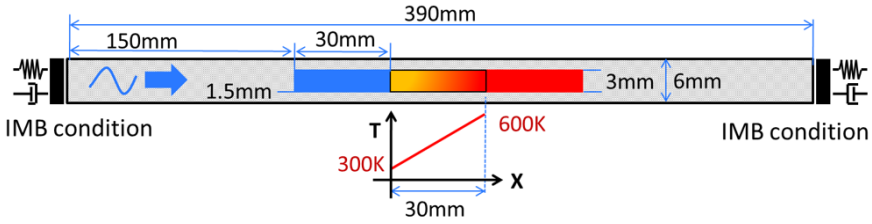

Figure 1: *Schematic of the computation domain.*

Discussions

In this work, the oscillatory flow structures around the parallel plates in a traveling wave thermoacoustic engine were studied. The flow structures formed around the plates and the heat transfer over a range of oscillation amplitudes and frequencies were discussed. The oscillation amplitudes were approximately 25%, 50%, 75%, 100%, 125%, and 150% of the

regenerator length (30mm). Meanwhile, applied frequencies were 10Hz to 70 Hz. Using the CFD simulation, nonlinear vortex generation around the plates were studied. It was found that at small amplitudes the shear layers in the wake remain symmetric and produced attached symmetrical vortex structures. However, for larger oscillation amplitudes the flow lost its symmetry and stability, resulting unstable vorticity field behind the plates.
It was observed that the temperature oscillations at the edges of the plates were nonlinear. Moreover, the temperature oscillations near the plates had impact on heat transport processes and effected the enthalpy flux carried along the plates. The interaction of the acoustic wave with the regenerator plates having a temperature gradient, leaded to a significant enthalpy flux changes along the regenerator plates. The change in enthalpy flux significantly increased as the oscillation amplitude became larger. Acoustic power gain as a function of oscillation amplitude and frequency was investigated and it was noticed that the acoustic power gain were influenced significantly by oscillation amplitude.

Conclusions

CFD simulations with IMB condition were performed. The oscillating flow fields in the vicinity of a thermoacoustic couple over a range of particle oscillations amplitudes and frequencies were investigated. It was confirmed that the temperature oscillations at the edges of the plates were nonlinear and the change in enthalpy flux significantly increased as the oscillation amplitude became larger. Furthermore, the acoustic power gain as a function of oscillation amplitude and frequency was investigated and it was obtained that the acoustic power gain influenced significantly by oscillation amplitude. However, the results will be presented in detail at the workshop.

Acknowledgements

This study was partially supported by ALCA project of Japan Science and Technology Agency (JST).

References

[1] X. Mao, "A study of fluid flow phenomena around parallel-plate stacks in a standing wave thermoacoustic device", PhD thesis, The University of Manchester, England, 2011.

[2] P. Blanc-Benon, E. Besnoin, and O. Knio, "Experimental and computational visualization of the flow field in a thermoacoustic stack", C. R. Mecanique 331, (2003), 17-24.

[3] X. Mao, and AJ. Jaworski, " Oscillatory flow at the end of parallel plate stacks – phenomenological and similarity analysis", Fluid Dynamics Research, 42(5), (2010)

[4] S. Takahashi, T. Nonomura, K. Fukuda, " A Numerical scheme based on an immersed boundary method for compressible turbulent flows with shocks", Journal of Applied Mathematics 2014(2014), Article ID 252478, 1-21.

[5] S. Hasegawa, T. Yamaguchi, Y. Oshinoya, "A thermoacoustic refrigerator driven by a low temperature-differential, high-efficiency multistage thermoacoustic engine", Applied Thermal Engineering 58 (2013) 394–399.

[6] S. Takahashi, S. Hasegawa, T. Nonomura, "Impedance matching boundary condition for flow simulation on thermoacoustics", International Journal of Heat and Mass Transfer, (2015- under review).

[7] P. H. Ceperley, "A pistonless stirling engine the traveling wave heat engine", Journal of the Acoustical Society of America 66 (1979) 1508–1513.

[8] T. Yazaki, A. Iwata, T. Maekawa, A. Tominaga, "Traveling wave thermoacoustic engine in a looped tube", Physical Review Letters 81 (1998) 3128–3131.

SIMULATION OF FLOW AND HEAT TRANSFER IN THERMOACOUSTIC REFRIGERATOR USING A 3-D PERIODIC CELL STRUCTURE

A.I. Abd El-Rahman*, W.A. Abdelfattah, and M.A. Fouad

The Department of The Mechanical Power Engineering, Faculty of Engineering, Cairo University, Giza 12613, Egypt.
**Corresponding author's e-mail: aiarahman@eng.cu.edu.eg*

Keywords: *Thermoacoustic Refrigerator/Cooler, Oscillating-Flow behavior, Flow Streaming, 3-D Simulation, CFD Analysis*

Introduction

The thermoviscous behavior of the oscillating gas within the porous medium of a thermoacoustic refrigerator enables the conversion of sound into heat in the process of typical standing thermoacoustic refrigeration systems. Several nonlinear mechanisms, such as harmonics generation, self-induced streaming and possible turbulence, cause complicated flow behavior and influence the performance of such devices. Few analytical and 2-D numerical approximations [2, 5] describe the flow field and the energy flux density in standing devices comprising stacks of parallel plates, but almost no 3-D simulation has been developed that directly models the large-amplitude excitations and enables the prediction of the oscillating-flow behavior within a porous medium made of square channels. This work builds on existing effort [1], and has the objective of extending the 2-D analysis of thermoacoustic couples into a 3-D CFD simulation of a thermoacoustic refrigerator. The stack is made of cordierite and consists of a large number of small square channels (600 CPSI). Each channel is 60-mm-in-length and has a transveral width h of 0.92 mm and a wall thickness t of 0.12 mm. This work also investigates the existence of non-linear phenomenons, such as DC-streaming.

Numerical Model Setup

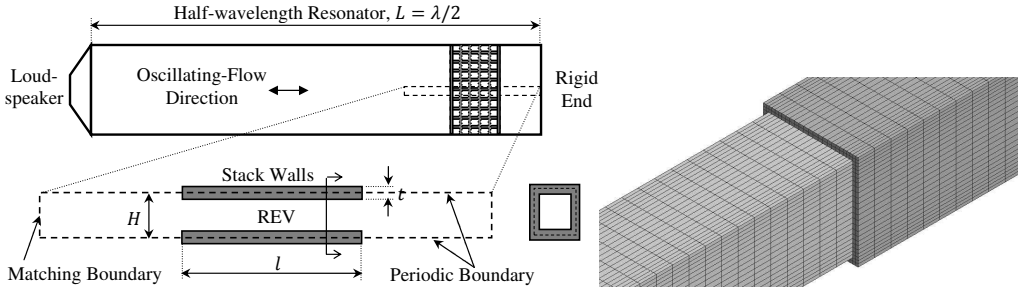

Figure 1: *Left-Top: Schematic of the thermoacoustic refrigerator. Left-Bottom: The representative element volume REV is drawn with two periodic surfaces along with an acoustically-matching adiabatic boundary condition imposed at the left end ($H = h + 2t$). The layering dynamic meshing technique is used for this purpose. Right: A 3-D illustration of the computational mesh of the periodic cell structure. The solid and gas domains are represented by large numbers of hexahedral elements. Here, the solid mesh is suppressed for clarity.*

The cooler geometry and domain meshing are shown in Fig. 1. For the sake of simulation and model validation, the current geometry and operating conditions follow the experimental setup of Lotton et al. [3]. The system is excited with an acoustic frequency of 200 Hz and acoustic

pressure amplitude of 1500 Pa. The resonator has a square cross section and filled with air at atmospheric pressure and ambient temperature. The numerical model is constructed such that the stack centre is positioned at a distance 140 mm from the resonator closed end. The domain is carefully discretized to properly capture the thermoviscous interactions of the oscillating-flow with the stack walls. In the transversal direction, the mesh is distinguished into three concentric regimes, depth of each corresponds to the viscous diffusion thickness $\delta_\nu = \sqrt{2\nu/\omega}$. Here, ν and ω are the gas kinematic viscosity and angular frequency, respectively. For instance, a typical run involves a million of computational cells. The second-order upwind finite-volume implicit-time algorithm is used along with the conjugate heat transfer algorithm (ANSYS FLUENT).

Prelimnary Results

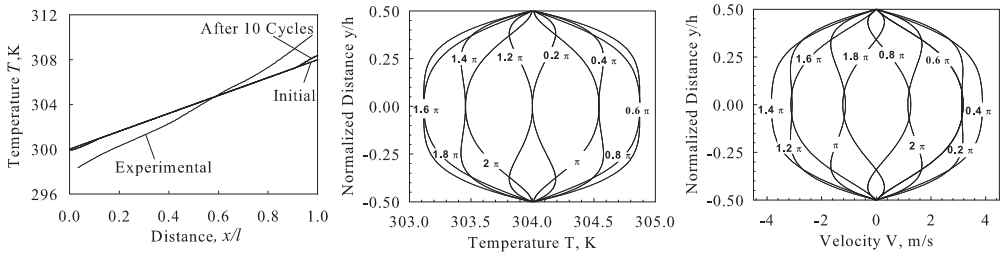

Figure 2: *The initially-imposed temperature distribution and its further development (Left). Laminar fully-developed temperature (Middle) and axial-velocity profiles (Right) at 10 different instants. The flow behavior is generally in agreement with that theoretically reported by Panton [4].*

Figure 2 shows the instantaneous temperature and velocity profiles for 36°-increments over one period. The stationary system response is predicted and the numerical values are presented in comparison with reported test data. Figure 3 illustrates the non-zero mean (cycle-average) velocity field, calculated over the last acoustic cycle.

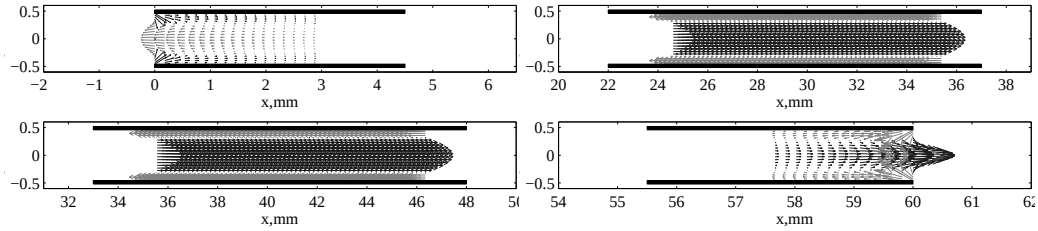

Figure 3: *Vector plot of the non-zero mean velocity field within the stack and at the stack extremities, demonstrating the existence of the DC-streaming.*

References

[1] Abd El-Rahman, A. I. and Abdel-Rahman, E. "Computational Fluid Dynamics Simulation of a Thermoacoustic Refrigerator". Journal of Thermophysics and Heat Transfer, **28**, (2014), 78 – 86.

[2] Cao, N., Olson, J. R., Swift, G. W., and Chen, S. "Energy flux density in a thermoacoustic couple". The Journal of the Acoustical Society of America, **99**, (1996), 3456–3464.

[3] Lotton, P., Blanc-Benon, P., Bruneau, M., Gusev, V., Duffourd, S., Mironov, M., and Poignand, G. "Transient temperature profile inside thermoacoustic refrigerators". International Journal of Heat and Mass Transfer, **52**, (2009), 4986 – 4996.

[4] Panton, R. L. *4^{th} Ed., Incompressible Flow.* John Wiley & Sons, Inc. (**2013**).

[5] Worlikar, A. S. and Knio, O. M. "Numerical Simulation of a Thermoacoustic Refrigerator: I. Unsteady Adiabatic Flow around the Stack". Journal of Computational Physics, **127**, (1996), 424 – 451.

ACOUSTIC TO ELECTRIC CONVERSION

EVALUATION OF BI-DIRECTIONAL TURBINES USING THE TWO-SENSOR METHOD

K. Kaneuchi[1*], K. Nishimura[1]

[1] *Osaka Gas CO., LTD, 6-19-9, Torishima, Konohana-ku, Osaka, Japan.*
** e-mail: k-kaneuchi@osakagas.co.jp*

Keywords: *Bi-directional turbine, two-sensor method*

Introduction

Various forms of thermal energy: solar heat, waste heat, and geothermal etc., can be converted to acoustic power utilizing thermo-acoustic phenomena. Acoustic power can be used for refrigeration and power generation. For power generation, linear alternators are typically used. However linear alternators are limited when it comes to cost and scalability. Kees de Blok proposed the use of a bi-directional turbine (BDT) which converts acoustic power into rotational energy [1]. His study determined that fluid density and frequency contributed to conversion efficiency. However, BDT behavior in thermoacoustic systems is not clear. The purpose of this study is to confirm the influence of a BDT on the sound field. Both the upstream and downstream sound fields were evaluated by two-sensor method.

Experiment

The BDT consists of a rotor with symmetric blades and two guide vanes (Figure 1). The rotor rotates in the same direction regardless of flow. Prototypes were made using a 3D-printer (Figure 2). Tim Kloprogge's document [2] was referred to when determining the blade shape. In this experiment, three types of turbines with different blade pitch (Figure 3) were evaluated.

The experiment consisted of two loudspeakers (FOSTEX, FW208N), polyvinyl chloride tubes and a BDT (Figure 4). A 40Hz sine wave was generated from the source speaker; past the BDT we used the second speaker to eliminate reflections off the end of the tube. Pressure sensors (JTEKT, PD104K-30K) were placed in both the upstream and downstream of the BDT. Pressure, particle velocity, work flow, and impedance were evaluated using the two-sensor method.

A brushless motor (HADKER, A20-26M) was used as a power generator. The output of the generator was connected to a 2Ω resistor. With this setup, generated power and rotation speed were measured.

Result

Using the two-sensor method: pressure, particle velocity, work flow, impedance and phase difference between pressure and particle velocity were approximated (Figure 5). Electrical conversion efficiency of the BDT was evaluated using the difference in work flow across the BDT. Generated power was measured using a series circuit with the motor and resistor. Results for each turbine are shown in table 1. We determined that differences in blade number contribute to electrical conversion efficiency.

Conclusions

Sound fields around the BDT were evaluated using the two-sensor method. We determined that blade pitch contributes to electrical conversion efficiency from acoustic power. For

practical use, further studies are required. For example, evaluation in a pressurized condition and an evaluation regarding blade shape.

Acknowledgements

We wish to thank Kees de Blok in Aster Thermoacoustics for his helpful discussions regarding the BDT and applications of thermoacoutics.

References

[1] Kees de BLOK, Pawel OWCZAREK, Maurice-Xavier FRANCOIS "Bi-directional turbines for converting acoustic wave power into electricity", 9th PAMIR International Conference, Riga,Latvia (2014) , 433-438

[2] Tim Kloprogge, "Turbine Design for Thermoacoustic Generator", Document of FACT foundation, FACT-5

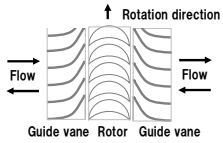

Figure 1: *Conceptual diagram of BDT.*

Figure 2: *Appearence of BDT.*

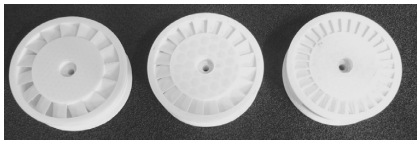

Figure 3: *Rotors of different pitch.*

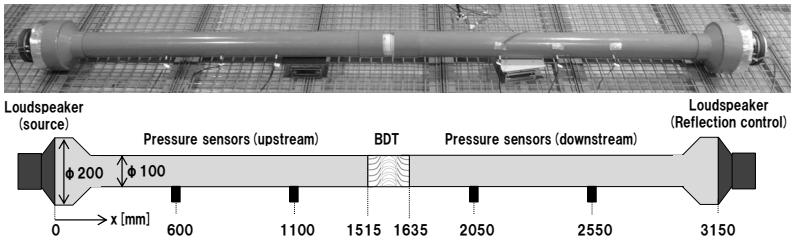

Figure 4: *Photograph and cross-section of the experimental setup*

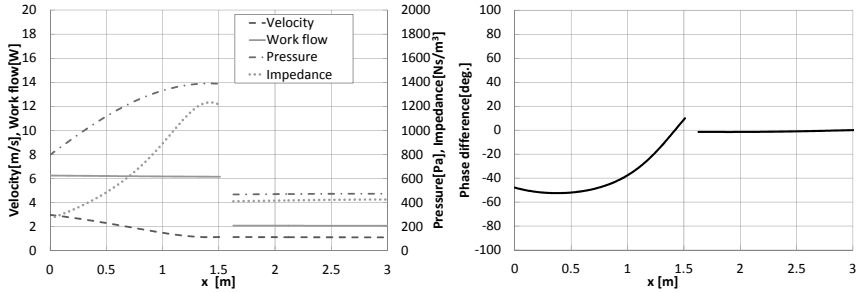

Figure 5: *Pressure, particle velocity, work flow, impedance and phase difference approximated by two-sensor method.*

Table 1: *Results of our evaluation.*

Number of blades		Rotation speed [rpm]	Difference in Work flow across the BDT[W]	Electric-generating capacity[W]	Acousitic-electric conversion efficiency[%]
Rotor	Guide vane				
15	12	2353	7.8	0.89	11.3
20	16	2473	8.3	0.97	11.7
30	24	2076	9.1	0.70	7.7

HIGH-FIDELITY SIMULATIONS OF A STANDING-WAVE THERMOACOUSTIC-PIEZOELECTRIC ENGINE

J. Lin[1*], C. Scalo[2], and L. Hesselink[1]

[1] *Department of Electrical Engineering, Stanford University, Stanford, CA 94305, USA.*
**Corresponding author's e-mail: linjef@stanford.edu*
[2] *Department of Mechanical Engineering, Purdue University, West Lafayette, IN 47907, USA.*

Keywords: *thermoacoustics, impedance, piezoelectric, energy conversion, energy extraction, Navier-Stokes, standing-wave*

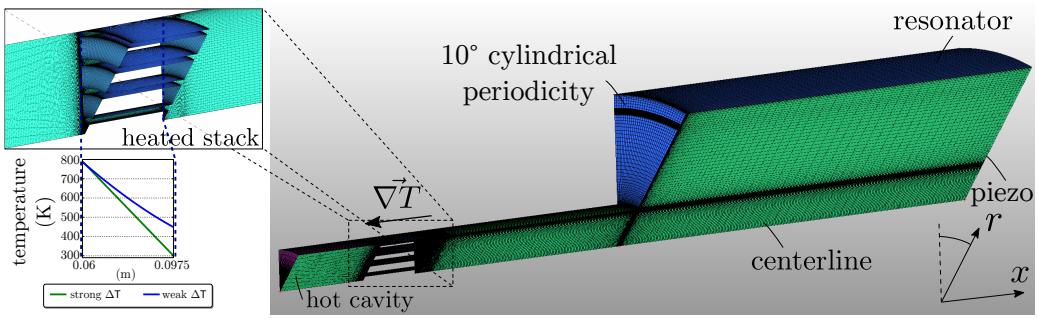

Figure 1: *Computational grid meshing of a 10° wedge of the axially-symmetric engine geometry. Linear temperature gradient profiles are introduced in the heated stack.*

We have carried out fully compressible Navier-Stokes numerical simulations of a standing-wave thermoacoustic piezoelectric (TAP) engine model inspired by the experiments of Smoker *et al.* (2012) [2]. The TAP model is composed of a 51 cm long cylindrical resonator divided into two constant-area segments of 19.5 mm and 71 mm in diameter. The smaller diameter segments contain a thermoacoustic stack while the larger diameter segment is capped by a PZT-5A piezoelectric diaphragm. The diaphragm is tuned to the engine's natural operating frequency (388Hz) for maximization of acoustic energy extraction.

The adopted numerical setup allows for both the evaluation of the nonlinear effects of scaling and the effect of a fully electromechanically-coupled impedance boundary condition, representative of a piezoelectric element. No signs of acoustic nonlinearities are present. Building upon the computational platform as presented by Scalo *et al.* (2015) [1], the stack geometry is now fully resolved without the use of source terms representing drag and heat transfer. Geometry meshing and example temperature profiles are shown in figure 1. To our knowledge, fully broadband-matching impedances have not been coupled with Navier-Stokes thermoacoustic engine simulations, and prior research has been performed on this engine using models such as the impedance model in DELTAEC.

We have performed simulations without the piezoelectric diaphragm with different temperature gradients across the stack, including values at $\Delta T = 490$K and $\Delta T = 340$K, which respectively reach limit cycles at cavity amplitudes of $P_{\text{lim}} = 356$Pa and $P_{\text{lim}} = 6109$Pa. Intermediate values of ΔT were also investigated and growth rates in the linear regime were validated with linear stability analysis of the engine.

To construct an energy extraction boundary condition, we imposed a time-domain impedance

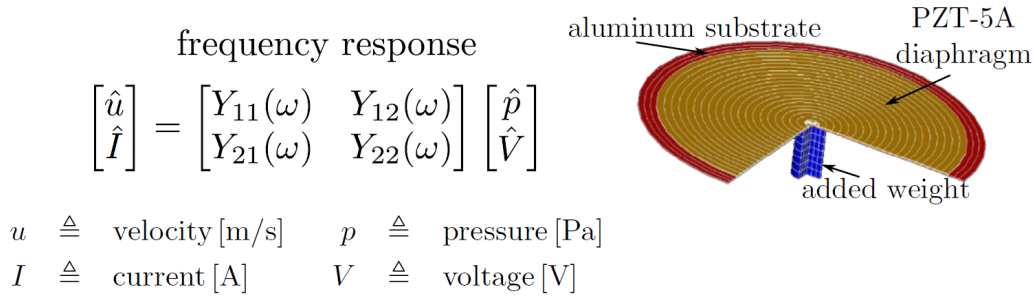

Figure 2: *The piezoelectric diaphragm used by Smoker et al. was tuned and weighted to the engine operating frequency and was reported as a two-port model with associated transfer functions Y. In order to construct computationally-compatible impedances, the two-port model was reduced to a one-port model of the form $\hat{p} = Z(\omega)\,\hat{v}$.*

boundary condition as a representation of the piezoelectric diaphragm as shown in figure 2. We have collapsed the two-port model provided by the PZT-5A piezoelectric patch by using the reference resistance of 3170Ω and constructed both single-frequency and broadband acoustic, causal impedances, as shown in figure 3. These impedance boundary conditions were coupled with the Navier-Stokes solver, producing both a high-fidelity simulation of the engine and simulation results for acoustic-to-electric energy conversion.

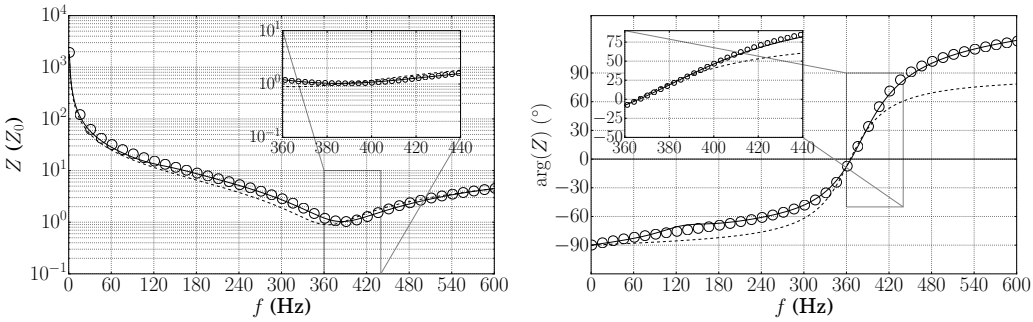

Figure 3: *Broadband fitting of a set of Helmholtz pairs and fitting of a Helmholtz pair to the transmittance-matrix derived impedance; measured impedance from experimental data collapsed into one-port model (∘ ∘ ∘), single-frequency Helmholtz oscillator (fitted around 388Hz)(- - - -), and broadband impedance using multiple basis frequencies (—). Fitting around the engine operating frequency is shown in the inset, demonstrating a reasonable ability for single-pole impedances to be sufficient for monotonic simulations.*

Results at a low-amplitude regime were validated against results obtained from experimental results in literature. Energy extraction results are within 10% difference.

References

[1] Scalo, C., Lele, S. K., and Hesselink, L. "Linear and nonlinear modeling of a theoretical traveling-wave thermoacoustic heat engine". **766**, , 368–404.

[2] Smoker, J., Nouh, M., Aldraihem, O., and Baz, A. "Energy harvesting from a standing wave thermoacoustic-piezoelectric resonator". Journal of Applied Physics, **111**, (2012), 104901.

Modeling and controlling the generator of a Thermoacoustic Stirling Engine

J.A. Brussen[1]

[1] *Electrical Engineering, HAN University of Applied Sciences , Ruitenberglaan 26, 6826 CC, Arnhem, The Netherlands.*
Corresponding author's e-mail: johan.brussen@han.nl

Keywords: *acoustic stirling engine, control, linear generator, efficiency*

Introduction

The acoustic waves consist of alternating pressures and flows. The used generator is a linear generator that converts acoustic waves into electric power. The linear movement of the generator is limited; exceeding these limits might damage the generator.
The total system, consisting of the thermoacoustics engine, generator and load, is tuned to get acoustic waves with the desired frequency and amplitude.
A source with a temperature difference delivers the heat power to the system. This temperature difference changes in time. The power delivered depends on the input power and the loading of the system.
To avoid destruction of the generator, the movement of the generator has to be controlled. The load should also be controlled to maximize the output power.

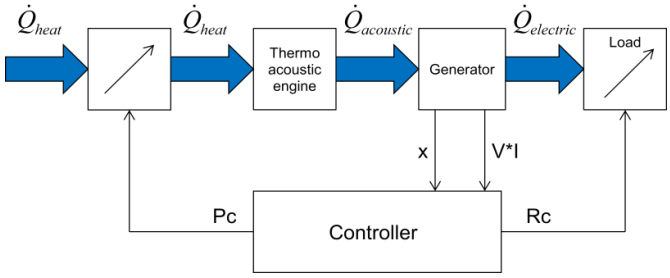

Figure 1: *Block diagram of the system*

Controller design

From the modeling it becomes clear a controller is needed to control the maximum electrical power delivered to the load. The maximum power is reached if the generator reaches its maximum excursion. The maximum power can be controlled by the value of the electrical load resistor. The control goal for this purpose can be stated as: Deliver maximum power to the electrical load resistor.
To deliver the maximum power to a given resistor the amplitude of the source has to be maximalized. At the start of the engine the amplitude is zero, to increase the amplitude the load resistance has to be higher than the calculated value. If the generator reaches its maximum excursion the load must be set to the calculated value. At this point the generated

voltage is at its maximum so the maximum power is delivered to the resistor. The derived control goal becomes: Keep generator at maximum generated voltage.

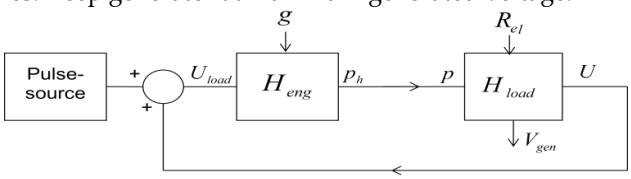

Figure 2: *Process with controls*

In Figure 2 the process is given. The feed forward loop make the system oscillate, the pulse source delivers the initial start-up energy. The temperature difference determines the gain of the engine (g). The gain can change in time due to the change in the source of the wasted heat, g is considered to be a disturbance. R_l is the input of the process and the V_{gen} the controlled variable. The process consists of a process with for $R_l > R_0$ the poles are in the right hand part of the pole plane, for $R_l < R_0$ the poles are be on the left site of the imaginary axis.. The controller keeps the poles on the imaginary axis. The system acts as an integrator. As the process is a non linear process, the process is linearized in an operating point. The operating point is given by the temperature difference. This difference dictates the R_l for stationary operation. The integrator behavior of the process makes a P controller sufficient. The control scheme is given in Figure 3.

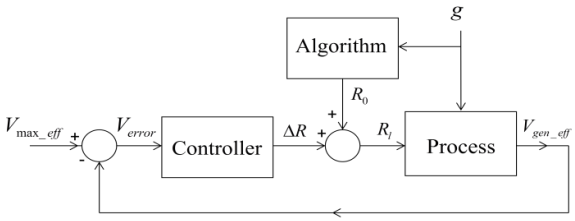

Figure 3: *Control scheme*

In this scheme, the output of the process is the rms value of the generated voltage, the V_{max_eff} is calculated and used as set point of the system. The error voltage is fed to the controller. The output of the controller is added to the R_0. R_0 is the value of the load resistor at which steady state conditions are met. The algorithm calculates R_0.
If R_0 is calculated correctly, the controller drives the V_{gen_eff} to the desired value, V_{error} will be zero. There is no steady state error as the process introduces an integrating action.

References

[1] L. L. Beranek, Acoustics, Cambridge: Acoustical Society of America, 1993.

[2] K. Thorborg, A. D. Unruh and C. J. Struck, "An Improved Electrical Equivalent Circuit Model for Dynamic Moving Coil Transducers," in *AES 122s Convention*, Vienna, 2007.

[3] N. S. Nise, Control Systems Engineering, John Wiley and Sons Ltd, 2008.

[4] C. M. De Blok and R. F. M. Van Den Brink, "Full Characterization of Linear Acoustic Networks," *J. Audio Eng. Soc., Vol. 40, No. 6,* pp. 517-523, june 1992.

[5] S. Backhaus and G. W. Swift, "A thermoacoustic-Stirling heat engine: Detailed study," *Acoustical Society of America,* pp. 3148-3166, june 2000.

SIGNAL CONDITIONING OF CARBON NANOTUBE LOUDSPEAKER

A. Hall [1*], J. Gaston[1], W. Wolde[1], S.Karna[1], E. Baker[2], M. Okada[2], Y. Wang[2],and B. Farouk [3]

[1] *U.S. Army Research Laboratory, Aberdeen Proving Ground, MD, 21005 USA.*
**Corresponding author's e-mail: asha.j.hall.civ@mail.mil*
[2]*Department of Chemistry and Biochemistry, University of Maryland, College Park, MD 20742, USA*
[3] *Mechanical Engineering and Mechanics Department, Drexel University, Philadelphia, PA, 19104, USA*

Keywords: *Thermophone, Carbon Nanotube Thin Film Loudspeaker, Thermoacoustics*

Introduction

Acoustic phenomena can be observed when conductors are electrically heated with alternating current when either free-standing or supported by a substrate. Materials with small heat capacity per unit area posses outstanding thermoacoustic properties and can be used in thermally driven loudspeakers such as thermophones. The thermal contraction and expansion of the surrounding medium determine the amplitude of the resulting sound waves [1]. The alternate expansion and contraction of the boundary layer of air in the immediate vicinity of the thin film causes a pressure otherwise known as a sound wave. It is important to note that the sound is produced from the thermal expansion and contraction of the air in the vicinity of the thin film, and not from the mechanical movement of the thin film. However at acoustic frequencies these waves are attenuated to a small fraction of their original amplitude and at under certain operating power we observe that distortion becomes a dominate feature [2]. Other studies have recommended to add a dc offset voltage or a pulse width modulated signal to eliminate the doubling of frequency [3]. The focus of this paper is to verify their recommendation via measurements and numerical simulations of the generated thermoacoustic waves.

Sample Preparations and Thermal Characterization

The CNT film was directly pulled across two copper electrodes that serve as the points of contact for the ground and current flow across the sample as shown in Figure 1. A small amount of conducting silver electrode paint (DuPont CB028 Silver Paint) was applied to the poles prior to the deposition of the thin film. The silver paint serves as an adhesive for the thin film but also improves the electrical contact between the CNT film and the copper electrode. The heat capacity and in-plane thermal conductivity of the super-aligned CNTs were determined by digital scanning calorimetry (DSC) (Perkin Elmer). The average heat capacity of the super- aligned CNT film is 490 kJ $kg^{-1}K^{-1}$ and the thermal conductivity is 0.23 W/mK.

Figure 1: A super-aligned CNT film placed across two copper electrodes

Numerical model

A fully compressible form of the Navier-Stokes equations was numerically solved to track the thermoacoustic waves generated by the CNT film heated by passing alternating current.

Results and Discussion

The CNT thin film produces a pressure oscillation in the surrounding air as it is periodically heated and cooled. This pressure oscillation leads to the generation of thermoacoustic sound

over a wide frequency range. The experimental measurements follow a trend where the sound pressures level-off with increasing frequencies; this trend is demonstrated as a transition from the far field to the near field sound propagation as the frequency is increased. The measurements were performed in an anechoic chamber with a pure sinusoidal voltage applied to a free standing CNT thin film positioned 5 cm from a microphone. The output of the free-standing film reaches 90 dB of sound pressure at 30 W of power. The thermal excitation was acquired with an MIKRON TS7300 IR camera. At a power of 45 W and an acoustic output of 90 dB, the maximum temperature across the surface of the free standing thin film peaked at 320°F.

The audio frequency produced was twice the frequency of the AC current applied to the thin film speaker. This signal distortion is due to the power dissipated as being proportional to the square of the input current. In the experiment, a squared alternating current $I^2\sin^2(\omega t)$ was supplied, wherein the Joule heating is proportional to

$$RI^2 sin^2(\omega t) = \frac{RI^2}{2}\left(-cos(2\omega t)\right) \quad (1)$$

the acoustic frequency given by $\omega = 2\pi f$. Experimental measurements confirmed that the squared sinusoidal input caused a frequency doubling in the sound pressure waveform.

Experimental test were conducted with an AC sine wave, 50 V dc offset, and PWM signal with an applied voltage ranging from 100-300V to a free-standing CNT thin film. Preliminary tests show that when a 50 V dc offset was applied to the ac input voltage ranging from 50-350V to the CNT thin films, the energy of the dominate tones at 2 kHz and 4 kHz was equivalent. As the power increases, there is a linear increase in the energy of the dominate tones as well as the resulting harmonics.

Sample solutions from the numerical model developed are shown in Figure 2 below. A CNT thin film is sinusoidally heated with a frequency of 1 kHz, Figure 3(a). The resulting thermoacoustic pressure wave evolution 5.0 cm from the film is shown for early and longer times at Figures 3(b) and 3(c). The characteristic frequency doubling phenomena is predicted.

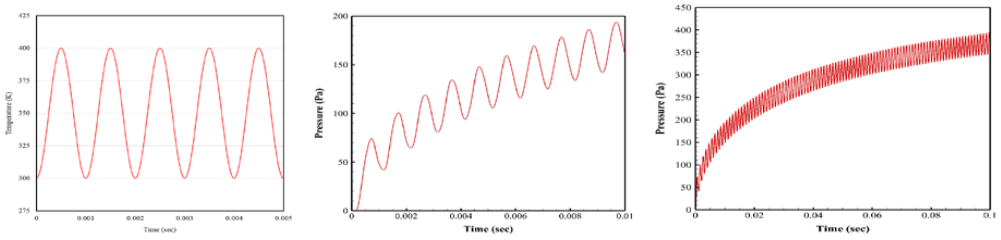

Figure 2: (a)Temperature variation of the heated film (b) predicted early time pressure variation 5.0 cm from the film (c) longer time pressure variation

Conclusions

The acoustic outputs consistently reached over 80 dB. At a critical power threshold of 57W a significant amount of distortion occurred. The goal of the study is not only to eliminate distortion, but to also understand the distortion effects as a function of temperature, power, or even possible direction of air flow or trapped air surrounding the thin film.

References

[1] Arnold and Crandall, "Thermophone as a Precision Source of Sound", Phys. Rev. 10 [1] (1917) 22-38

[2] Wente, "The Thermophone", Phys Rev. 19 [4] (1922), 333-345,

[3] Aliev et al. "Thermal Transport in MWCNT sheets and yarn, Carbon 45(2007) 2880-2888.

[4] Baloch et al. "Remote Joule heating by a carbon nanotube", Nature Nanotechnology, 39, (2012),1-4

[5] Jiang et al. "Superaligned Carbon Nanotube Arrays, Films, and Yarns: A Road to Applications", Advanced Materials, 23, (2011) 1154-1161

DEVELOPMENT OF A COMPACT THERMOACOUSTIC-STIRLING ELECTRIC GENERATOR

D. Wilcox*, P. Spoor

Chart Inc. - QDrive, 302 Tenth Street, Troy, NY 12180
**Corresponding author's e-mail: douglas.wilcox@chartindustries.com*

Keywords: *Power generation, Thermal-to-Electric Conversion, Commercialization*

Thermoacoustic-Stirling engines, or acoustic traveling-wave heat engines, have been shown to convert high temperature heat into acoustic power while maintaining a simple design with few moving parts. Previous experiments have demonstrated that a thermoacoustic-Stirling heat engine can convert thermal power to acoustic power with a conversion efficiency of 30% in the laboratory. [1] Typically, laboratory prototypes rely on embedded hot zones placed directly inside the pressure vessel to apply heat to the working fluid, have a long, bulky acoustic resonator, and deliver their work to an acoustic load rather than as electricity. While these features are acceptable for examining the fundamental acoustic and thermodynamic cycles in a laboratory setting, they do not address the challenging design requirements necessary for a commercially acceptable product. Recently, a compact thermoacoustic-Stirling electric generator, or TaSEG, consisting of two mirrored thermoacoustic engines coupled to a pair of electrodynamic alternators has been designed, constructed and is being tested. The main focus of this work has been developing a TaSEG design that has an acceptable thermal-to-electric conversion efficiency and moves this technology away from the laboratory towards a commercially viable product. This talk will explore the TaSEG design, touch on the tradeoffs between performance and manufacturability and present the TaSEG's experimental performance. Based on the TaSEG's performance results, recommendations for future work that might improve the overall efficiency of the TaSEG will also be discussed.

References

[1] Backhaus, S. and Swift, G. "A thermoacoustic-Stirling heat engine: detailed study". The Journal of the Acoustical Society of America, **107**, (2000), 3148–66.

Space Thermoacoustic Radio-Isotopic Power System: SpaceTRIPS

Antoine Alemany, Maurice Francois[1*], Kees de Blok[2], Roux Jean Pierre, - Poli Gerard[3], Eleonnora Zeminiani - Enrico Gaia[4], Phillipe Jeantet – Emmanuel Roy - Christian Chillet[5], Janis Freiberg, - Raimonds Nikoluškins[6], Gunter Gerbeth - Sven Eckert[7]

[1] Company HEKYOM Fr, [2] Company ASTER Ne, [3] Company AREVA T.A Fr., [4] Company Thales Alenia Space It, [5] CNRS Fr, [6] Institute of Physics of the University of Latvia IPUL Lv, [7] Helmholtz-Zentrum Dresden-Rossendorf HZDR De.
** Corresponding author's e-mail: Maurice.francois@hekyom.com*

Objective

The project relates to an advanced thermal to electric conversion for radio-isotopic power systems (RPS). Indeed RPSs are a key for space exploration as the solar power is very low in deep space, notably in Jupiter orbit and beyond. These systems will be also useful for Mars exploration, where solar power is subject to nights and dust storms. Thus, Europe aims to get its independence for such missions, and ESA have initiated development of RPS. If thermoelectricity fits well with small RPS (e.g.20We), for 100We range, high efficiency conversion is desirable. Indeed this leads to save between 2/3 up to 3/4 of the radioisotope mass. This is of real importance in term of cost and safety. Stirling converters under development in USA have low reliability due to pistons (sensitive to launch vibrations and shocks, subject to wear). Thermoacoustic (TAC), coupled with magneto hydrodynamic (MHD) generator is innovating technology free of moving parts. Unfortunately, the Technological Readiness Level is low and the priority is given to Stirling in ESA's programme, even if ESA has supported the first studies of TAC-MHD systems. This project is complementary with ESA's approach. So, the objective of this Project is to raise the TRL of this technology from 2 to 3-4 and show that this option is viable for European RPSs. The approach is based on 3 axes: Theoretical modeling, which has been already developed but needs to be validated, Experimentation of a thermo acoustic engine coupled with a MHD generator, Design of the space RPS, equipped with this conversion system, to check if the technology is suitable for space mission. The targets are: 1/ to validate the process efficiency (close to 20% or above), 2/ to justify the compatibility of the technology with space missions,

Methodological approach and results

The project is based on numerical calculation, design construction and test of a thermoacoustic loop coupled with an MHD generator using liquid sodium (cold source temperature above 400K), to convert mechanical energy furnished by the thermoacoustic loop in electricity. The TAC loop is of toroidal shape and is used in push pull action using two 'heat driven' thermoacoustic engine. In the facility the hot sources will be electrical resistances able to furnish 1400 w. the temperature at the hot source can reach 1200K. The other characteristic of this loop is given in Table 1.

Pressure values	Heat exchangers	40±0.6bars
	Three way connections	40±1bars
	MHD Adapters	40±7bars
Temperature	Hot heat exchangers	1100K
	Cold heat exchangers	400K
	Loop pipes	~400K

Table 1: *main values of the Thermo acoustic loop*

The MHD generator is used to convert the mechanical energy into electricity. For this purpose the proposed system is based on the oscillation of a liquid metal (sodium is considered the best fluid), imposed by the thermo acoustic effect. The interaction of the fluid oscillation with an imposed DC magnetic field produces an AC electric current circulating in the sodium with the same frequency than the oscillating velocity. This AC current generates itself an AC induced magnetic field, and an AC current in the coil connected with the load. The main elements of the MHD generator are given on figure 2. The oscillating flow (in blue) imposed by thermoacoustic loop, produces AC current in the liquid sodium. The AC current produces AC magnetic field that is transformed by induction process in AC current in a coil connected with the load (Fig. 2)

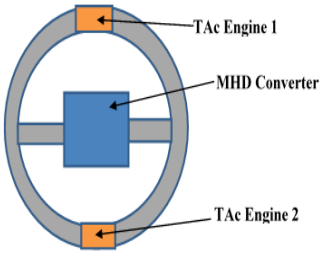

Fig. 1: *schematic structure of the thermos acoustic loop*

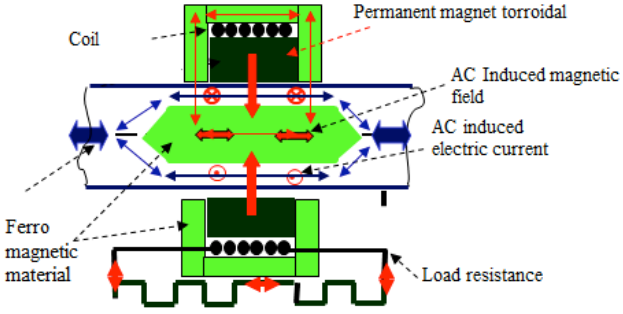

Fig. 2: *schematic structure of the MHD generator*

The real configuration of the built thermoacoustic prototype is given on figure 3. The different elements of the loop are represented and the MHD generator (Fig 4) is located in between the two green adaptors.

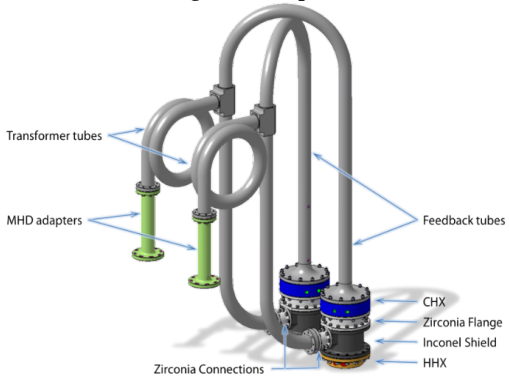

Fig. 3: *Main elements of the thermos acoustic loop*

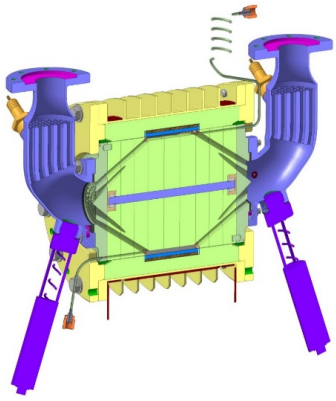

Fig. 4: *The MHD generator*

First results will be presented at the workshop. The targets below show the expected performances.

Electrical power	Expected efficiency	Thermal power	Temp Hot source	Temp Cold source	Carnot efficiency	Efficiency/ Carnot efficiency
200 W	η= 0.2	1200 W	1100 K	400 K	η = 60%	η = 0,35

Table 2: *The principal performances of thermoacoustic loop connected with MHD generator*

[1] Réf: The Space TRIPS Project: SPACE THERMOACOUSTIC RADIO-ISOTOPIC POWER SYSTEM: Maurice-Xavier François, Antoine Alemany, Emmanuel Roy, Janis Friebergs, Gerard Poli, Eleonora Zeminiani, Gunter Gerbeth. 23rd Conference of the Italian Association of Aeronautics and Astronautics. AIDAA2015, Torino,17-19 November 2015.

STREAMING
&
NON-LINEARITIES

SIMPLIFIED MODELING OF A THERMO-ACOUSTO-ELECTRIC ENGINE FORCED BY AN EXTERNAL SOUND SOURCE

C. Olivier, G. Poignand*, G. Penelet, and P. Lotton

*Laboratoire d'Acoustique de l'Université du Maine, UMR CNRS 6613, Avenue Olivier Messiaen, 72085 Le Mans cedex 9, France . *Corresponding author's e-mail: gaelle.poignand@univ-lemans.fr*

Keywords: *Thermoacoustics, Nonlinear dynamics, Active Control*

Introduction

Thermoacoustic wave-generators are usually designed and optimized using software tools [1, 2] based on the linear thermoacoustic theory. These tools enable to predict the operating point of a thermoacoustic engine from the balance between the thermoacoustic amplification process and the numerous nonlinear effects saturating wave amplitude growth, the latter effects being very difficult to describe properly. A non exhaustive list of these effects includes (apart from the thermoacoustic heat pumping accompanying wave amplification) different kinds of streaming, nonlinear acoustic propagation or aerodynamical and thermal entrance effects. These nonlinear effects are responsible for both dissipation of acoustic power and perturbations of the temperature field in the thermoacoustic core, that work together to limit the overall performances of thermal-to-acoustic conversion. Therefore, the development of adequate simulation tools is still needed to describe the high level of complexity of the processes involved above the onset of thermoacoustic instability. Direct numerical simulation seems to be the only way to reproduce quantitatively the effects mentioned above, but it is still limited by large computation times inherent to the complicated physics and multiple time and space scales involved in the description of thermoacoustic engines. Simplified analytical models can help in getting a deeper physical insight about the processes involved, but they are also based on substantial approximations. In this study, we use a simplified modeling of thermoacoustic engines to help understanding recent experimental observations dealing with the external forcing of thermoacoustic oscillations [3–5].

Aims and scope of the study

Recent proof of concept studies [3,4] performed at LAUM have already shown that the external forcing of thermoacoustic oscillations could be an interesting way to increase the efficiency of a thermoacoustic prime-mover. In particular, we have shown that the adjunction of an adequately tuned electroacoustic feedback loop to a thermo-acousto-electric transducer can lead to the increase of its global efficiency [4]. Using a reference pressure signal from the engine as an input, an auxiliary acoustical source is used to control self-sustained thermoacoustic oscillations in the engine. By tuning the properties of this feedback (in terms of amplification gain and phase-shift relative to the reference signal), the efficiency of the transducer can either be reduced down to the death of the auto-oscillations, or increased, thus generating a greater output power for the same heat input. More recently, we have shown on the same device that the electroacoustic feedback loop is also responsible for the occurrence of hysteretic behavior [5] of both the temperature difference across the regenerator and the efficiency versus the heat input. However, at the present time the multiplicity of the involved nonlinear effects and their complexity does not allow to understand why and how the mechanisms at stake in this process of "active control" enable to increase the global efficiency of the thermoacoustic engine. It is there-

fore worth considering to make theoretical studies on the topic. This task is however arduous because a pre-requisite is to understand deeply and to describe properly the self-sustained oscillator itself before describing its nonlinear coupling with external sound sources. However, we plan as a first step to find a qualitative description of the dynamics of the system which would be well-suited for the analysis of its bifurcation diagram and its response to external forcing. Such kind of approach is very common in nonlinear dynamics in which complicated systems are sometimes summarized by a few ordinary differential equations.

In this study, a simplified model of a thermo-acousto-electric generator is proposed. This reduced-order model is based on a lumped element approach for the description of the acoustic propagation in the engine, coupled with a resolution of unsteady heat transfer through the thermoacoustic core based on a finite difference scheme. This description allows the study of both transient and steady-state operation of the engine. Applying an external forcing to that model also allows to get a better overview of the effects of the feedback loop on the engine. Notably, by gradually increasing its degree of complexity, it enables to study various parameters, such as the coupling of the auxiliary electrodynamic source with the engine, and the influence of the feedback on both the acoustic field and on the distribution of the temperature field within the thermoacoustic core. This simplified model of a forced thermoacoustic transducer will help to get a better understanding of the phenomena responsible for the complex behaviors induced by the electroacoustic feedback loop on the actual prototype: death of oscillations, efficiency improvement accompanied by a temperature gradient reduction, as well as a hysteretic behavior induced by the electroacoustic feedback loop during the processes of gradual heat input increase followed by a gradual decrease.

References

[1] Ward W.C., Swift G.W., Design Environement for low Amplitude ThermoAcoustic Engines, J. Acoust. Soc. Am., 95:3671-3672, 1994.

[2] G.W. Swift, *Thermoacoustics: A unifying perspective for some engines and refrigerators* (Acoustical Society of America, Melville NY, 2001).

[3] C. Desjouy, G. Penelet, P. Lotton, Active control of thermoacoustic amplification in an annular thermoacoustic engine, J. Appl. Phys., 108:114904, 2010.

[4] C. Olivier, G. Penelet, G. Poignand, P. Lotton, "Active control of thermoacoustic amplification in a thermo-acousto-electric engine", J. Appl. Phys., 115:174905, 2014.

[5] G. Poignand, C. Olivier, G. Penelet, P. Lotton, ÂńÂăHysteretic behavior induced by an electroacoustic feedback loop in a thermo-acousto-electric generatorÂăÂż, submitted to Appl. Acoust., 2015

NUMERICAL SIMULATION OF MINOR LOSSES IN OSCILLATING FLOW

S. Mukhopadhyay* and B. J. Boersma

Process and Energy Department, Delft University of Technology, Delft, The Netherlands.
**Corresponding author's e-mail: s.mukhopadhyay@tudelft.nl*

Keywords: *oscillating flow, diffuser, minor loss, RANS*

Introduction

Thermoacoustic devices operate on conversion of heat into acoustic energy and vice versa for use in heat engines or refrigerators [2]. Normally the conversion between thermal and acoustic energies is realised by oscillating gas flow. The main advantages are lack of moving mechanical parts and use of non polluting inert gases as working medium. The present efficiency levels are as high as 49% of the Carnot efficiency [3] but the efficiency levels need further improvement to take them to commercial scales. Significant improvement can be achieved by reducing losses in pipe bends, expansions or entrances (other than in a straight passage) which are generally termed as minor losses. Minor losses in oscillating flows can dissipate significant acoustic power in thermoacoustic heat pumps and refrigerators [2]. Numerical simulation of minor losses can help in improving the design of thermoacoustic devices. In this work, we investigate performance of Reynolds-Average Navier-Stokes (RANS) method in capturing minor losses in incompressible oscillating flow by comparing with available experimental data.

Problem Formulation and Numerics

Air flow in a 2-D diffuser section with 30° angle is chosen from the experimental studies of oscillating flows in 2-D diffuser [1]. Oscillation amplitude and a measure of driving frequency are required to define oscillating flow in a channel. The amplitude can be described by Reynolds number defined as- $Re_\delta = \frac{u_{max}\delta}{\nu}$ where u_{max} is the maximum velocity through the cycle in the channel, ν is the kinematic viscosity and $\delta = \sqrt{\nu/\pi f}$, f is the oscillation frequency.

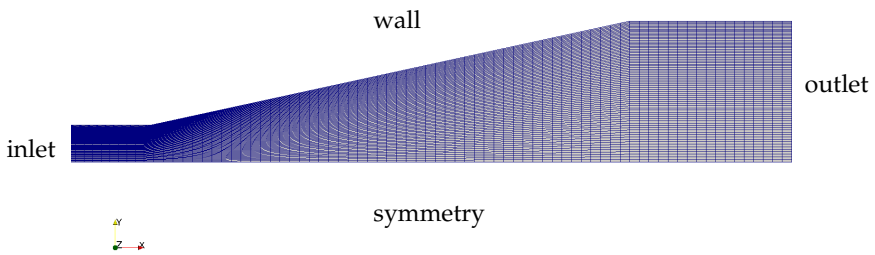

Figure 1: *Schematic representation of the computational domain, mesh and boundary conditions.*

The Computational Fluid Dynamics (CFD) code Open Source Field Operation and Manipulation (OpenFOAM) based on the finite volume method (FVM) is used for the numerical simulations. The standard high Reynolds number k-ϵ model along with wall function is applied as it is most commonly used in industry. The OpenFOAM transient solver pimpleFoam (based on merged PISO-SIMPLE algorithm) for incompressible flow is used with second order dis-

cretisation schemes. Only half of the domain is simulated taking advantage of symmetry and boundary conditions are shown in Figure 1. At inlet a sinusoidal velocity profile is prescribed. To capture the unsteady flow physics and ensure convergence small time steps are used, automatically adjusted by the solver to maintain Courant number below 0.9. Flows with $Re_\delta = 740$ are investigated for different dimensionless displacement amplitude, L_0/h as given in Table 1.

Table 1: *Oscillation frequencies simulated at $Re_\delta = 740$ for 30° diffuser*

L_0/h	25	28	31	35	40
f (Hz)	20.41	16.27	13.27	10.41	7.97
u_{max} (m/s)	26.67	23.81	21.51	19.05	16.67

Results and Discussion

The results for sum of minor losses ($K_B - K_S$) and normalized acoustic power dissipation ($\dot{E}/\rho A u^3$) computed like [1] are presented as function of L_0/h in Figure 2. The results are in line with experimental findings with the deviations more pronounced at low oscillating frequencies. It is found that minor losses and acoustic power dissipation grow with increasing displacement amplitude (or decreasing oscillating frequency). Thus standard high Reynolds number k-ϵ model is able to predict the trend but further investigation is required to improve quantitative prediction. Additional studies will be presented during the workshop.

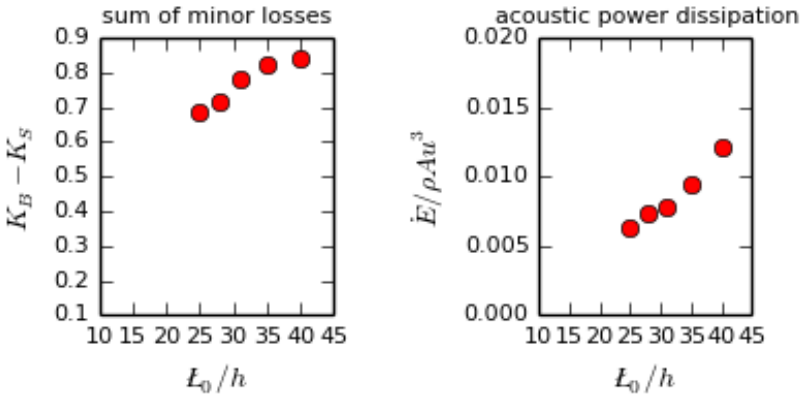

Figure 2: *Minor losses ($K_B - K_S$) and normalized acoustic power dissipation ($\dot{E}/\rho A u^3$).*

Acknowledgements

The authors are grateful to Energy research Centre of the Netherlands (ECN) for funding this research work.

References

[1] King, C. V. and Smith, B. L. "Oscillating flow in a 2-D diffuser". Experiments in Fluids, **51**, (2011), 1577–1590.

[2] Swift, G. *Thermoacoustics: A Unifying Perspective for Some Engines and Refrigerators*. Acoustical Society of America (**2002**).

[3] Tijani, M. E. H. and Spoelstra, S. "A high performance thermoacoustic engine". Journal of Applied Physics, **110**, 093519.

ON GENERAL EXPRESSIONS OF TEMPORAL MEANS OF MASS FLUX, SHEAR STRESS AND HEAT FLUX DUE TO THERMOACOUSTIC WAVES

N. Sugimoto

Department of Pure and Applied Physics, Faculty of Engineering Science, Kansai University, Suita, Osaka 564-8680, Japan.
e-mails: n_sugimo@kansai-u.ac.jp, sugimoto@me.es.osaka-u.ac.jp

Keywords: *nonlinear, diffusion-wave equation, temperature gradient, regenerator, acoustic streaming, mass flux, heat flux, shear stress.*

Introduction

Performance of thermoacoustic heat engines is determined crucially by various nonlinear phenomena. Among them, steady streaming of mass and energy impacts on it significantly. To aim at making its quantitative description, nonlinear theory of thermoacoustic waves in a channel and a tube has been developed by the author and a nonlinear diffusion-wave equation has been derived for a case that a diffusion layer is thick enough compared with a span length [1]. Within the same framework, this paper derives general expressions of temporal means of mass flux, shear stress and heat flux on a wall by assuming time-periodic wave. It is shown that the mean pressure is set down and that all mean values are expressed in terms of the mean pressure and its spatial gradients.

Nonlinear diffusion-wave equation and general expressions for the temporal mean values

When a typical diffusion layer is thick enough compared with a span length of a channel and a tube as in a gas in regenerators, propagation of nonlinear thermoacoustic waves therein is governed by the following diffusion-wave equation in an axial coordinate x and a time t as

$$\frac{\partial p'}{\partial t}-\frac{\partial}{\partial x}\left(\alpha_e\frac{\partial p'}{\partial x}\right)+\frac{\alpha_e}{T_e}\frac{\mathrm{d}T_e}{\mathrm{d}x}\frac{\partial p'}{\partial x}$$
$$+[n\gamma-(\gamma-1)\mathrm{Pr}]\frac{\alpha_e}{a_e^2}\frac{\partial^2 p'}{\partial t^2}-m(1+\beta+\mathrm{Pr})\frac{\alpha_e H^2}{\nu_e T_e}\frac{\mathrm{d}T_e}{\mathrm{d}x}\frac{\partial^2 p'}{\partial t\partial x}-\frac{p'}{p_0}\frac{\partial p'}{\partial t}-\frac{\alpha_e}{p_0}\left(\frac{\partial p'}{\partial x}\right)^2=0, \qquad (1)$$

where p_0 and p' denote, respectively, a uniform pressure in a quiescent state and an excess pressure from it; T_e denotes a wall temperature non-uniform axially, which is assumed to be fixed temporarily; $\alpha_e(=ma_e^2H^2/n\gamma\nu_e)$ denotes a diffusivity of acoustic waves in a channel of span length of $2H$ and in a tube of radius $R(=H)$, respectively, with the pair of constants $m=2/5$ and $n=6/5$, and the one of $m=1/6$ and $n=8/6$, a_e, ν_e, β, γ and Pr being, respectively, an adiabatic sound speed, a kinematic viscosity, a factor in the temperature dependence of viscosity, the ratio of specific heats and Prandtl number.

Assuming time-periodic solutions to (1), it is found that

$$\frac{\alpha_e}{T_e}\widetilde{\left(\frac{\partial p'}{\partial x}\right)^2}=-p_0\frac{\partial}{\partial x}\left(\frac{\alpha_e}{T_e}\frac{\partial\widetilde{p'}}{\partial x}\right), \qquad (2)$$

where a tilde designates a temporal mean over one period. This shows that the gradient of the mean pressure $\tilde{p}'$ is of quadratic order in disturbance and that the mean of the pressure gradient squared is expressed in terms of the derivative of the mean pressure gradient. It is noted that finite effects of span length, represented by the first two terms on the second line in (1), do not contribute to (2).
In a similar fashion, mean values of the mass flux, shear stress and heat flux on the wall are expressed in terms of the mean of the products of spatial and/or temporal gradients of the excess pressure, which are in turn expressed in terms of the mean pressure gradient through (2). Hence once the mean excess pressure is available, all means are obtained in terms of it.

Summary

Because thermoacoustic heat engines do not consist of the regenerator only, (1) should be solved in conjunction with other nonlinear wave equations for propagation in a buffer tube, a heat exchanger and a tube without temperature gradient. In fact, the linearized version of (1) has been solved in this way to derive marginal conditions for the onset of thermoacoustic oscillations in a gas-filled tube [2]. Although no attempt to include the nonlinear terms has been made, it is expected to obtain autonomous excitation of thermoacoustic waves of finite amplitude. When these time-periodic waves are available, it is straightforward to have mean values due to steady streaming of mass and energy. Their expressions may illuminate a way how to control the streaming.

Acknowledgements

The author acknowledges the support of the Grant-in-Aid for Scientific Research (KAKENHI #26289036) by the Japan Society of Promotion of Science.

References

[1] Sugimoto, N. "Nonlinear Diffusion-Wave Equation for a Gas in a Regenerator Subject to Temperature Gradient", to be presented at the 20th International Symposium on Nonlinear Acoustics, June 29-July 2, 2015 in Lyon, France.

[2] Hyodo, H. and Sugimoto, N. "Stability analysis for the onset of thermoacoustic oscillations in a gas-filled looped tube", J. Fluid Mech., **741**, (2014), 585-618.

A MATHEMATICAL MODEL OF ACOUSTIC THERMAL EXCITATION FOR PULSE TUBE ENGINE

E.A. Zinovyev, A.I. Dovgyallo, S.O. Nekrasova*

Thermal Engineering and Heat Engines, Aircraft Engines and Power Plants, Samara State Aerospace University, 34, Moskovskoe shosse, 443086 Samara, Russia. Corresponding author's e-mail: yhoji@yandex.ru

Keywords: *pulse tube engine, nonlinear processes, transient mode, standing-wave.*

Introduction

The most of works applied for the pulse tube converters contain the workflow description implemented through the use of mathematical models on stationary modes. However, the study of the thermoacoustic systems unsteady behavior in the start, stop, acoustic load changes modes is in the particular interest. Yuan et.al. [1] offered a simplified quasi-one-dimensional model of a thermoacoustic engine that described the amplification of acoustic oscillations and their subsequent "saturation" at the launch phase. For the study of the standing wave thermoacoustic engines functioning in the start mode Karpov et.al. [2] applied a weakly non-linear theory of the thermoacoustic instability in a channel with temperature gradient. The motivation for this work was provided by the research results of the lumped thermal capacity model presented by Matveev [3]. The aim of the present study is to develop a mathematical thermal excitation model of acoustic oscillations in pulse the tube engine (PTE) (Figure1) in more general formulation of the mathematical description. A half-length cylindrical resonator length is 240 mm, resonator radius – 10 mm, regenerator length – 60 mm, porosity – 0.89, piston mass – 0.02 kg.

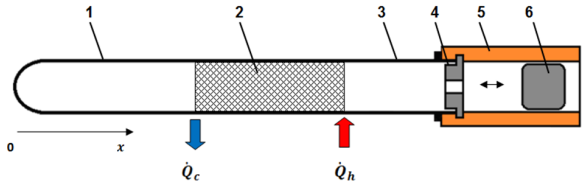

Figure 1: *Scheme of the pulse tube engine*

1 – resonator; 2 – regenerator; 3 – pulse tube; 4 – jet nozzle; 5 – cylinder; 6 – piston.

The model assumes the assignment of any porosity (for stack or regenerator), takes the piston weight and the friction in the cylinder and piston unit into account, and determines the operating frequency (in contrast to [3], where the fundamental acoustic mode was considered). The numerical method is based on the relation equations between the pressure and volume velocity variables at the ends of each element of PTE which is recorded through the appropriate transformation matrix. A solution demonstrates that the PTE operation frequency is the complex value, and it depends on the piston mass and the dynamic friction due to its movement in the cylinder. The real part of frequency variable determines the actual operating frequency of the engine, and the imaginary determines the damping factor of the oscillations. On the basis of the determined frequency thermoacoustically induced heat transport and generation of acoustic power equations were solved for channel with temperature gradient on its ends. This model was applied to a small-scale scheme of pulse

tube engine (Figure1) operating at atmospheric air. Unlike the work [3] this standing wave configuration is a fully closed system. The results of numerical simulation demonstrate the features of the initialization process of PTE and show that high-amplitude acoustic oscillations can occur in the initial moment of time (Figure2) as [3] presented. The fact that generated acoustic power more than power on the steady mode in a factor of 3…4 doesn`t mean the possibility of its it`s further continuous utilizing due to its existence only in transient mode which lasts only for a 30-40 sec.

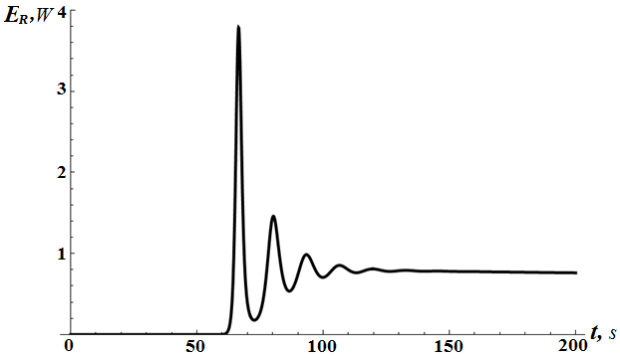

Figure 2: *Acoustic power generated in the regenerator.*

The experiments were carried out on small-scale scheme of the pulse tube engine. The data registration of the pressure changing as a function of the piston length displacement on the oscilloscope was implemented. The results shows that the value of acoustic power W_{ac} is in the range of 0.7..1.05 W for the defined frequency range f = 13... 18 Hz and pressure amplitudes 11...12 kPa. These experimental data are satisfactorily correlated with the numerical modeling results. The mathematical model can be straightforwardly applied for the thermoacoustic devices with variable temperatures of thermal reservoirs and variable transduction loads which are expected to occur in practical implementations of portable thermoacoustic engines.

References

[1] Yuan H., Karpov S., Prosperetti A. "A simplified model for linear and nonlinear processes in thermoacoustic prime movers. Part II. Nonlinear oscillations", J. Acoust. Soc. Am., **102 (6)**, (1997), 3497-3506.

[2] Karpov S., Prosperetti A. "Nonlinear saturation of the thermoacoustic instability", J. Acoust. Soc. Am., **107 (6)**, (2000), 3130-3147.

[3] Matveev K.I. "Unsteady model for standing-wave thermoacoustic engines", J. Non-Equilib. Thermodyn., **35(2)**, p. 85-96.

ESTIMATION OF DIFFERENT NUMERICAL PULSE TUBE THERMOACOUSTIC REFRIGERATOR MODELS

Nekrasova S.O.[1*], Sarmin D.V.[1], Shimanov A.A.[1] ,Uglanov D.A.[1]

[1] *Department of heating engineering and heat engines, Samara State Aerospace University, Moskovskoe shosse 34, 443086, Samara, Russia, *yhoji@yandex.ru*

Keywords: *thermoacoustic refrigeration, oscillatory flow, computational modeling, pulse tube, porous media.*

Introduction

The design of the pulse tube refrigerators has continually evolved since the invention of the main PTR [1] with the aim of improving their performance. Last modification of the design was the refrigerator with the inertance tube (IPTR), which established the necessary phasing between speed and pressure, Cha et al. [2] presented the results of numerical simulations in FLUENT, Ashwin et al. [3] used a thermal non-equilibrium model for the simulation of processes in cryocooler. Thus, the aim of the research was the estimation of applicability of parallel methods: thermodynamic and finite-difference simulation in an integrated approach for the design engineering methodology of the thermoacoustic pulse tube refrigerator.

For the first step of OPTR design engineering methodology to get the optimum dimensions in terms of a minimum level of cooling the thermodynamic model of calculating parameters of the cryocooler was used [10]. The geometry, dimensions of OPTR and cases of studies are the same of [4] to be able to compare the calculated results with the experimental data presented in this paper (Fig. 1). The theoretical model of an idealized operating cycle describes 1) the filling process of cryocooler, 2) pressing of the fluid through the OPTR axis, 3) isentropic expansion in the pulse tube with heat rejection in the hot heat exchanger and 4) irreversible adiabatic compression of the gas in the compliance volume, 5) irreversible adiabatic and 6) isentropic expansion of the gas during the return stroke of the piston. The calculation was made with the assumption of an ideal heat transfer in the both heat exchangers, regenerator; the processes in the pulse tube and the compliance volume were assumed adiabatic, hydraulic resistance along the length of the OPTR was not considered, operating cycle was described as step-like process with instantaneous changes of flow parameters in cryocooler. The energy conservation equation for an open thermodynamic system, the equation of state and equation considering pressure changing as a function of temperature of the fluid was solved for each element of the OPTR geometry. Three different cases of mass fluid distribution from the pulse tube into the compliance volume during the OPTR operating cycle were considered [5]. The calculation was performed for the three cryocooler operating modes (Table 1) similar [4], the pressure in the compliance volume for the each operating mode were obtained by the authors using OPTR numerical simulation in ESI ACE +. Computational results show deviations from the experimental values of 5-8% (Table 2).

An integrated approach of design methodology was to execute an additional modeling of OPTR in two software products ESI CFD ACE + and Fluent.

Table 1. *List of operating modes at 65 Hz simulated*

№	Mean pressure P_0 (MPa)	Mean pressure in compliance volume P_{P1} (MPa)	Pistone displacement A_0, m	T_{exp}, K [9]	Gas temperature in cold heat exchanger $\bar{T}$, K
1	1.4	1.375	0.00210	142	154.4
2	1.74	1.715	0.00195	129	134.5
3	2.2	2.167	0.00175	126.5	123.2

The simulation of 10 seconds duration of each OPTR operating mode was produced. Temperatures on the cold heat exchanger were recorded every 0.1 s. For modeling the processes in OPTR using the program Ansys Fluent was built similar 2-D model in size [4] and it was set the appropriate settings of the boundary conditions. Depending on the frequency step is changed from $0.11 \cdot 10^{-3}$..$0.15 \cdot 10^{-3}$s. The results of the calculation are presented in table 2.

Table 2: *The temperature of the gas in the cold heat exchanger 10 seconds of work*

№ mode/frequency	1/55	1/55	1/55	2/65	2/65	2/65	3/75	3/75	3/75
CFD-ACE	155	155	152	152	151	150	150	150	142
Fluent	167	148	137	174	144	136	164	153	128

Thermodynamic model demonstrated the discrepancy 5-8% between the results of the cold heat exchanger temperature from the experimental data [4] that is quite acceptable for a preliminary assessment of the OPTR cooling level and the amount of heat that can get the load heat exchanger. Comparative analysis of simulation results in OPTR based on the three methods showed similar temperatures and geometrical relations coolers. This fact allows us to conclude that the design phase of the newly created OPTR it is enough to use one of the methods, or their combination. This enables better-informed and more rational use of high-level techniques for revised calculations.

References

[1] Gifford, W., Longsworth, R. "Pulse-tube refrigeration. Trans ASME", J Eng Ind (series B) 1964; 86: 264–268.

[2] Cha, J.S., Ghiaasiaan, S.M., Desai, P.V., Harvey, J.P., Kirkconnell C.S., "Multi-dimensional flow effects in pulse tube refrigerators", Cryogenics, 46, (2006), 658–665.

[3] Ashwin, T.R., Narasimham, G.S.V.L.., Subhash Jacob. "CFD analysis of high frequency miniature pulse tube refrigerators for space applications with thermal non-equilibrium model", Applied Thermal Engineering , 30 (2010), 152–166.

[4] Dion Savio Antao, Bakhtier Farouk. "Experimental and numerical investigations of an orifice type cryogenic pulse tube refrigerator" Applied Thermal Engineering, 50 ,(2013), 112-123.

[5] Mikulin,E., Tarasov, A., Shkrebyonock , M. "Low-temperature expansion pulse tubes". Adv. Cryogen. Eng., 29, 629–637.

NUMERICAL INVESTIGATION OF HEAT EXCHANGE BETWEEN FLUID AND SOLID WALL OF OSCILLATORY FLOW

K. Kuzuu[1*] and S. Hasegawa[1]

[1] *Department of Prime Mover Engineering, Tokai University, Hiratsuka, Kanagawa, 2591292, Japan.*
**Corresponding author's e-mail: kuzuu@tokai-u.jp*

Keywords: *CFD, large displacement amplitude, heat flux, heat exchanger, self-oscillation, thermoacoustic device*

Introduction

With respect to the estimation of heat transfer of oscillatory flow inside the engine, some numerical approaches combined with the classical linear thermoacoustic theory are suggested [1][2]. In their studies, the heat transfer of oscillatory flow considering heat exchange between wall and fluid is discussed, and phase dependent heat transfer rates and Nusselt numbers are investigated. However, for the oscillatory flow with larger displacement amplitude, which can be occurred in the actual engine, we have to consider the interaction of heat transfers among the heat exchangers, the stack and the resonator, and the conventional approach cannot reproduce those interactions.

Numerical Simulation

The present numerical simulation is based on three-dimensional unsteady compressible Navier-Stokes equation. Figure 1 shows the computational domain and the boundary conditions of the present simulation. Here, the thermoacoustic device is composed of two resonance tubes, two heat exchangers and a stack, and the engine core has six flat plates. The wall temperature is given as shown in Fig.1.

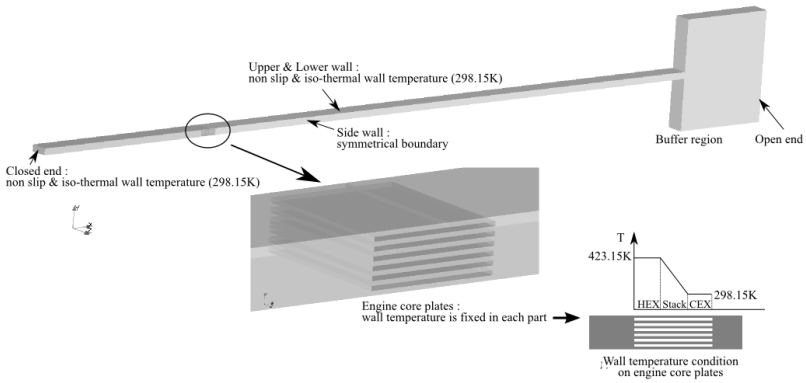

Figure 1: *Configuration of the computational domain and the boundary conditions.*

Results

The present simulation reproduces the self-oscillatory flow. To generate the self-oscillation, we execute the following procedures in the simulation. First, after the start of the simulation, we continue supplying the acoustic wave from the open end of the resonance tube for a

while. After 2.5 seconds, which corresponds to 1250000 time steps of the simulation, the supply of the acoustic wave is stopped. After that, we judge whether the self-oscillation is reached or not by monitoring the variation of the pressure and velocity amplitudes. The obtained self-oscillatory flow has large displacement amplitude in this condition. The amplitude is about 30 mm, the length of each engine core component (heat exchanger and stack).

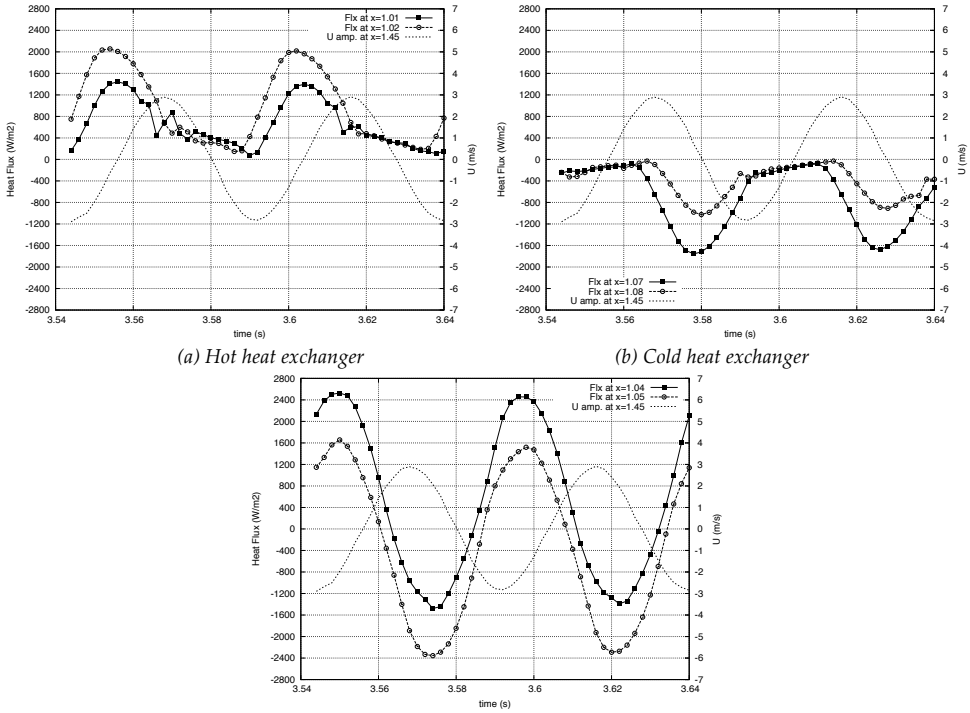

(a) Hot heat exchanger *(b) Cold heat exchanger*

(c) Stack

Figure 2: *Time variation of heat flux on the wall of each component of the engine core (from wall to fluid : positive).*

From the CFD results, we investigate the heat flux of each engine core component. Figure 2 shows the heat flux on the wall of the hot and cold heat exchangers and the stack. As shown in the figures, with respect to the heat flux of the heat exchangers, the symmetry of the harmonic oscillatory flow collapses while the velocity amplitude keeps the sinusoidal curve. On the other hand, the symmetry is kept in the region of the stack. These results might be due to the fact that the convective heat transfer in the axis direction is affected by the large displacement of fluid element. Furthermore, it is clear that this behavior can be regarded as nonlinear effect, and we have to consider this effect for estimating the performance of the thermoacoustic engine. In the present study, we have a plan to investigate these mechanisms more in detail.

Acknowledgements

This work was supported by the Japan Science and Technology Agency through the Advanced Low Carbon Technology Research and Development Program.

References

[1] Piccolo, A. and Pistone, G., *Int. J. Heat Mass Tran*, 49, 1631-1642 (2006).

[2] Jaworski , A. J. and Piccolo , A., *Applied Thermal Engineering* 42, 145–153 (2012).

HIGH-FIDELITY AND LOW-ORDER MODELING OF A TRAVELING-WAVE THERMOACOUSTIC ENGINE

Carlo Scalo[1*], Sanjiva K. Lele[2], Lambertus Hesselink[3]

[1]*School of Mechanical Eng. and Aeronautics and Astronautics, Purdue University, IN, 47907, USA*
[*]*Corresponding author's e-mail: scalo@purdue.edu (current affiliation)*
[2]*Dept. of Aeronautics and Astronautics and Mechanical Eng., Stanford University, CA, 94305, USA*
[3]*Dept. of Aeronautics and Astronautics and Electrical Eng., Stanford University, CA, 94305, USA*

Keywords: *thermoacoustic instability, streaming, traveling-wave, thermal-buffer tube, Stirling cycle, Lagrangian dynamics*

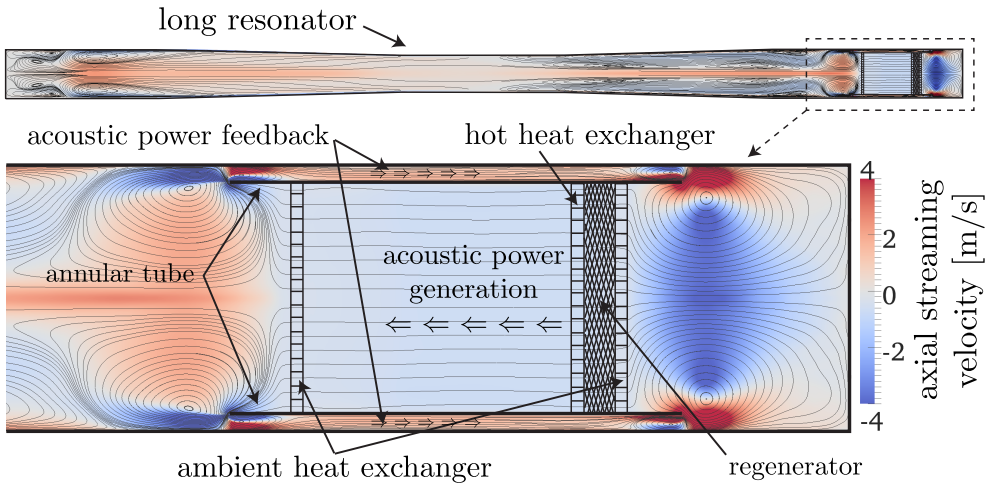

Figure 1: *Contours of axial component of time-averaged streaming velocity $\langle \tilde{u}_x \rangle$ for $T_h = 500K$. Full-scale visualization (a) and zoom on the right end (b).*

Inspired by the work of Lycklama à Nijeholt et al. (2005) [1], Scalo *et al.*, (2015) [2] have devised a simple traveling-wave TAE model that could serve as a benchmark case for high-fidelity numerical simulations of similar devices. We have extended such setup to three-dimensions and introduced a second ambient heat-exchanger to achieve a limit cycle, modeling typical fluid dynamic conditions found in thermal buffer tubes. While the simplicity of the adopted REG/HX heat-transfer and drag models allows for the straightforward development of companion linear and nonlinear models (necessary for verification of the Navier-Stokes calculations), other important processes typically occurring in REG/HX are, inevitably, not directly simulated.
The time integration is carried out from initial quiescent conditions to the limit cycle. It is shown that the mechanisms responsible for the acoustic energy generation and propagation in the system during the start-up phase can be explained with linear acoustics, despite the high amplitude ($\sim$ 1% of the mean) of the initial perturbation resulting from the activation of the source terms modeling the heat transfer. An analytical linear Lagrangian model shows that the thermoacoustic instability occurring in the regenerator/heat-exchanger (REG/HX) unit intensifies plane waves traveling in the direction of the imposed temperature gradient via a process resembling a thermodynamic Stirling cycle. The result is the establishment of a network of self-amplifying traveling waves looping around the REG/HX unit. A system-wide linear stability

model based on Rott's theory accurately predicts the frequency of the (only) unstable mode as well as the critical temperature ratio, despite not accounting for viscous and other nonlinear losses. The dependency of growth rates and limit-cycle pressure amplitudes on the temperature ratio are shown to be consistent with a supercritical Hopf bifurcation model. No evidence has been found to support subcritical or non-modal instability arguments.

At the limit cycle acoustic amplitudes exceed +170dB and nonlinear effects dominate the flow field in the form of transitional turbulence and acoustic streaming. The latter is the occurrence of a quasi-steady flow evolving over time scales much longer than the period of the waves inducing it. The data from the full three-dimensional simulations has allowed to identify the governing processes driving the streaming flow, which are viscous wave amplitude decay in the feedback inertance, periodic vortex ring roll-up and break-up around the sharp edges of the annular tube, and near-wall acoustic shear-stresses in the variable-area resonator.

An axially-symmetric numerical model based on Stokes-streamfunction formulation has been adopted to directly simulate the streaming flow as the solution of the incompressible Navier-Stokes equations driven by the divergence of the wave-induced Reynolds stresses extracted from the fully compressible three-dimensional calculations. The model correctly reproduces the streaming flow patterns and, in spite of the strong assumptions made and numerical issues associate with geometric singularities, it correctly predicts the intensity of the Gedeon streaming. The latter is responsible for the decrease of the engine's efficiency as the drive ratio is increased, and a robust parametrization for it is warranted. The investigation of the scaling of nonlinear fluxes reveals the importance of prior knowledge of the critical temperature ratio, which may not be straightforwardly achieved by simply relying on linear theory, for more complex systems. More details can be found in Scalo *et al.*, (2015) [2].

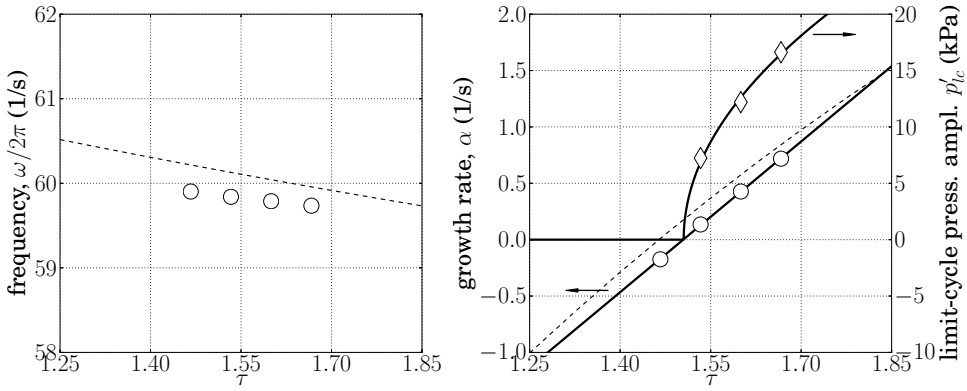

Figure 2: *Frequency, $\omega/2\pi$ (a), growth rate, α, and limit-cycle pressure amplitude p'_{lc} (b) versus hot-to-cold temperature ratio, $\tau = T_h/T_c$. Linear stability model (- - -), numerical simulations (symbols) with corresponding fitting (—) yielding critical temperature ratio $\tau_{cr} = 1.505$ and $p'_{lc}|_{\delta\tau=1} = 41,000$ Pa.*

References

[1] Lycklama à Nijeholt, J., Tijani, M., and Spoelstra, S. "Simulation of a traveling-wave thermoacoustic engine using computational fluid dynamics". J. Acoust. Soc. Am., **118**, (2005), 2265–2270.

[2] Scalo, C., Lele, S. K., and Hesselink, L. "Linear and Nonlinear Modeling of a Theoretical Traveling-Wave Thermoacoustic Heat Engine". J. Fuid Mech., **766**, (2015), 368 – 404.

PERFORMANCE MEASUREMENTS OF JET PUMPS WITH MULTIPLE HOLES

J.P. Oosterhuis[1*], S. Bühler[1], D. Wilcox[2], and T.H. van der Meer[1]

[1] *Thermal Engineering, Engineering Technology, University of Twente, P.O. Box 217, 7500AE, Enschede, The Netherlands.*
**Corresponding author's e-mail: j.p.oosterhuis@utwente.nl*
[2] *Chart Inc., Troy, New York, USA.*

Keywords: *jet pumps, minor losses, flow separation, acoustic streaming*

Introduction

In order to cancel Gedeon streaming in traveling wave thermoacoustic devices, a jet pump can be used [2, 3]. Due to its asymmetric shape an asymmetry in the minor losses during each acoustic cycle occurs that yields a time-averaged pressure drop across the jet pump. By balancing the time-averaged pressure drop across the jet pump with that which exists across the regenerator of a thermoacoustic device, Gedeon streaming can be suppressed.
The current state of the art in jet pump design methodology is based on a quasi-steady approximation [2]. In a recent numerical study we have shown that the applicability of this approximation is limited [4]. Currently, the previous numerical work is extended to the experimental domain to investigate the influence of three-dimensional geometry variations. By "splitting" a jet pump with a single hole into a geometry with multiple parallel holes, the size of the jet pump can be reduced while maintaining the taper angle and the total cross-sectional area. Reducing the size of the jet pump will aid in the design of compact thermoacoustic engines.

Method

The experimental setup is shown schematically in Figure. 1 and is similar to the setup previously used by Aben [1]. A 40 Hz acoustic wave is generated using a loudspeaker. Both the pressure amplitude p_1 and the time-averaged pressure p_2 are measured at four different locations as indicated by P1–P4 in Fig. 1. From the measured pressure amplitude the velocity amplitude inside the jet pump $u_{1,JP}$ and the acoustic power dissipation $\Delta\dot{E}_2$ are calculated. Eight different jet pump samples are investigated having a various number of holes (1, 2, 4, 8 and 16) and two different taper angles (7° and 15°). The total cross-sectional area is kept constant at both openings and the jet pump length is varied in order to maintain the correct taper angle among the different samples.

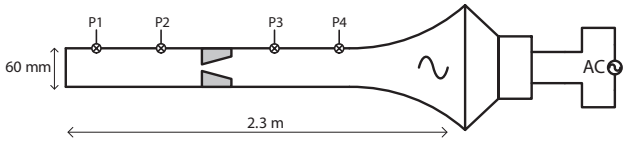

Figure 1: *Schematic of experimental setup with pressure sensors and jet pump sample indicated. Dimensions not to scale.*

Results and discussion

Figure. 2 shows the jet pump performance in terms of the dimensionless pressure drop and acoustic power dissipation which are defined using [5],

$$\Delta p_2^* = \frac{8\Delta p_2}{\rho_0 |u_{1,JP}|^2}, \qquad \Delta \dot{E}_2^* = \frac{3\pi \Delta \dot{E}_2}{\rho_0 A_s |u_{1,JP}|^3}, \tag{1}$$

with A_s the total cross-sectional area at the jet pumps small opening. On the horizontal axis, KC_D is the Keulegan–Carpenter number based on the diameter of the small jet pump opening and represents the wave amplitude. While the samples with one or two holes (● and ■) show a comparable performance for $KC_D > 10$, the pressure drop is significantly decreased for jet pump samples with 4 or more holes (▼, ♦ and ★). This is observed for both the 7° and 15° taper angles. However, the time-averaged pressure drop for the 15° taper angle is generally lower which is probably caused by stronger flow separation in the diverging flow direction. The dimensionless acoustic power dissipation shows a mixed trend. Albeit the 16 hole jet pump shows higher acoustic power dissipation compared to the single or double hole jet pump samples, a definitive trend could not be distinguished based on these results.

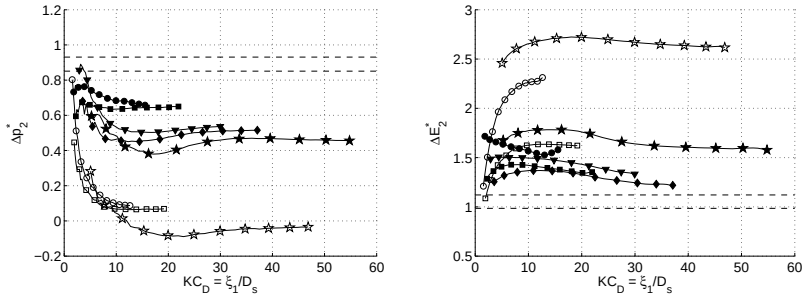

Figure 2: *Dimensionless pressure drop (left) and dimensionless acoustic power dissipation (right) for all jet pump samples. Solid markers correspond to 7° taper angle, open markers to 15° taper angle. Different marker types are used to indicate the number of holes: 1 (●), 2 (■), 4 (▼), 8 (♦) and 16 (★). For clarity, markers are shown only in one fifth of the measured points. Dashed lines represent bounds of values calculated using the quasi-steady approximation.*

Conclusions and outlook

Switching from single to multiple hole jet pump geometries certainly has an effect on the performance in terms of the time-averaged pressure drop and acoustic power dissipation. A lower dimensionless time-averaged pressure drop is measured when increasing the number of holes. Possible causes for this phenomenon are the interaction between jets from the different holes and the effect of turbulence on the jet pump performance. The latter will be investigated using hot-wire anemometry and flow visualization.

Acknowledgements

The authors would like to gratefully thank Jos Zeegers and the Eindhoven University of Technology for the provision of the experimental apparatus. Bosch Thermotechnology and Agentschap NL are thankfully acknowledged for the financial support as part of the EOS-KTO research program under project number KTOT03009.

References

[1] Aben, P. C. H. *High-Amplitude Thermoacoustic Flow Interacting with Solid Boundaries*. Phd thesis, Technische Universiteit Eindhoven (**2010**).

[2] Backhaus, S. and Swift, G. "A thermoacoustic-Stirling heat engine: detailed study". J. Acoust. Soc. Am., **107**, (2000), 3148–66.

[3] Biwa, T., Tashiro, Y., Ishigaki, M., Ueda, Y., and Yazaki, T. "Measurements of acoustic streaming in a looped-tube thermoacoustic engine with a jet pump". Journal of Applied Physics, **101**, (2007), 064914.

[4] Oosterhuis, J. P., Bühler, S., Wilcox, D., and Van der Meer, T. H. "A numerical investigation on the vortex formation and flow separation of the oscillatory flow in jet pumps". J. Acoust. Soc. Am., **137**, (2015), 1722–1731.

[5] Smith, B. L. and Swift, G. W. "Power dissipation and time-averaged pressure in oscillating flow through a sudden area change". J. Acoust. Soc. Am., **113**, (2003), 2455–2463.

REDUCING FLOW SEPARATION IN JET PUMPS

M.A.G. Timmer[1*], J.P. Oosterhuis[1], S. Bühler[1], D. Wilcox[2] and T.H. van der Meer[1]

[1] *Thermal Engineering, Engineering Technology, University of Twente, P.O. Box 217, 7500AE, Enschede, The Netherlands.*
**Corresponding author's e-mail: timmer.mag@gmail.com*
[2] *Chart Inc., Troy, New York, USA.*

Keywords: *jet pump, flow separation, acoustic streaming, minor losses*

Introduction

Jet pumps are static components that can be used in closed-loop, traveling wave thermo-acoustic devices to suppress a time-averaged mass flux (Gedeon streaming) that can exist [2]. The minimization of convective heat transport caused by this mass flux is of vital importance due to the detrimental effect it has on the device's efficiency. Jet pumps have an asymmetric shape, resulting in asymmetric minor losses. This causes a time-averaged pressure drop that suppresses Gedeon streaming when the minor losses are tuned correctly [1].
Current jet pump designs are mainly based on a quasi-steady approximation using minor loss coefficients [1]. A recent numerical study on conventional jet pump designs has shown that the quasi-steady approximation is only accurate in a small range of operating conditions [4]. It is shown that, above certain wave amplitudes, flow separation occurs during the half-cycle where the bulk flow is moving in the diverging direction of the jet pump. The flow separation originates from the small jet pump opening as a result of the local adverse pressure gradient. Due to the flow separation the asymmetry in minor losses diminishes, resulting in a severe downgrade of the jet pump performance compared with the quasi-steady approximation. The current work will investigate the flow separation behavior by varying the geometry of the jet pump. The goal is to minimize the flow separation and shift it to higher wave amplitudes, therewith increasing the effectiveness and robustness of jet pumps.

Method

In a similar manner as in Oosterhuis [4], an axisymmetric computational fluid dynamics model is developed which solves the unsteady, fully compressible Navier-Stokes equations. The boundary conditions enforce a 20 Hz traveling wave, with a wave amplitude that maintains flow in the laminar regime according to Ohmi and Iguchi [3].

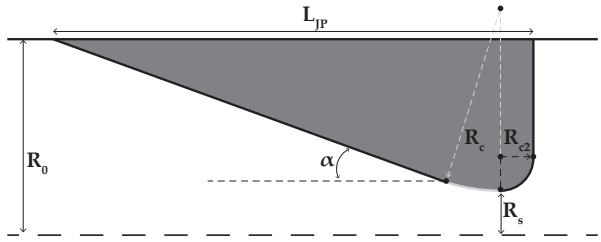

Figure 1: *Axisymmetric representation of the jet pump geometry. Bottom dashed line depicts the symmetry axis, top solid line indicates the outer tube wall.*

The investigated jet pump geometry is depicted in Figure 1. Conventional jet pumps use a single radius of curvature to reduce the minor loss coefficient at the small opening ($R_c = R_{c2}$), with the corresponding jet pump length defined as the reference length $L_{JP,ref}$. In an effort to minimize and shift flow separation, the adverse pressure gradient is reduced by increasing

the radius of curvature R_c. This introduces a longer and smoother transition from the small opening to the tapered surface. The extra jet pump length introduced by this longer transition with respect to $L_{JP,ref}$ is defined as ΔL_{JP}. Six cases are compared with the reference, namely: $\Delta L_{JP} = 3, 5, 10, 20, 30$ and 50 mm. The other dimensions are kept constant and are given by: $R_0 = 30$ mm, $R_s = 7$ mm, $R_{c2} = 5$ mm, $\alpha = 15^\circ$ and $L_{JP,ref} = 91.5$ mm (for $R_c = 5$ mm).

Results and discussion

The jet pump performance is studied in terms of the dimensionless time-averaged pressure drop Δp_2^* and acoustic power dissipation $\Delta \dot{E}_2^*$ [4], which are depicted in Figure 2 as a function of the Keulegan-Carpenter number. The latter is a dimensionless measure of the wave amplitude scaled with the jet pump waist diameter ($2R_s$). For larger transition lengths, the maximum pressure drop increases significantly. Additionally, the point at which the pressure drop is at its maximum shifts to higher amplitudes. A flow field investigation shows that this is the result of flow separation being shifted to higher KC_D values. Before flow separation occurs, the pressure drop of the cases with the largest transition lengths is similar to the quasi-steady approximation. The acoustic power dissipation is reduced for larger transition lengths.

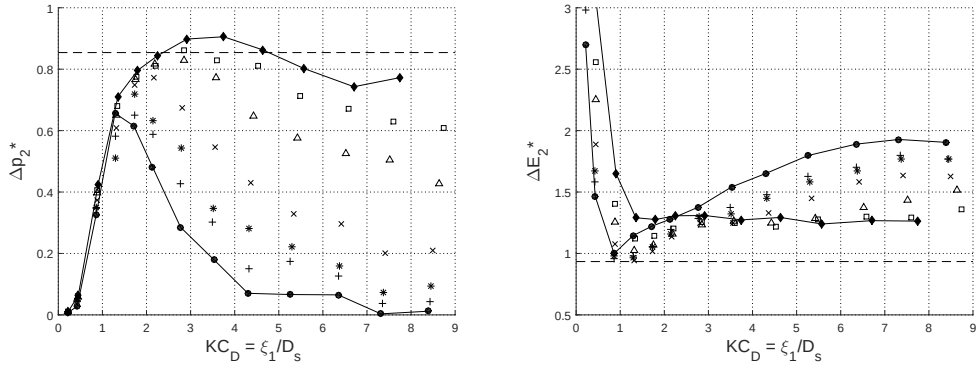

Figure 2: *Dimensionless pressure drop (left) and dimensionless acoustic power dissipation (right) for all cases, with: $\Delta L_{JP} = 0$ mm (●, reference), 3 mm (+), 5 mm (∗), 10 mm (×), 20 mm (△), 30 mm (□) and 50 mm (⧫). The dashed lines represent the quasi-steady approximation and the solid lines the cases with the smallest and largest transition length.*

Conclusions and outlook

By prolonging the transition length between the small opening and the tapered surface of jet pumps, flow separation is shifted to higher amplitudes and the pressure drop is increased significantly. This results in an improvement of the effectiveness and robustness of jet pumps. Future work will focus on reducing the jet pump length without downgrading its performance.

Acknowledgements

Bosch Thermotechnology and Agentschap NL are thankfully acknowledged for the financial support as part of the EOS-KTO research program under project number KTOT03009.

References

[1] Backhaus, S. and Swift, G. "A thermoacoustic-Stirling heat engine: detailed study". J. Acoust. Soc. Am., **107**, (2000), 3148–3166.

[2] Gedeon, D. "DC Gas Flows in Stirling and Pulse Tube Cryocoolers". In: "Cryocoolers 9", (**1997**), 385–392.

[3] Ohmi, M. and Iguchi, M. "Critical Reynolds number in an oscillating pipe flow". B. JSME, **25**, (1982), 165–172.

[4] Oosterhuis, J. P., Bühler, S., van der Meer, T. H., and Wilcox, D. "A numerical investigation on the vortex formation and flow separation of the oscillatory flow in jet pumps". J. Acoust. Soc. Am., **137**, (2015), 1722–1731.

CFD Modelling of the Effect of Oscillating Jets on Streaming Heat Losses in a Torus-shaped Thermoacoustic Engine

J.A. Lycklama à Nijeholt[1*], M.E.H. Tijani[1], N.B. Siccama[2]

[1]*Heat & Biorefinery Technology, Biomass & Energy Efficiency, ECN, P.O. Box 1, 1755 LE, Petten, The Netherlands.*
**Corresponding author's e-mail: lycklama@ecn.nl*
[2] *Safety and waste, Research& Innovation, NRG, The Netherlands.*

Keywords: *Thermoacoustics, CFD, Acoustic Streaming, Oscillating Heat Transfer, Heat Engine*

Introduction
A thermosacoustic engine converts heat into acoustic energy. A high temperature engine utilizes heat from a burner to drive the engine. Due to the high driving temperature acoustic streaming can be a strong heat loss mechanism that should be limited as much as possible. Linear acoustic simulation tools cannot be used to predict streaming nor its resulting heat loss. Therefore, computational fluid dynamics (CFD) has been used to simulate the streaming in a torus-shaped thermoacoustic engine. The present study builds upon previous CFD modeling and experimental studies from ECN on the high temperature TA engine and presented in [1] and [2]. Aim of the present work is to investigate the effect of oscillating helium jets originating from the heat exchangers on the degree of the streaming heat losses in the thermal buffer tube (TBT).

CFD model
The CFD model simulates the engine which consists of a torus-shaped part with heat exchangers and regenerator. The engine is connected to the resonator with an acoustic load. The resonator has also been included in the CFD geometry. The experimental geometry has been simplified into a two dimensional model in order to save CPU time. The streaming velocity field in the torus has been calculated by means of time-averaging of the oscillating flow. The convective streaming heat loss in the TBT has been calculated from the predicted thermal load of the TBT heat exchanger. The helium slots in the heat exchangers have been included in the CFD model in order to investigate the effect of the oscillating jets on the streaming flow pattern and streaming heat loss in the TBT.

Results
Jets from the heat exchangers enhance thermal mixing because of the additional production of turbulence. The CFD study shows however, a previously unknown and much stronger adverse effect of the helium jets. The helium jets enhance the convective streaming vortex present in the TBT resulting in much higher streaming velocities. Consequently, the convective heat loss in the TBT is also strongly increased. The physical flow mechanism for enhancement of the streaming flow rate by means of the jets is not yet fully understood.

The calculated temperature profile in the TBT and the thermal load of the TBT heat exchanger have been compared to the experimental data. The CFD results showed similar temperature profiles in the TBT and similar trends in the convective streaming heat loss. This

qualitative good agreement showed that the two-dimensional model approximation could be applied to demonstrate the effect of jets.

References

[1] Lycklama a Nijeholt, J.A.; Tijani, M.E.H.; Spoelstra, S.; Loginov, M.S.; Kuczaj, A.K.; "CFD modeling of streaming phenomena in a torus-shaped thermoacoustic engine ", 19th International Congress on Sound and Vibration (ICSV19), Vilinius, Litouwen, July 8-12, 2012.

[2] Tijani,M.E.H.; Spoelstra,S.; "A hot air driven thermoacoustic-Stirling engine", Applied Thermal Engineering (Elsevier), 2013, Ed.61, p.866-870.

A FAST ONE-DIMENSIONAL NONLINEAR THERMOACOUSTIC CODE

J.A. de Jong[1*], Y.H. Wijnant[1], D. Wilcox[2] and A. de Boer[1]

[1] *Applied Mechanics, Engineering Technology, University of Twente, P.O. Box 217, 7500AE, Enschede, The Netherlands.*
**Corresponding author's e-mail: j.a.dejong@utwente.nl*
[2] *Chart Inc. - Qdrive, 302 Thenth St., Troy, NY 12180, USA*

Keywords: *Nonlinear thermoacoustics, numerical modeling, design tool*

Introduction

The design of thermoacoustic (TA) systems is often aided with computational models. These computational models should be both fast, to quickly obtain feedback on design decisions, and accurate to know that the results are representative for a real TA system. However, in many cases these demands counteract each other. This often leads to a trade-off between computational cost and accuracy when choosing a specific design tool.

Currently, several computer codes are available to aid the design of TA systems. For example, the linear TA theory is implemented in the widely used computer code DeltaEC [5]. DeltaEC also has capabilities to compute nonlinear effects such as Gedeon streaming up to second order. For detailed simulations of the full nonlinear governing equations, commercial Computational Fluid Dynamics (CFD) software can be used. However, CFD tends to be computationally costly and time consuming.

This abstract describes the development and the first tests of a new one-dimensional nonlinear TA code, called the *ThermoAcoustic System Modeling Environment Twente* (TASMET). The code is capable of solving one-dimensional TA systems in a computationally efficient manner. It makes use of one-dimensional models to retain a low computational cost. However, to achieve better accuracy for high amplitude oscillations, the existing one-dimensional linear thermoacoustic theory is extended to the nonlinear domain.

The code

The low computational cost of the code is achieved by directly solving the periodic steady state of a TA system. For solving a TA system, a periodic (but not harmonic) solution is assumed *a priori*. This solution is expressed in terms of a truncated Fourier series. For an arbitrary dependent variable ξ this Fourier series is

$$\xi(t) \approx \sum_{n=0}^{N_f} \hat{\xi}_n e^{in\omega t},$$

where N_f is the number of frequencies (harmonics) taken into account to describe the solution, $\hat{\xi}_n$ are the Fourier coefficients, n is the harmonic number and ω the fundamental angular frequency. Then, instead of doing a time integration, the numerical algorithm solves for the Fourier coefficients of each dependent variable in the system [2].

The actual numerical routines are written in C++ and use the Armadillo [4] linear algebra package. The nonlinear system of equations is solved using the Newton-Raphson method with an exact evaluation of the Jacobian matrix. At each Newton iteration, the sparse algebraic system is solved

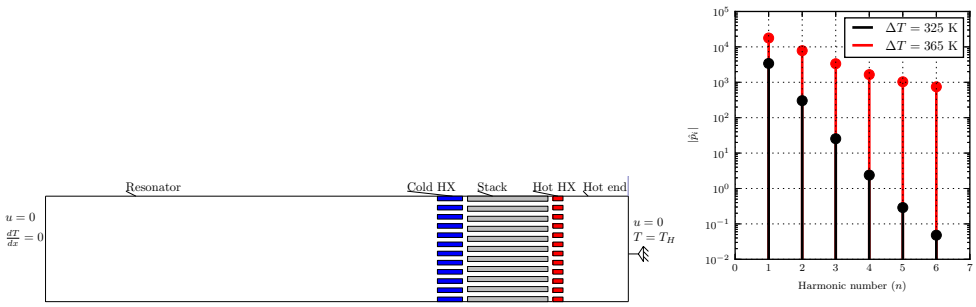

Figure 1: *Left: schematic picture of the geometry of a standing wave thermoacoustic engine. On the bottom, the wall temperature as a function of the position is shown. Right: results for the amplitudes of 6 pressure harmonics at the leftmost end of the geometry for two temperature differences across the stack.*

using the SuperLU [3] sparse system solver. The interface to the code has been made accessible using the portable and publicly available scripting language Python [1].

Example

A TA system consists of several tube-like segments, such as heat exchangers, a stack/regenerator and a feedback tube. In these segments, for the fluid domain the one-dimensional governing equations are solved, including the thermal equation of state. An example of a simple TA system is given in Figure (1). For each of the segments, a model is available. The segments are coupled at the ends, where the coupling equations dictate conservation of mass, momentum and energy.
Solving this system is done in less than a minute. The code outputs the Fourier coefficients for each of the dependent variables. For example, the spatial distribution of the absolute value of the first six acoustic pressure phasors is given on the right in Figure (1).

Future work

In future work, the modeling capabilities of the code will be expanded. Several commonly used models will be added, such as a model for a thermal buffer tube, and a porous material (random fiber, stacked screen) regenerator model.

Acknowledgements

This research has been carried out as a part of the Agentschap NL EOS-KTO (KTOT03009) research program. The financial support is gratefully acknowledged.

References

[1] Guido van Rossum. "The Python Programming Language - www.python.org" (**2015**).

[2] de Jong, J. A., Wijnant, Y. H., Wilcox, D., and de Boer, A. "Modeling of thermoacoustic systems using the nonlinear frequency domain method". To be published.

[3] Li, X. S., Demmel, J. W., Gilbert, J. R., Grigori, i., Shao, M., and Yamazaki, I. *SuperLU Users' Guide*. Technical Report LBNL-44289, Lawrence Berkeley National Laboratory (**1999**).

[4] Sanderson, C. *Armadillo: An Open Source C++ Linear Algebra Library for Fast Prototyping and Computationally Intensive Experiments*. Technical report, NICTA, Australia (**2010**).

[5] Ward, W. C. and Swift, G. W. "Design environment for low-amplitude thermoacoustic engines". The Journal of the Acoustical Society of America, **95**, (1994), 3671–3672.

EXPERIMENTAL TECHNIQUES

A TRAVELING WAVE TERMINATION FOR A THERMOACOUSTIC SETUP

M.C. Vidya*, J.P. Oosterhuis, and T.H. van der Meer

Thermal Engineering, Engineering Technology, University of Twente, P.O. Box 217, 7500AE, Enschede, The Netherlands.
**Corresponding author's e-mail: m.c.vidya@utwente.nl*

Keywords: *traveling wave, impedance tube, reflection coefficient, sound absorption.*

Introduction

A modification of a thermoacoustic experimental setup is performed to obtain traveling wave conditions. The setup has been used previously at the University of Twente to conduct experiments in a standing wave environment. One method to obtain a traveling wave inside the setup is to use a sound absorbing device. Two classes of sound absorbing structures can be distinguished: porous materials and resonance absorbers [4]. A traveling wave termination in the form of a resonance absorber was designed and tested.

Method

The experimental setup is depicted in Figure 1. For a detailed description, readers are referred to [1, 5]. The termination of the main impedance tube can be removed, thus a traveling wave termination can be attached to the end of the setup at $x = 0$. The termination is made of a quarter-wavelength tube with a diameter such that the wave is dissipated.

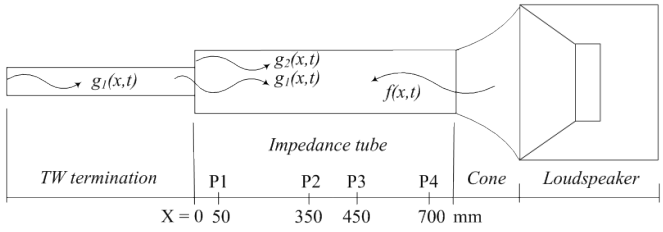

Figure 1: *Experimental setup with attached traveling wave termination. P1 – P4 represents the location of pressure sensors. Figure not to scale.*

The idea of adding a traveling wave termination is to cancel the reflections at the end of the setup. When an incoming wave $f(x,t)$ is generated from the loudspeaker, it will be reflected at the end of the setup (wave $g_2(x,t)$). The incoming wave $f(x,t)$ will also be reflected by the end wall of the traveling wave termination (wave $g_1(x,t)$). Wave $g_2(x,t)$ should have equal amplitude but 180° phase difference to $g_1(x,t)$ such that all reflected waves cancel each other at $x = 0$.

To model the wave propagation inside the impedance tube and the traveling wave termination, a one dimensional Low Reduced Frequency Model [3] is used. From the solution of the Low Reduced Frequency Model, the reflection coefficient and subsequently, absorption coefficient can be obtained as follows,

$$R(x) = \frac{\hat{p}_A e^{\Gamma k x}}{\hat{p}_B e^{-\Gamma k x}} \qquad \alpha(x) = 1 - |R|^2 \tag{1}$$

where $\hat{p}_A$ and $\hat{p}_B$ are the complex pressure amplitudes of the backward and forward propagating wave, respectively.

Results

The one dimensional model was used to obtain the relation between tube radius, tube length, absorption coefficient, and frequency. For each tube radius, there is one frequency and tube length that correspond to the theoretical 100% absorption. The manufactured tube has an inner radius of 5.985 mm and length of 73.7 cm. According to the model, it has a theoretical absorption coefficient of 100% at a frequency of 113 Hz.

Once the traveling wave termination was built, two sets of experiments were conducted: (1) a frequency sweep at pressure amplitude of 100 Pa and (2) a pressure amplitude sweep at 113 Hz. The results are presented in Figure 2.

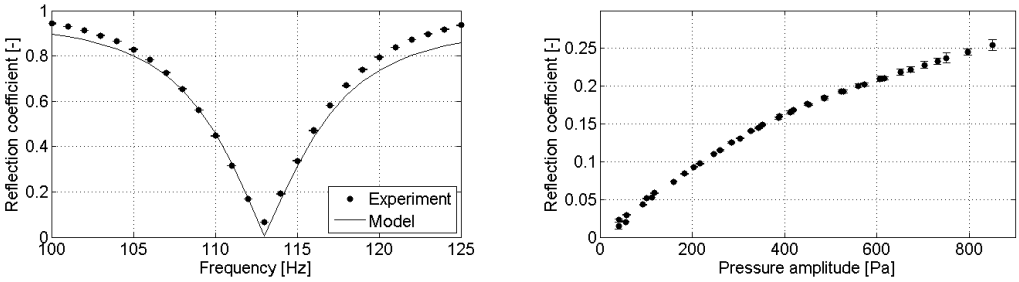

Figure 2: *Experimental results of frequency sweep at P2 = 100 Pa (left) and pressure amplitude sweep at 113 Hz (right). Error bars represent standard deviation within one measurement point.*

The traveling wave termination works well at low amplitudes and at the predicted frequency. At higher pressure amplitude, the reflection coefficient increases nonlinearly. Possible causes for this phenomenon are tube imperfection or nonlinear effects [1, 2] that occur at high pressure amplitude or due to flow disruption at $x = 0$.

Conclusions

A standing wave thermoacoustic setup is converted into a traveling wave setup by using a traveling wave termination. The termination works best at 113 Hz with absorption of 99.9%.

Acknowledgements

The authors would like to gratefully thank Jos Zeegers and the Eindhoven University of Technology for the provision of the experimental apparatus. Bosch Thermotechnology and Agentschap NL are thankfully acknowledged for the financial support as part of the EOS-KTO research program under project number KTOT03009.

References

[1] Aben, P. C. H. *High-Amplitude Thermoacoustic Flow Interacting with Solid Boundaries.* Phd thesis, Technische Universiteit Eindhoven (**2010**).

[2] in 't Pahuis, P. H. M. W. *Mathematical aspects of thermoacoustics.* Phd thesis, Technische Universiteit Eindhoven (**2009**).

[3] Tijdeman, H. "On the Propagation of Sound Waves in Cylindrical Tubes". *J. Sound and Vibration,* **39(1),** (1975), 1-33.

[4] van der Eerden, F. J. M. *Noise Reduction with Coupled Prismatic Tubes.* Phd thesis, University of Twente (**2000**).

[5] van der Gun, D. *Design and Realization of an Experimental Thermoacoustic Setup.* Master thesis, University of Twente (**2013**).

COMPARISON OF ACOUSTIC POWER AMPLIFICATION BY WET/DRY-WALLED THERMOACOUSTIC ENGINE

M. Senga[1*], Y. Ashigaki[1], and S. Hasegawa[2]

[1]*Course of Mechanical Engineering, School of Engineering, Tokai University, 4-1-1 Kitakaname, Hiratsuka-shi, Kanagawa, 259-1292 Japan.*
**Corresponding author's e-mail: senga.mariko@gmail.com*
[2]*Department of Prime Mover Engineering, School of Engineering, Tokai University, 4-1-1 Kitakaname, Hiratsuka-shi, Kanagawa, 259-1292 Japan.*

Keywords:
traveling wave heat engine, phase change, wet regenerator, acoustic power amplification

In 1979, Ceperley proposed acoustic amplification in a traveling wave heat engine [1]. This proposal was verified by Biwa et al. in 2011[2], whose results indicated that the maximum gain of the traveling wave thermoacoustic heat engine is asymptotic to the temperature ratio when there is no phase change. Meanwhile, Raspet et al. performed numerical calculations for a wet-walled regenerator[3]. They found that in comparison to a thermoacoustic heat engine with a dry regenerator, the critical temperature at which self-induced oscillation occurs is lower and the acoustic power amplification is higher in a thermoacoustic heat engine using a wet regenerator. Ueda et al. investigated experimental verification of the reduction in critical temperature ratio[4]. However, the acoustic power amplification of a wet regenerator has yet to be experimentally verified. In this study, we measured the acoustic power amplification gain of a wet regenerator and compared it with that of dry regenerator.
Figure 1 shows the schematic of our experimental apparatus in this study. The apparatus was consists of ducts and a unit which made of an ambient heat exchanger, a hot heat exchanger, and a regenerator. Loudspeakers were installed on each end of the apparatus. In the experiment, the ambient heat exchanger was set at T_R=307 K and the hot heat exchanger at T_H=332 K, and the temperature of each heat exchanger was measured with a thermocouple. To satisfy the same conditions as in the Ceperley's proposal, the acoustic field was regulated to make a traveling wave phase at the downstream end of the unit by adjusting the phase and voltage of the loudspeakers. Three pressure transducers were attached to each duct at the upstream and downstream ends, and the acoustic field was calculated by the two-sensor method[5,6] from the measured complex pressure amplitude. The gain G of an acoustic power W was measured for both a dry and a wet regenerator. G was found by the following equation using the acoustic power at the upstream end of the unit W_{in}, and acoustic power at the downstream end of the unit W_{out}.

$$G = W_{\mathrm{out}} / W_{\mathrm{in}} \tag{1}$$

Figure 2 shows the experimentally observed acoustic power distribution, normalized by W_{out} for ease of comparison. The solid line shows the results for the wet regenerator and the dushed line shows the results for the dry regenerator. The black dots in the figure are measurement points. Here, the acoustic power attenuates without amplifying in the dry case

for the temperature ratio T_H/T_R= 1.08. In the wet case, however, amplification of acoustic power was observed and *G* value was 1.12. Since temperature ratio(T_H/T_R) is 1.08, the mentioned *G* value is higher than the temperature ratio. This result indicates that an acoustic power amplification exceeding the temperature ratio is possible when using a wet regenerator, though gain essentially does not exceed the temperature ratio in a dry case.

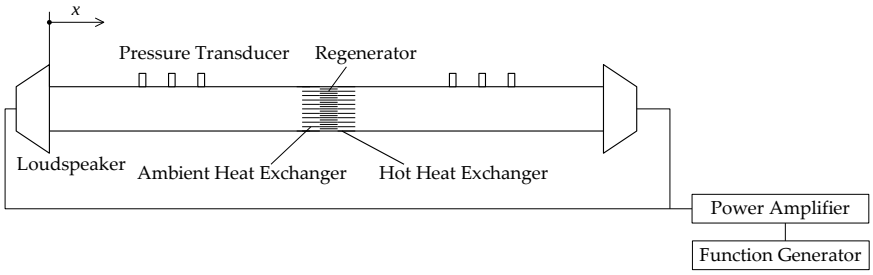

Figure 1: *Experimental apparatus*.

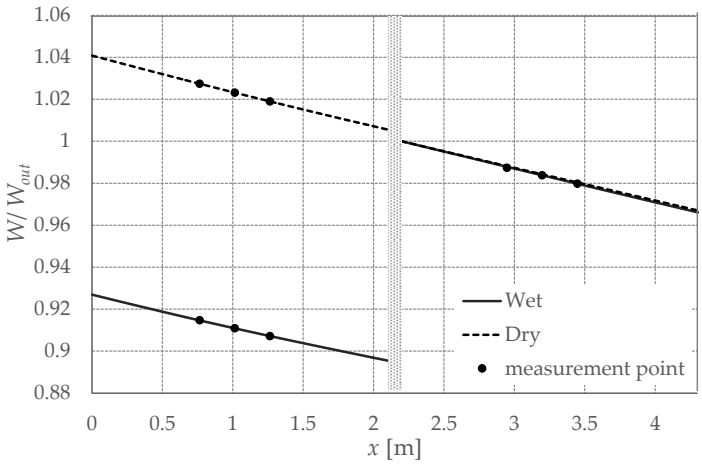

Figure 2: *Distribution of normalized acoustic power* W/W_{out}.

Acknowledgements

This study was financially supported by the Advanced Low Carbon Technology Research and Development Program (ALCA) in 2013 (Grant No. 13414425) from Japan Science and Technology Agency.

References

[1] Ceperley, P. H. "A pistonless Stirling engine - the traveling wave heat engine", J. Acoust. Soc. Am., **66**, (1979), 1508–1513.

[2] Biwa, T., Komatsu, R., and Yazaki, T. "Acoustical power amplification and damping by temperature gradients", J. Acoust. Soc. Am., **129**, (2011), 132–137.

[3] Raspet, R., Slaton, W.V., Hickey, C. J, and Hiller, R. A. "Theory of inert gas-condensing vapor thermoacoustics: Propagation equation", J. Acoust. Soc. Am., **112**, (2002), 1414–1422.

[4] Noda, D., and Ueda, Y. "A thermoacoustic oscillator powered by vaporized water and ethanol", Am. J. Phys., **81**, (2013), 124–126.

[5] Fusco, A. M., Ward, W. C., and Swift, G. W. "Two-sensor power measurements in lossy ducts", J. Acoust. Soc. Am., **91**, (1992), 2229–2235.

[6] Biwa, T., Tashiro, Y., Nomura, H., Ueda, Y., Yazaki, T. "Experimental verification of a two-sensor acoustic intensity measurement in lossy ducts", J. Acoust. Soc. Am., **124**, (2008), 1584–1590.

ANALYSIS OF THE ACOUSTIC FIELD IN A THERMOACOUSTIC SYSTEM USING TIME-RESOLVED PARTICLE IMAGE VELOCIMETRY AND CONSTANT-VOLTAGE ANEMOMETRY

P. Blanc-Benon [1*], E. Jondeau[1], and G. Comte-Bellot[1]

[1] *Laboratoire de Mécanique des Fluides et d'Acoustique, UMR CNRS 5509, Université de Lyon, École Centrale de Lyon, 36 avenue Guy de Collongue, 69134 Ecully-Cedex, France.*
*. *Corresponding author's e-mail: philippe.blanc-benon@ec-lyon.fr*

Keywords: *nonlinear acoustic, oscillating flows, temperature fluctuation, velocity fluctuation , time-resolved particle image velocimetry, constant-voltage anemomety, thermoacoustic,*

The development of high-performance thermoacoustic systems requires efficient heat transfer between the stack or the regenerator and the heat-exchangers. So far, the coupling between these elements has been addressed using theoretical models and numerical simulations[1]. These analyses demonstrate that, at the high acoustic levels found in realistic thermoacoustic systems, acoustic velocities and instantaneous temperatures exhibit nonlinear interactions. However, there is a lack of controlled experimental data to validate these results. In this paper we consider a standing-wave thermoacoustic refrigerator. It consists of a stack of plates placed in an acoustic resonator. Two heat exchangers are located at each stack extremity. The thermoacoustic effect takes place in the thermal and viscous boundary layers along each plate of the stack. It results in a heat transport along the plates and in a temperature difference between the two stack ends. The full understanding of the heat transfer between the stack and the heat exchangers is a key issue to improve the global efficiency of these devices.

The aim of this analysis is to investigate the vortex structures, which appear at the ends of the stack and modify the heat transfer. Here, the aerodynamic in the gap stack-exchanger is characterized using a time-resolved particle image velocimetry technique[2] (TR-PIV). Measurements are performed in a device operating at a frequency of 200 Hz. Instantaneous velocity fields are recorded at a frequency of 3125 Hz (ie 15 maps per acoustic period). Measurements show that vortex shedding occur at high pressure levels, when a nonlinear acoustic regime prevails, leading to an additional heating generated by viscous dissipation in the gap and a loss of efficiency.

In order to analyze the structure of the instantaneous temperature field we have developed a new thermal anemometry technique using a constant-voltage anemometer (CVA) prototype[3,4,5]. This technique is well adapted to unsteady and oscillating flows as the thermal lag of the sensors is corrected instantaneously. It is based on an additional measurement of the flow velocity and its influence on the heat transfer balance of the sensor. Using specifically designed probes with very fine wires, high frequency signals can be recorded and analysed. In a first part we present a validation of this new procedure using a standing-wave acoustic tube for which the fluctuating temperature field is well known even for high acoustic pressure levels. In a second part, measurements are performed behind the stack of a standing-wave thermoacoustic refrigerator. They confirm the existence of temperature harmonics near the stack edge, which should not be overlooked when designing the stack and the heat exchangers.

In summary, the TR-PIV gives access to the real time evolution of the flow rather than to rely on phase-averaging and it allows measurements even when the flow loses its periodicity at high drive ratio. The development of a new procedure for the measurement of temperature fluctuations which relies on the unique features of the CVA, allows measurement of temperature fluctuations in oscillating flows. With these two experimental techniques, it is now possible to have an estimation of the nonlinearities which occur in efficient thermoacoustic systems.

References

[1] Marx, D. and Blanc-Benon, P., "Numerical simulation of stack-heat exchangers coupling in a thermoacoustic refrigerator", AIAA Journal, (2004), 42(7), 1338-1347.

[2] Poignand G., Jondeau E. and Blanc-Benon P., "Investigation of the aerodynamic field in a standing-wave thermoacoustic refrigerator using Time-Resolved Particle Image Velocimetry", 17th AIAA/CEAS Aeroacoustics Conference, (2011) ,AIAA Paper 2011-2932.

[3] Berson, A., Poignand, G., Blanc-Benon P. and Comte-Bellot, G., "Nonlinear temperature field near the stack ends of a standing-wave thermoacoustic refrigerator", Int. J. Heat Mass Transfer, (2011),54(21-22), 4730-4735

[4] Berson A., Poignand G., Blanc-Benon P. and Comte-Bellot G., "Capture of instantaneous temperature in oscillating flows: Use of constant-voltage anemometry to correct the thermal lag of cold wires operated by constant-current anemometry", Review of Scientific Instruments, (2010) 81(1), 015102.

[5] Taifour A. M., Weiss J., Sadeghi A., Vétel J., Jondeau E. and Comte-Bellot G., "A detailed procedure for measuring turbulent velocity fluctuations using constant voltage anemometry", Experiment in Fluids (2015) 56:17, DOI 10.1007/s00348-015-2045-0.

NOTES